

Aus dem Zentrum für Hygiene und medizinische Mikrobiologie
der Philipps Universität Marburg
Institut für Virologie
Geschäftsführender Direktor: Prof. Dr. Stephan Becker



**Potent inhibition of highly pathogenic influenza virus
infection using a peptidomimetic furin inhibitor alone or
in combination with conventional antiviral agents**

Dissertation

**Zur Erlangung des Doktorgrades der Naturwissenschaften
(Dr. rer. nat.)**

dem Fachbereich Biologie
der Philipps-Universität Marburg
vorgelegt von

Yinghui Lu

aus Shanghai, China

Marburg an der Lahn

2014

Die Untersuchungen zur vorliegenden Arbeit wurden im Institut für Virologie, Direktor: Prof. Dr. Stephan Becker, Fachbereich Medizin der Philipps-Universität Marburg, unter der Anleitung von Prof. Dr. Wolfgang Garten durchgeführt.

Vom Fachbereich Biologie der Philipps-Universität Marburg
als Dissertation angenommen am: 18.08.2014

Erstgutachter: Prof. Dr. Wolfgang Garten

Zweitgutachter: Prof. Dr. Wolfgang Buckel

Weitere Mitglieder der Prüfungskommission:

Prof. Dr. Erhard Bremer

Prof. Dr. Susanne Önel

Tag der mündlichen Prüfung: 01.10.2014

献给我亲爱的家人

For my parents and sister

Für meine Eltern und Schwester

Inhalt

Summary	1
Zusammenfassung	1
1. Introduction	3
1.1 Influenza	3
1.1.1 Classification	3
1.1.2 Clinical features and pathogenesis of influenza	3
1.1.2.1 Human influenza viruses	3
1.1.2.2 Avian influenza viruses	4
1.1.2.2.1 Avian influenza H7 viruses	4
1.1.2.2.2 Avian influenza H5 viruses	6
1.1.3 Epidemiology	7
1.1.3.1 Antigenic drift and antigenic shift	7
1.1.3.2 History of human influenza pandemics	8
1.1.4 Virus morphology, genome and proteins	9
1.1.5 Virus life cycle	12
1.2 Hemagglutinin	14
1.2.1 The structure of the hemagglutinin	14
1.2.2 Receptor binding specificity of hemagglutinin	15
1.2.3 Proteolytic activation of precursor hemagglutinin	16
1.2.3.1 Monobasic cleavage site	17
1.2.3.2 Multibasic cleavage site	18
1.3 Proprotein convertases	18
1.3.1 Furin	19
1.4 Prevention and treatment of influenza	21
1.4.1 Vaccination	21
1.4.2 Approved antiviral agents	22

1.4.2.1 Adamantane derivatives	23
1.4.2.2 Neuraminidase inhibitors	24
1.4.3 Other antiviral agents	25
1.4.3.1 Proprotein convertase inhibitors.....	26
1.4.3.1.1 Furin inhibitors	26
1.4.4 Combination therapy	28
1.5 Aim of the study.....	29
2. Materials	31
2.1 Chemicals	31
2.2 Consumed materials	32
2.3 Instruments.....	33
2.4 Kits	33
2.5 Protein markers	33
2.6 Antibodies	34
2.6.1 Primary antibodies	34
2.6.2 Secondary antibodies.....	34
2.7 Enzymes	34
2.8 Primers.....	34
2.9 Viruses	35
2.10 Consumed materials for cell cultures	35
2.10.1 Cell culture medium	35
2.10.2 Cell lines	36
2.11 Buffers.....	36
2.12 Others	38
3. Methods.....	39
3.1 Molecular and biological methods	39
3.1.1 Antiviral compounds.....	39

3.1.2 MTT viability assay.....	39
3.1.3 Stability measurements of furin inhibitors with high performance liquid chromatography	39
3.1.4 Sodium dodecyl sulfate polyacrylamide gel electrophoresis	40
3.1.5 Western blots	41
3.1.6 Viral RNA extraction.....	41
3.1.7 One-step reverse transcription polymerase chain reaction	42
3.1.8 Two-steps reverse transcription polymerase chain reaction	43
3.1.8.1 Reverse transcription	43
3.1.8.2 Polymerase chain reaction.....	43
3.1.9 DNA electrophoresis	44
3.1.10 DNA fragment extraction and purification.....	44
3.1.11 DNA purification	44
3.1.12 DNA-sequencing	44
3.2 Cell culture methods.....	45
3.3 Virological methods	45
3.3.1 Virus propagation in eggs	45
3.3.2 Virus propagation in cell cultures	46
3.3.3 Hemagglutination assay	46
3.3.4 Plaque assay	46
3.3.5 Plaque reduction assay	47
3.3.6 Immunostaining.....	47
3.3.7 Cleavage of HA0 protein in the presence of furin inhibitors	48
3.3.8 Virus spread in the presence of inhibitors	48
3.3.9 HPAIV multicycle replication in the presence of a single inhibitor	48
3.3.10 Control inhibition assay using FPV mutant.....	49
3.3.11 Combination treatment of HPAIV infection.....	49

3.3.12 Time of inhibitor addition	49
3.3.13 Neutral red uptake assay	50
3.3.14 Inhibitor efficiency calculation.....	50
3.3.15 Synergistic inhibition analysis.....	50
3.3.16 Vesicular Stomatitis Virus control infection experiment.....	51
3.3.17 Control infection experiment with apathogenic influenza virus	51
3.3.18 Serial propagation of FPV in the presence and absence of antivirals	52
3.3.19 Virus inactivation	54
3.3.20 Determination of neuraminidase activity	54
3.3.21 Virus susceptibility to oseltamivir.....	55
3.3.22 Growth kinetic of FPV mutants.....	55
3.3.23 Effect of MI-701 on replication of FPV mutants	56
4. Results.....	57
4.1 Screening of furin inhibitors	57
4.1.1 Determination of cytotoxicity	57
4.1.2 Determination of stability	59
4.1.3 Cleavage of HA0 in the presence of furin inhibitors	60
4.2 Inhibitory efficacy of furin inhibitor MI-701 against HPAIV infection.....	62
4.2.1 Cleavage of HA0 in the presence of inhibitor MI-701	62
4.2.2 Virus spread in the presence of inhibitor MI-701	63
4.2.3 Inhibitory efficacy of inhibitor MI-701 on HPAIV multicycle replication	64
4.2.4 Specificity of furin inhibitor MI-701	66
4.3 Combination therapy against HPAIV	67
4.3.1 Cell viability in the presence of different drugs	67
4.3.2 Virus spread in the presence of double drugs	68
4.3.3 Virus replication in the presence of double drugs	69
4.3.4 Virus replication in the presence of triple drugs	70

4.3.5 Determination of the 50 percentage effective concentration of MI-701, oseltamivir and ribavirin as single drugs or in combination	75
4.3.6 Synergy analysis	76
4.4 Effects of treatment initiation on antiviral activity	78
4.5 Development of drug-resistant FPV	80
4.5.1 Propagation of FPV in the presence of MI-701	80
4.5.2 Propagation of FPV in the presence of oseltamivir	81
4.5.3 Propagation of FPV in the presence of oseltamivir and furin inhibitor MI-701	83
4.5.4 Virus susceptibility to oseltamivir <i>in vitro</i>	86
4.5.5 Biological characterization of FPV variants	87
4.5.5.1 Growth kinetics of FPV variants in cell cultures	87
4.5.5.2 Effect of furin inhibitor MI-701 on replication of FPV mutants	88
5 Discussion	90
5.1 Furin as a drug target for prevention of HPAIV infection	90
5.2 Development and evaluation of furin inhibitors	91
5.3 Binding of furin inhibitors	94
5.4 Combinatorial drug treatment	95
5.5 Development of drug-resistance during drug treatment	98
5.6 Furin inhibitors block other viruses and bacterial pathogens	102
5.7 Conclusion	105
6. Supplementary data	106
7. References	118
Abbreviations	132
Figures	135
Curriculum vitae	137
Acknowledgements	140
Erklärung	142

Summary

Antiviral medication is an important option for treatment of influenza virus infections. Two classes of anti-influenza drugs are available for prophylaxis and treatment of the infections: M2 ion channel inhibitors and neuraminidase inhibitors. However, most of the currently circulating influenza A virus strains are resistant to M2 inhibitors, and wide spread application of neuraminidase inhibitors is increasing resistance to these drugs. Therefore, discovery of new antiviral drugs and more efficient therapeutic approaches are urgently needed.

The hemagglutinin (HA) protein is the major membrane glycoprotein of influenza A viruses. It facilitates binding of the virus to host cell receptors and mediates fusion between viral and endosomal membranes. Precursor HA0 must be activated by host proteases to gain its fusion capacity. The cleavage motif of HA is a major determinant of influenza virus pathogenicity. HA of highly pathogenic avian influenza virus (HPAIV) of subtypes H5 and H7 contains a multibasic cleavage motif, which is activated by the eukaryotic subtilase furin. Furin's essential role during the HPAIV infection makes it an attractive drug target. Novel peptidomimetics imitating the furin recognition motif -R-X-K/R-R- proved to be efficacious anti-HPAIV inhibitors. They interfered with the proteolytic activation of HA and suppressed virus replication in cell cultures. Combination of oseltamivir and ribavirin with a furin inhibitor had synergistic antiviral effects. Furthermore, it suppressed the development of oseltamivir-resistant variants. Therefore, combination treatment is considered as a promising approach for the control of HPAIV.

Zusammenfassung

Zur Therapie und Prophylaxe von Influenza beim Menschen Medikamente aus zwei Wirkstoffklassen sind zugelassen: die M2-Ionenkanalblocker und Neuraminidase-Inhibitoren (Oseltamivir). Die M2-Ionenkanalblocker Amantadin und Rimantadin hemmen die Freisetzung des viralen Ribonukleokapsids ins Zytoplasma. Sie führen aber bei ihrer Anwendung zu resistenten Virusmutanten und werden daher nicht mehr zur Prophylaxe und Therapie von Influenzavirusinfektionen empfohlen. Auch nehmen Oseltamivir-resistente Influenzaviren weltweit zu. Daher sind neuartige Wirkstoffe und neue Strategien zur Bekämpfung von Influenzavirusinfektionen dringend erforderlich. Die proteolytische Spaltung des Hämagglutinins (HA), eines Glykoproteins an der Oberfläche der Influenzaviren, ist Voraussetzung für deren Infektiosität. Bei den hoch pathogenen aviären Influenzaviren (HPAIV) der Subtypen H5 und H7 wird das HA-Vorläufermolekül (HA0) von der Wirtsprotease Furin am Carboxyterminus des basischen Peptidmotivs –Arg-X-Arg/Lys-Arg- in die Untereinheiten HA1 und HA2 gespalten. In dieser Arbeit wurde die Hemmung von HA-Spaltung und Virusvermehrung durch neuartige Protease-Inhibitoren untersucht. Es handelte sich dabei um Peptidomimetica, die strukturelle Ähnlichkeit mit den HA-Spaltstelle haben. Sowohl die Spaltung des HAs als auch die Ausbereitung von HPAIV in Zellkulturen wurde durch den Furininhibitor MI-701 besonders effizient gehemmt. Die Kombination von MI-701 mit Oseltamivir und Ribavirin steigerte die antivirale Hemmwirkung enorm. Darüber hinaus kam es bei gleichzeitige Gabe von MI-701, Oseltamivir und Ribavirin zur eine stark verzögerten Ausbildung von Oseltamivir-resistenten Viren (HPAIV). Den Kombination von Furininhibitoren mit konventionellen antiviralen Substanzen bietet sich deswegen als besonders wirksame Methode zur Behandlung von HPAIV-Infektionen an.

1. Introduction

1.1 Influenza

Influenza is a common infectious disease in human. The infection typically causes a transient respiratory illness, in severe cases, however, it may also lead to death. Influenza viruses spread worldwide and cause annual epidemics and sporadic pandemics. Influenza A viruses have been isolated not only from human, but also from many other mammalian species including pigs, whales, horses, seals, bats, but the original reservoir of all influenza A viruses are birds (Webster et al., 1992).

1.1.1 Classification

Influenza viruses belong to the family *Orthomyxoviridae*, which is a family of enveloped viruses with segmented, negative-stranded RNA genes. There are six different genera in this family; Influenza virus A, Influenza virus B, Influenza virus C, Isa virus, Thogoto virus and recently discovered Quaranja virus. These viruses are serologically differentiated by their internal proteins: the matrix protein and nucleoprotein (Fields, 2006; Presti et al., 2009). Influenza A viruses are further divided into 18 hemagglutinin, H1-H18, and 11 neuraminidase subtypes, N1-N11, based on different antigenicity of their HA and NA molecules (Fields, 2006; Tong et al., 2012; Tong et al., 2013). Influenza strains are named according to their genus, the host of origin (except for humans), the location of isolation, the number of the isolate, the year of isolation and the HA and NA subtypes. For example, A/Thailand/1(KAN-1)/2004 (H5N1) describes an influenza A virus subtype H5N1, which was isolated from a human in Kanchanaburi, a province of Thailand, in 2004 with the strain number 1 (Puthavathana et al., 2005).

1.1.2 Clinical features and pathogenesis of influenza

1.1.2.1 Human influenza viruses

Currently, influenza A virus, subtypes H1N1 and H3N2, and two lineages of influenza B virus, B/Victoria/2/87-like (Victoria lineage) and B/Yamagata/16/88-like (Yamagata lineage), are co-circulating among humans (WHO¹). Human influenza viruses usually affect the human respiratory tract: the nose, trachea, bronchi and lungs, resulting in mild upper respiratory diseases and rarely induce severe lower respiratory diseases (Fields, 2006). The flu syndrome is typically a sudden onset of high fever, chills, dry

cough, sore throat, runny nose, headache, muscle and joint pain, fatigue, and in severe cases breathing problems and pneumonia. The incubation period can be as short as 24 hours to 4 or 5 days (Fields, 2006). Influenza epidemics normally occur during the winter and affect people of all ages. However, children under 2 years old, the elderly aged more than 65 years, and people of any age with pre-existing medical conditions, metabolic diseases or weakened immune systems are at highest risks of developing flu-related complications (Rothberg et al., 2008).

1.1.2.2 Avian influenza viruses

Influenza A viruses isolated from birds are termed avian influenza viruses. The first outbreak of avian influenza was reported in Italy in 1878 by Perroncito (Perroncito et al., 1878). It caused high mortality in chickens and was originally termed as fowl plague. A filterable virus was first determined to cause this disease (Centanni et al., 1901). Influenza A viruses was identified as the causative agent of fowl plague in 1955 (Schäfer, 1955; Lupiani & Reddy, 2009).

Avian influenza viruses are categorized as either low pathogenic avian influenza virus (LPAIV) or highly pathogenic avian influenza virus (HPAIV) based on their pathogenicity in chickens. LPAIV usually cause little to no diseases in wild birds. Its infection is limited to the intestinal tract of birds. High concentrations of viruses are shed in feces (Alexander, 2007; Webster et al., 1992). HPAIVs are highly pathogenic for chickens and cause severe contagious illness and death among infected birds. Currently, only some strains of influenza A subtypes H5 or H7 have the potential to shift from low pathogenic to highly pathogenic by spontaneous insertion of basic amino acids at the HA0 cleavage site (Perdue et al., 1997; Garten & Klenk, 2008). Although most avian influenza viruses do not infect humans, human infections with LPAIV or HPAIV may sporadically occur after direct contact with infected poultry. Infection of LPAIV generally results in mild respiratory diseases, whereas infection of HPAIV can cause severe lower respiratory disease and high mortality in humans (Fields, 2006; Garten & Klenk, 2008).

1.1.2.2.1 Avian influenza H7 viruses

Over the past 60 years outbreaks of LPAIV and HPAIV H7 viruses, including H7N1, H7N2, H7N3, H7N4, H7N7 and H7N9 subtypes, occurred throughout the world, resulting in mass culling of poultry and domestic birds and devastating economic losses (Alexander, 2000; Capua & Alexander, 2004; Belser et al., 2009) (Table S1 in

supplementary). Some H7 strains crossed the species barrier and infected humans. Human infection with H7 viruses mainly results in conjunctival symptoms with occasional and generally mild respiratory illness (Belser et al., 2009). The first documented isolation of HPAIV H7 subtypes from human occurred in 1959 in the United States (Delay et al., 1967), while the first direct transmission of H7 subtype from infected birds to human occurred in 1996 in England (Kurtz et al., 1996). Since then, human infections with H7 subtype have been reported in countries worldwide, including Canada, Italy, Mexico, the Netherlands, the United Kingdom, and the United States (Table 1.1).

Table 1.1: Human cases of influenza A virus H7 subtype infection since 1996.

Year	Virus subtype	Pathogenicity	Location	Nr. of human cases (Nr. of deaths)	Symptoms
1996	H7N7	LPAIV	England	1	Conjunctivitis
2002	H7N2	LPAIV	Virginia (USA)	1	Respiratory
2003	H7N2	LPAIV	New York (USA)	1	Respiratory
2002-2003	H7N3	LPAIV	Italy	7	Conjunctivitis, respiratory
2003	H7N7	LPAIV	Netherlands	89 (1)	Conjunctivitis, respiratory, pneumonia, ARDS
2004	H7N3	LPAIV	Canada (British Columbia)	2	Conjunctivitis, respiratory
2006	H7N3	LPAIV/HPAIV	Norfolk (UK)	1	Conjunctivitis
2007	H7N2	LPAIV	Wales (UK)	4	Conjunctivitis, respiratory
2013	H7N9	LPAIV	China	375 (115)	Pneumonia, ARDS

*Table is taken from Belser et al., 2009 with modification.

ARDS: acute respiratory distress syndrome.

The largest outbreak of HPAIV H7N7 subtype in humans occurred in February 2003 in the Netherlands. More than 30 million birds and chickens were slaughtered during this outbreak, and 86 humans who handled infected poultry were infected, as well as three of their family members. The symptoms were generally mild; however, one case was severe and the patient died after developing an acute respiratory distress syndrome (ARDS) and pneumonia (Fouchier et al., 2004). In 2004 two people in Canada were infected with HPAIV H7N3 subtype and developed mild influenza-like illness and conjunctivitis (Tweed et al., 2004). In 2013 an outbreak of LPAIV subtype H7N9 occurred in China. Most patients developed severe pneumonia. By February 2014 a

total of 375 human cases of H7N9 infection had been confirmed, including 115 deaths. The source of the virus has not been identified and therefore the risk of infection with H7N9 is still present (WHO²).

1.1.2.2.2 Avian influenza H5 viruses

The first documented outbreak of avian influenza H5 viruses in poultry occurred in Scotland in 1959 (Becker et al., 1967). Within the past fifty years, over ten outbreaks of H5 viruses have occurred worldwide, including several large outbreaks of HPAIV H5 viruses that affected huge amounts of domestic poultry (Table S2 in supplementary). The outbreak of HPAIV H5N1 in 2003 in Asia, affecting South Korea, Japan, Indonesia, Vietnam, Thailand, Laos, Cambodia and China, resulted in high mortality in poultry and wild birds. Since 2003, the HPAIV H5N1 viruses extended from Asia to Europe, the Middle East and Africa, and caused endemics in Bangladesh, China, Egypt, India, Indonesia and Vietnam (Lupiani & Reddy, 2009).

The first human infection with avian influenza virus H5N1 was reported in Hong Kong in 1997. Eighteen people were infected with this virus and six of them died (Shortridge et al., 1998). No other additional cases were reported until 2004, when human infections with HPAIV H5N1 were reported in Vietnam (Tran et al., 2004). Infection of HPAIV H5N1 causes severe pneumonia and multi-organ failure (Abdel-Ghafar et al., 2008). Since 2003, a total of 650 human infection cases have been confirmed and 386 people died (Table. 1.2) (WHO³). Until now, the HPAIV H5N1 virus is not able to efficiently and sustainably transmit from human-to-human. Most cases of H5N1 infection in humans are linked to direct contact with infected poultry. However, the frequent occurrence of H5N1 infections in wild birds and poultry increases the risk of human exposure to H5N1 viruses. Therefore, the HPAIV H5N1 virus is considered to have potential to cause a new pandemic.

Table 1.2: Confirmed human H5N1 cases from 2003 to 2014.

Country	Nr. of human cases (Nr. of deaths)	Mortality rate (%)
Azerbaijan	8 (5)	62.5
Bangladesh	7 (1)	14.3
Cambodia	47 (33)	70.2
Canada	1 (1)	100
China	45 (30)	66.7
Djibouti	1 (0)	0
Egypt	173 (63)	36.4
Indonesia	195 (163)	83.6
Iraq	3 (2)	66.7
Lao People's Democratic Republic	2 (2)	100
Myanmar	1 (0)	0
Nigeria	1 (1)	100
Pakistan	3 (1)	33.3
Thailand	25 (17)	68
Turkey	12 (4)	33.3
Vietnam	125 (62)	49.6
Total	650 (386)	59.4

This table is taken from cumulative number of confirmed human cases for avian influenza A (H5N1) reported to WHO, 2003-2014, with modification (WHO⁴).

1.1.3 Epidemiology

1.1.3.1 Antigenic drift and antigenic shift

Influenza A viruses exhibit rapid evolutionary dynamics, consistent with a high average mutation rate, ranging from 10^{-3} to 8×10^{-3} substitutions per site per year during viral genome replication (Chen & Holmes, 2006). Influenza viruses can rapidly change in two different ways: antigenic drift and antigenic shift. Antigenic drift refers to small changes that are caused by point mutations such as amino acids substitution in HA and NA or a cluster of mutations in antigenic epitopes. It occurs frequently and may result in minor changes in antigenicity that allow the virus to escape host pre-existing immunity induced by previous infection or vaccination. Antigenic drift occurs in all strains of influenza A and B viruses and much more often in influenza A virus H3 subtype (Carrat & Flahault, 2007). Antigenic shift is defined as major antigenic change

in HA or NA proteins, which produces a new virus subtype. This has only been found in influenza A viruses and occurs when different viruses, from either different subtypes or different host species co-infect the same host cell and new influenza subtypes are produced by genetic reassortment (Fields, 2006) (Fig. 1.5).

1.1.3.2 History of human influenza pandemics

In the past hundred years 4 major human influenza pandemics have occurred at intervals of 10 to 50 years with varying severity and caused millions of fatalities worldwide (Fig.1.1).

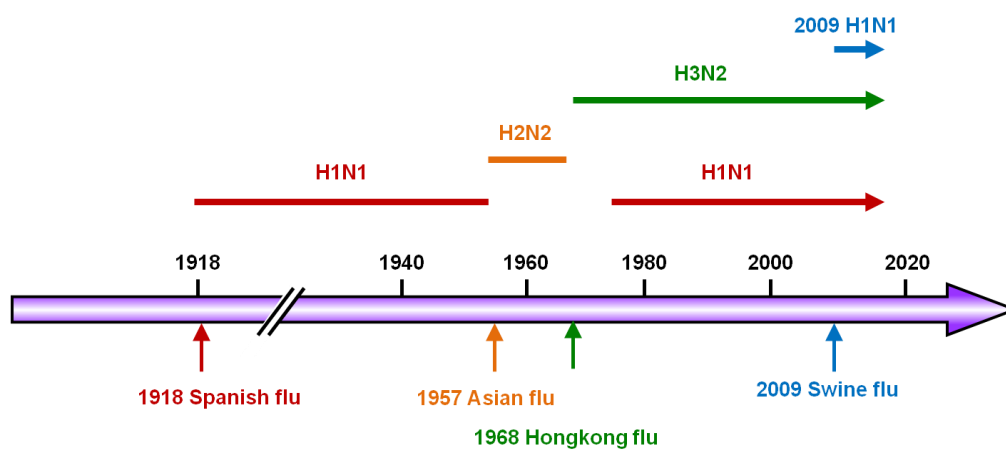


Fig. 1.1: Recorded human influenza pandemics since 1918. Figure is taken from Ahmed et al., 2007 with modification.

1918 Spanish flu (H1N1): The “Spanish flu” was the most devastating influenza pandemic, killing more than 40 million people worldwide. In 1997, the genomic RNA of the 1918 virus was recovered from preserved lung tissue from a victim of the 1918 pandemic, as influenza virus could not be isolated before 1933 (Fields, 2006; Taubenberger et al., 1997).

1957 Asian Flu (H2N2): This pandemic originated in southern China and quickly spread to Singapore in February 1957, to Hong Kong in April and reached the US by June. It killed approximately 2 million people and mostly affected younger individuals aging 5-19 years old. Genetic and biochemical analysis indicated that the 1957 pandemic virus was the result of genetic reassortment of previously circulating human H1N1 virus and avian viruses (Fields, 2006; Kilbourne, 2006).

1968 Hong Kong Flu (H3N2): The Hong Kong flu began in Southern Asia and killed at least 1 million people around the world. It was caused by an influenza A H3N2 strain, which shared the same NA with previously circulating Asian flu H2N2 viruses, but contained a different HA. The Hong Kong pandemic was not as severe as the H2N2 pandemic. It is believed that the pre-existing antibody to the NA (N2) protein in people moderated the severity of this pandemic (Field, 2006; Cox & Subbarao, 2000).

2009 Pandemic swine flu (pandemic 2009 H1N1): The 2009 pandemic swine flu is the first global influenza pandemic of the 21st century. The novel H1N1 virus was first identified in Mexico and the United States in March and early April 2009. It is a triple-reassortant swine influenza virus, possessing NA and M genes from Eurasian avian-like swine virus (H1N1), HA, NP and NS genes from classical swine virus, PB2 and PA genes from North American avian virus and the PB1 gene from human H3N2 virus (Smith et al., 2009). Shortly after its emergence, the virus spread quickly across the world and on 11th June 2009 WHO declared a phase 6 influenza pandemic alert, which is the maximum phase of a pandemic alert (WHO⁵).

1.1.4 Virus morphology, genome and proteins

Influenza viruses are pleomorphic, spherical, and sporadically also filamentous. Spherical particles are of about 80-120nm in diameter, filamentous particles can reach more than 20µm in length (Noda, 2011). The genomes of influenza A and B viruses are segmented into 8 single-stranded RNA molecules, while influenza C viruses have only 7 RNA segments.

The segmented genomes of influenza A virus encode for at least 10 major viral proteins, polymerase basic 1 (PB1), polymerase basic 2 (PB2), polymerase acid (PA), hemagglutinin (HA), nucleoprotein (NP), neuraminidase (NA), matrix protein 1 (M1), matrix protein 2 (M2), nonstructural proteins 1 (NS1) and 2 (NS2, also called nuclear export protein, NEP) (Fields, 2006) (Fig.1.2).

Two viral glycoproteins, HA and NA are inserted in the viral lipid membrane, which is derived from the host cells. HA is more abundant than NA. The HA protein is a rod-like shaped homotrimer, which mediates the binding of viral particles to the cellular glycoconjugates with terminal sialic acid (N-acetyneuraminic acid). It is also responsible for the fusion between viral and endosomal membranes. The NA protein is a mushroom-shaped homotetramer. It removes sialic acid residues from virus and

host cell receptors after infection and thereby prevents self-aggregation of progeny viruses and facilitates the release of mature virions.

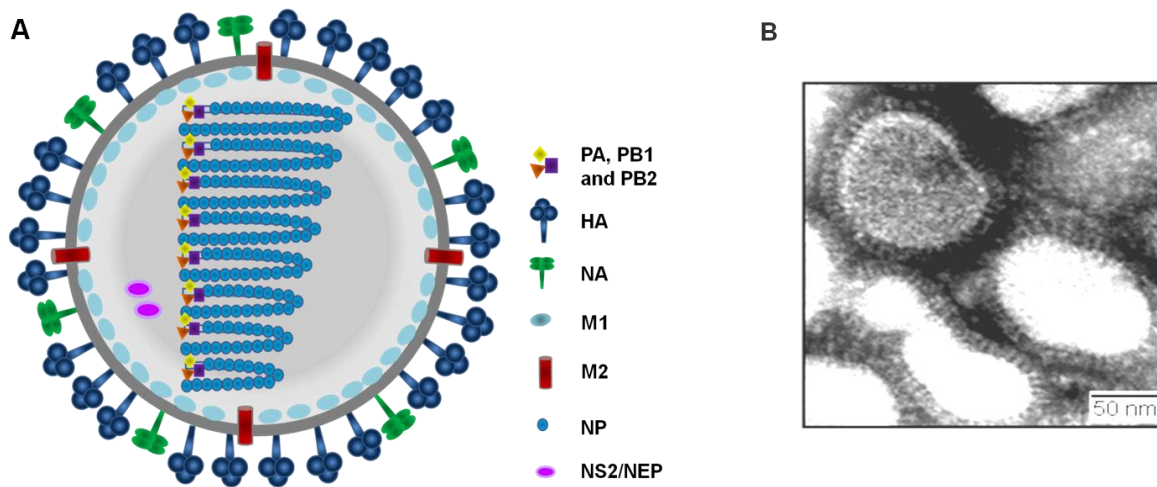


Fig. 1.2: Structure of influenza A virus. (A) Scheme of influenza A virus. Influenza A virus is an enveloped virus containing 8 segmented RNA genomes. Three membrane proteins, hemagglutinin (HA), neuraminidase (NA) and matrix protein 2 (M2) are inserted in the viral membrane which is derived from host cell membrane. The matrix protein (M1) lies beneath the viral membrane. The viral RNA genome segments are associated with nucleoprotein (NP) and three polymerase subunits (PA, PB1 and PB2), (B) EM image was kindly provided by Dr. Larissa Kolesnikova, Institute of Virology, Marburg.

The M2 protein, a homotetrameric, type III integral membrane protein, is also embedded in the viral lipid envelope. It functions as an ion channel, which allows the passage of protons into the interior of virus leading to acidification and dissociation of the matrix protein M1 and the release of viral RNP complex into the cytoplasm (Fields, 2006). The M2 protein is also involved in the virus assembly process at the plasma membrane (Lamb et al., 1985).

The M1 protein lies beneath the lipid membrane. It is the most abundant protein in viral particles. It mediates the interaction between the envelope and the viral RNPs. Within the interior of the viral particle are the segmented RNA genomes. Each RNA segment is coated with NP and a viral polymerase complex and forms rod-shaped, double-helical RNPs. The RNPs play an important role in virus transcription and replication.

Table 1.3: Functions of influenza viral proteins

RNA segment	Proteins	Functions
1	PB2	▪ Initiation of transcription by the cap-snatching mechanism and contains endonuclease activity
2	PB1	▪ Possesses the polymerase activity
2	PB1-F2	▪ A proapoptotic virulence factor
2	PB1-N40	▪ Nonessential for virus viability ▪ Regulates virus replication in particular genetic backgrounds
3	PA	▪ Contains endonuclease activities
3	PA-X	▪ Modulates the host cell response and affects the pathogenicity of the virus
3	PA-N155	▪ Possess important functions in the replication cycle of influenza A virus
3	PA-N182	
4	HA	▪ Mediates virus-binding to sialic acid receptors on host cell surface ▪ Induces the fusion of viral and endosomal membranes
5	NP	▪ Capsidation of viral RNA and binding of viral polymerase subunits to form ribonucleoprotein (RNP) complex
6	NA	▪ Cleavage of sialic acid on host cells, promoting release of progeny viruses ▪ Cleavage of sialic acid residues from virions, preventing virus aggregation
7	M1	▪ Nuclear export of vRNPs
7	M2	▪ Uncoating of virus ▪ Virus assembly and budding
7	M42	▪ Compensates for the loss of M2 in tissue culture cells and animals
8	NS1	▪ Protection against host-cell antiviral responses
8	NS2/NEP	▪ Nuclear export of vRNPs from host-cell nucleus

The NS1 protein is a homodimeric RNA-binding protein that is highly expressed in infected cells (Fields, 2006). It exhibits multiple functions during virus infection (Hale et al., 2008), including the regulation of mRNA splicing and translation (Chien et al., 1997), the nuclear export of viral mRNA (Qian et al., 1994), inhibition the host interferon (IFN)-mediated antiviral response (García-Sastre et al., 1998) and also interacts with several host factors.

The NS2/NEP protein is derived through splicing of NS1 mRNA. NS2/NEP is localized in the cell nucleus and interacts with the M1 proteins, thereby mediating the translocation of vRNPs across nuclear pores (O'Neill et al., 1998).

Since influenza virus RNA replication takes place in the host cell nucleus, it has the advantage of using the host splicing mechanism to enhance its genomic coding

capacity. In addition to the splicing products, M2, PB1-F2 and NS2/NEP, several novel influenza A virus proteins have currently been identified: PB1-N40, encoded by segment 2 mRNA (Wise et al., 2009), PA-X, PA-N155, PA-N182, three additional products of segment 3 (Jagger et al., 2012; Muramoto et al., 2013) and M42, which is generated by segment 7 (Wise et al., 2012).

1.1.5 Virus life cycle

Influenza virus infection is initiated by HA protein binding to sialic acid (SA)-containing host cell receptors. After binding, the virus is internalized by receptor-mediated endocytosis. The low pH in the endosomes induces conformational changes of cleaved HA, which exposes the HA2 fusion peptide, allowing the fusion between viral and endosomal membranes and the uncoating of viral RNPs, resulting in the release of viral RNPs into the cytoplasm. By using nuclear transport signals of NP, the viral RNPs are transported via the classical importin- α/β_1 pathway from the cytoplasm into the nucleus, where the viral transcription and replication take place (Fields, 2006; Gabriel et al., 2011). Once the vRNPs enter the nucleus, the incoming negative-stranded RNAs are transcribed to messenger RNAs (mRNAs). This transcription process is catalyzed by the influenza viral polymerase complex, which uses a short-capped primer, derived from the 5'-capped RNA fragments from host pre-mRNAs by a unique 'cap-snatching' mechanism. This primer aligns on the templates and provides a starting point for positive stranded RNA synthesis (Fig. 1.3).

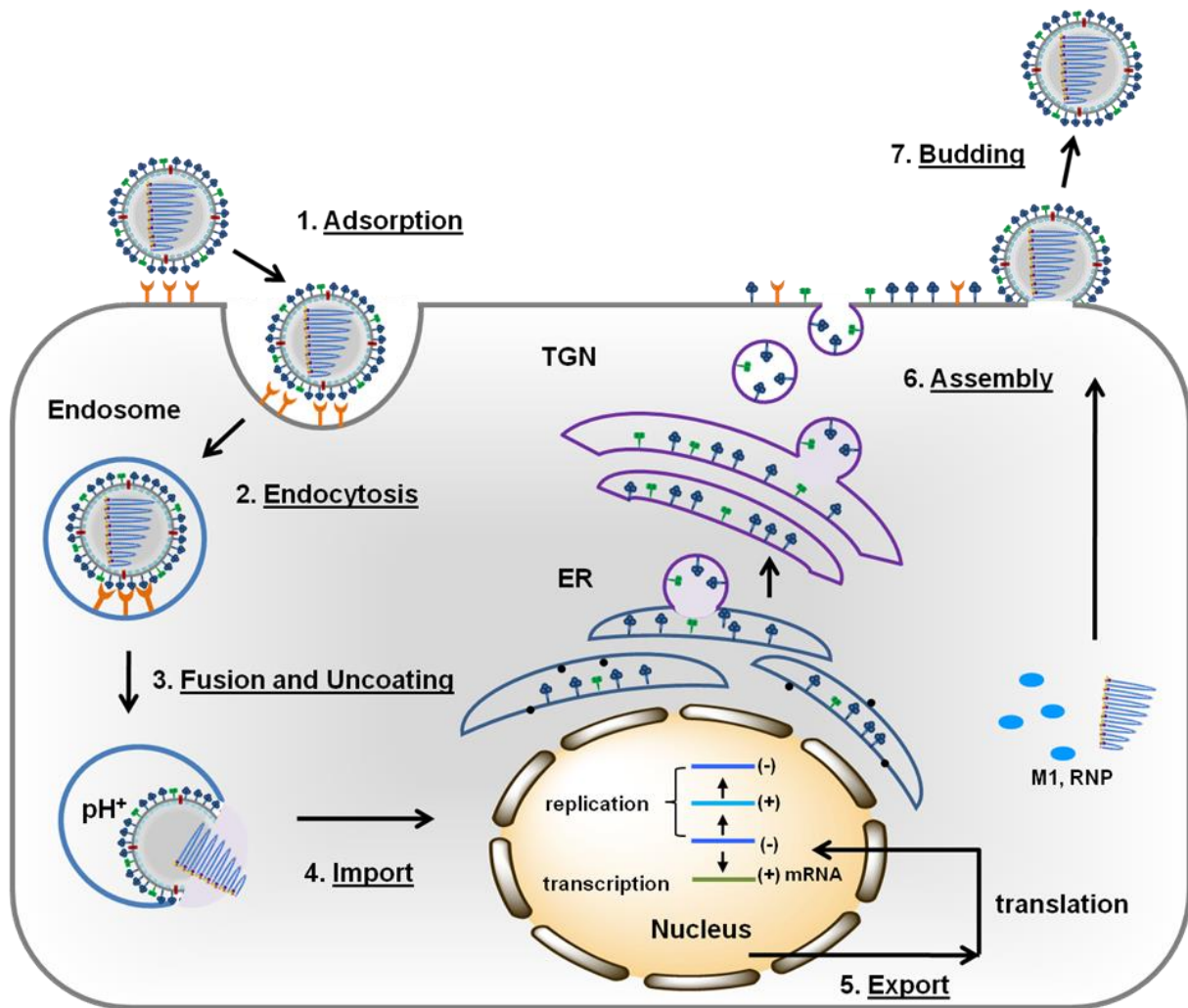


Fig. 1.3: Influenza virus life cycle. With the help of HA influenza virus binds to sialic acid-containing host receptors. After receptor-mediated endocytosis and HA-mediated fusion between viral and endosomal membrane, viral ribonucleoprotein (vRNP) complexes are released into the cytoplasm and then transported into the nucleus, where replication and transcription take place. Translation of messenger RNAs (mRNAs) occurs in the cytoplasm. Newly synthesized vRNPs are exported out of the nucleus with the help of the M1 and NS2 proteins. The assembly and budding of progeny virions occurs at the plasma membrane.

Three membrane proteins, HA, NA and M2 proteins are synthesized in the endoplasmic reticulum (ER) and then transported from the ER through *cis*-, *trans*-Golgi network (TGN) to the apical plasma membrane in polarized epithelial cells. Finally virus particles are assembled at the plasma membrane where raft lipids are enriched (Nayak et al., 2009) During transport to the cell surface, these transmembrane proteins are folded, oligomerized (HA: trimer, NA and M2: tetramer), N-glycosylated (HA and NA), palmitoylated (HA and M2) and phosphorylated (M2).

The NP, M1, NS1 and NS2/NEP proteins are transported from the cytoplasm back into the nucleus and bind to newly formed vRNAs. Replication of viral genomes occurs in a two-step process in the nucleus. The full-length complementary RNAs (cRNAs) of positive polarity are first generated and in turn are used as templates for synthesis of additional negative-sense vRNAs. With the help of M1, NEP and NP proteins newly synthesized vRNAs are exported out of the nucleus via the cellular chromosomal maintenance 1 (Crm1) also known as Exportin 1-mediated nuclear export pathway (Elton et al., 2001; Chen & Krug, 2000) and are transported to the assembly sites. The assembly and budding of progeny virions occur at the plasma membrane.

1.2 Hemagglutinin

The HA protein is the major glycoprotein of influenza virus. HA is an important determination factor of host range, cell tropism and infectivity of influenza virus (Klenk et al., 1975). It is responsible for viral attachment to the sialic acid (SA) containing host receptors. Human and classical H1N1 swine influenza viruses bind preferentially to 2,6-linked SA, whereas most avian and equine viruses exhibit a strong binding affinity for 2,3-linked SA (see 1.2.2). Cleavage of HA is a prerequisite for mediating fusion between viral and endosomal membrane (see 1.2.3). In addition, the HA protein also plays an important role in host immune responses by harboring the major antigenic sites responsible for the generation of neutralizing antibodies.

1.2.1 The structure of the hemagglutinin

The HA protein is a type I glycoprotein with an N-terminal signal peptide, a large ectodomain, a transmembrane domain and a short C-terminal cytoplasmic tail. Each HA monomer consists of a globular head unit HA1 (blue), which contains a SA binding site, and a stalk unit HA2 (red), which is responsible for the pH-triggered membrane fusion between viral and endosomal membranes (Fields, 2006; Klenk et al., 1975; Skehel & Wiley, 2002; Harrison, 2008) (Fig. 1.4 and Fig. 1.6A).

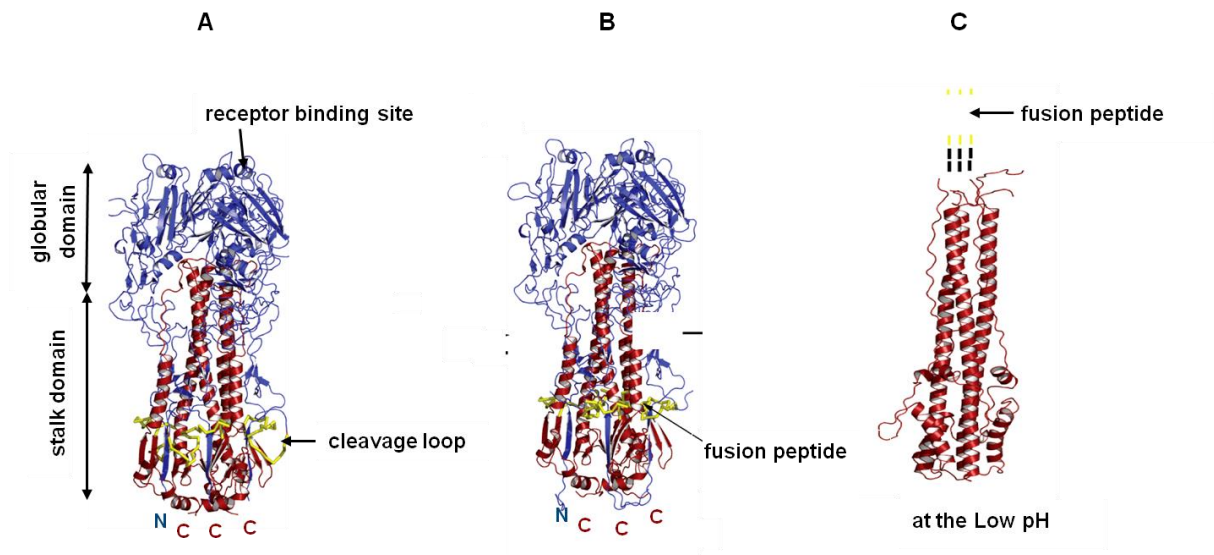


Fig. 1.4: Crystal structure of the hemagglutinin (HA). (A) Non-cleaved trimeric precursor HA0. (B) Cleaved HA trimer. (C) HA2 subunits after conformational changes at low pH. HA1 subunits are in blue, HA2 are in red. The cleavage loop and fusion peptide (yellow) are indicated by arrows. Figures were modified from Skehel & Wiley, 2002 and Galloway et al., 2013.

1.2.2 Receptor binding specificity of hemagglutinin

To initiate the infection in host cells the HA protein must bind to the SA on the host cell surface. SA is a diverse family of monosaccharides with a 9-carbon backbone. It is widely distributed on many cell types and is usually found as the terminal sugar of glycoconjugates. The carbon-2 of SA can bind in trans to the carbon-3 or carbon-6 of galactose, forming α -2,3-linked SA or α -2,6-linked SA linkages. Human and classical H1N1 swine influenza viruses bind preferentially to α -2,6-linked SA, whereas most avian and equine viruses exhibit a strong binding affinity for α -2,3-linked SA. The α -2,6-linked SA are dominant in non-ciliated cells of the human upper respiratory tract such as nasopharynx and trachea. The 2,3-linked SA are more commonly located in epithelial cells in the gastrointestinal tract of birds and on the ciliated cells and type II pneumocytes in the human respiratory tract (Matrosovich et al., 2004; Kumlin et al., 2008; Ibricevic et al., 2006; Wilks et al., 2012). The epithelial cells in pig trachea contain both α -2,3-linked SA and α -2,6-linked SA, which makes pigs susceptible to infection of both human and avian influenza viruses and thus act as 'mixing vessel' for influenza viruses (Scholtissek, 1990) (Fig. 1.5).

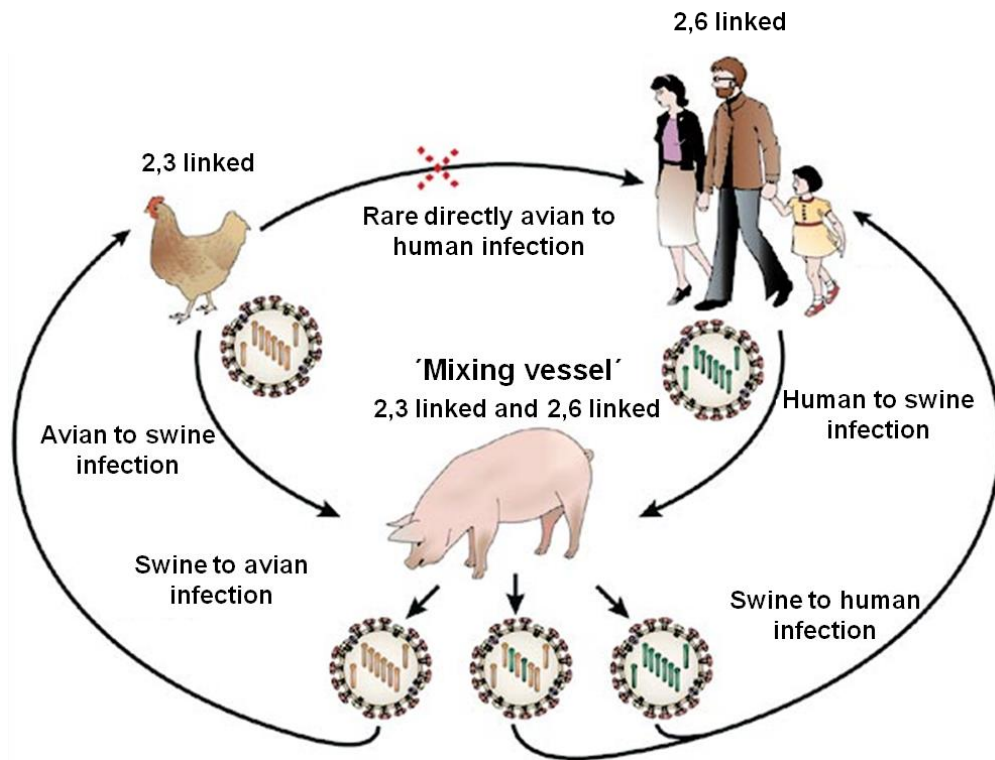


Fig. 1.5: The role of swine for influenza virus genetic reassortment. Since the trachea of swine contains both α -2,3-linked and α -2,6-linked SA, swine is considered to be an appropriate intermediate host for generation of novel influenza virus strains by genetic reassortment. Image was taken from Stevens et al., 2006 with modification.

1.2.3 Proteolytic activation of precursor hemagglutinin

Proteolytic cleavage of precursor HA0 into disulfide-linked subunits HA1 and HA2 is essential for infectivity of influenza viruses. The cleavage occurs at the C-terminus of a conserved arginine residue connecting HA1 and HA2 (Klenk et al., 1975; Lazarowitz & Choppin, 1975) (Fig.1.6).

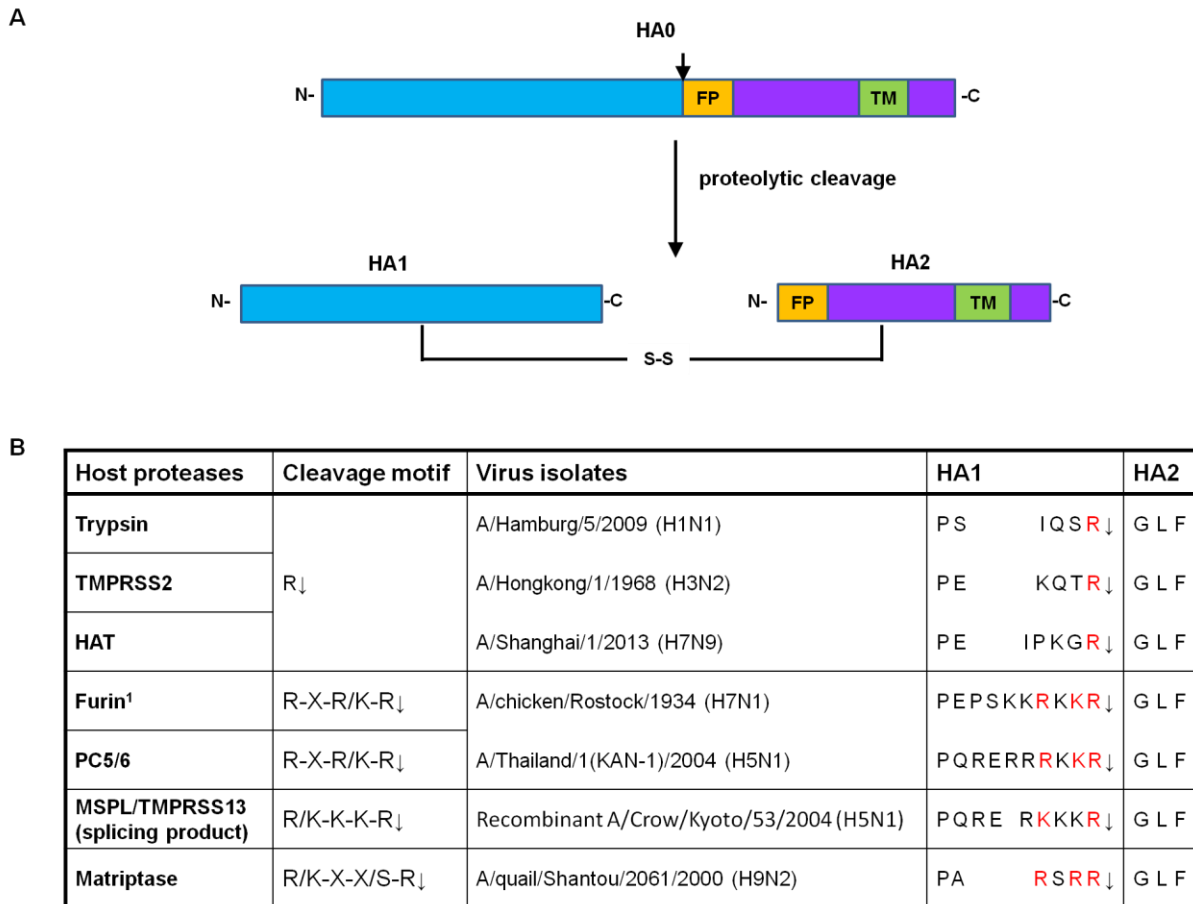


Fig. 1.6: Cleavage of hemagglutinin of influenza A viruses. The hemagglutinin precursor (HA0) must be cleaved by the host proteases to initiate the infection in the host. (A) Schematic images of the HA0 precursor and its cleaved form consisting of the disulphide-linked subunits HA1 and HA2. The HA1 subunit is shown in blue and the HA2 subunit in purple, the fusion peptide (FP) in orange and transmembrane domain (TM) in green. (B) HA-activating host cell proteases and their cleavage specificity. Table is taken from Böttcher-Friebertshäuser et al., 2013 with modifications. ¹Details about furin see 1.3.1.

1.2.3.1 Monobasic cleavage site

Most influenza viruses, including LPAIV and mammalian influenza viruses contain a single arginine (R) or in rare cases a lysine (K) at the cleavage site (Garten & Klenk, 2008). Previously, cleavage of HA with monobasic cleavage site has been thought to occur extracellularly when viruses are released from the infected cells. Trypsin (Klenk et al., 1975) or trypsin-like proteases such as plasmin (Lazarowitz & Choppin, 1975), the factor Xa-like protease (Gotoh et al., 1990), mini-plasmin (Murakami et al., 2001), tryptase Clara (Kido et al., 1992) and tryptase TP30 (Sato et al., 2003) have been identified for HA0 activation *in vitro*. However, a study by Boycott *et al.* indicated that

an endosomal protease might be responsible for the proteolytic activation of influenza A H1N1 in MDBK cells (Boycott et al., 1994) and the study by Zhirnov *et al.* showed the intracellular activation of influenza viruses in human intestinal Caco-2 cells (Zhirnov et al., 2003). In 2006, two serine proteases: transmembrane serine protease 2 (TMPRSS2) and HAT (human airway trypsin-like protease) in human airway epithelium (Böttcher et al., 2006; Garten & Klenk, 2008) were identified for cleavage of HA with a monobasic cleavage motif. Cleavage of newly synthesized HA0 by TMPRSS2 occurs intracellularly during the transport to the plasma membrane, whereas HAT activates HA0 of incoming viruses during attachment and entry into the cell. It also activates the progeny viruses during assembly and budding at the plasma membrane (Böttcher-Friebertshäuser et al., 2010).

1.2.3.2 Multibasic cleavage site

In contrast to LPAIV, the HA protein of HPAIV contains a multibasic amino acids motif at the cleavage site. HA of most HPAIV contains the consensus sequences R-X-K/R-R (R= arginine, L=lysine, X = any amino acid) at the cleavage site (Fig. 1.6). This cleavage motif is recognized by subtilisin-like endoproteases, furin and PC5/6, which are ubiquitously expressed in human tissues (see 1.3) (Stieneke-Gröber et al., 1992; Horimoto et al., 1994, Garten & Klenk, 2008). However, there are exceptions. LPAIV influenza virus subtype H9N2 isolated in America, Europe, and Africa contains monobasic cleavage site, whereas many isolates from Asia and the Middle East possess the multibasic cleavage sites R-S-S-R or R-S-R-R, which are proteolytically activated by human protease TMPRSS2, HAT and matriptase. Sequences analysis showed that these multibasic motifs were formed by amino acids substitution rather than by insertion and therefore are not accessible to furin (Baron et al., 2013). Recently, the serine protease TMPRSS13 and its splicing product MSPL were shown to cleave HA with the multibasic cleavage site -R/K-K-K-R- in the absence of calcium, whereas cleavage by furin is strictly calcium-dependent (Okumura et al., 2010).

1.3 Proprotein convertases

Proprotein convertases (PCs) are calcium-dependent eukaryotic subtilisin-like endoproteases. They are responsible for activating many biologically inactive precursor proteins by limited endoproteolysis. There are nine identified members in the PCs family, PC1/3, PC2, PC4, PC5/6, PC7, furin (Fuller et al., 1989; Thomas, 2002; Seidah & Prat, 2012), paired basic amino acid cleaving enzyme 4 (PACE4) (Kiefer et

al., 1991), subtilisin kexin isozyme-1 (SKI-1)/site-1 protease (S1P) (Espenshade et al., 1999), and proprotein convertase subtilisin/kexin type 9 (PCSK9) (Seidah et al., 2002). They commonly contain a prodomain, a conserved catalytic domain, a P domain and a variable C-terminal domain. In particular, a catalytic triad, consisting of serine, histidine and aspartic acid, is present at corresponding positions in the catalytic domain of all members (Nakayama, 1997; Chrétien et al., 2008). The first seven members, PC1/3, PC2, PC4, PC5/6, PC7, furin, PACE4, are structurally closer to kexin. They cleave precursors at specific single or paired basic amino acids within the motif (K/R)-X_n-(K/R)↓, where the arrow indicates cleavage site, X_n corresponds to a 0-, 2-, 4- or 6-amino-acid spacer, and position 1 of the cleavage site is preferred to be an arginine. The other two members SKI-1 and PCSK9 cleave the motifs at non-basic residues. SKI-1 is a pyrrolisin-like serine protease that cleaves precursors within the motif R-X-(L/V/I)-X↓, where X can be any amino acid except for cysteine and proline. PCSK9 is a protease K-like protease that cleaves at VFAQ¹⁵²↓ (Seidah & Chrétien, 1999; Seidah & Prat, 2012).

1.3.1 Furin

The prototypic eukaryotic subtilase furin is encoded by gene *fur* (fes upstream region), which is in the upstream region of the *fes* oncogene (Roebroek et al., 1986). Furin is a calcium-dependent, human prohormone-processing endoprotease, which shares 50% homology with the catalytic domain of the yeast prohormone convertase Kex2 (Fuller et al., 1989).

Furin is a type I transmembrane protein and exists in all tissues and cells that have been examined thus far (Seidah et al., 1994). It is mainly localized in the TGN in a steady state. It also can be transported through the constitutive secretory pathway to the plasma membrane, where it can be shed or recycled back to the TGN (Schäfer et al., 1995; Thomas, 2002). Furin is first synthesized as a pro-furin molecule and translocated across the membrane due to its signal peptide into the endoplasmic reticulum (ER) lumen (Fig.1.7). After the loss of the signal peptide in the ER, furin undergoes a pH-dependent conformational change, resulting in a rapid autocatalytic cleavage after R107 of its N-terminal prodomain. This step is a prerequisite for furin to leave the ER and enter vesicles of the exocytic pathway (Leduc et al., 1992; Creemers et al., 1995). It must be noted that after its autocatalytic cleavage, the prodomain remains associated with the mature furin and acts as a chaperone inhibitor, which

retains furin in an inactive state. After translocation into a more acidic environment, the TGN, furin undertakes a slower internal secondary autocatalytic cleavage between R75 and S76 in the middle of its prodomain, which is not the consensus cleavage site of furin (VTKR↓SLSP⁷⁹). And this cleavage results in the release of its prodomain and generates an enzymatic active form of furin, which is membrane anchored (Nakayama, 1997; Thomas, 2002).

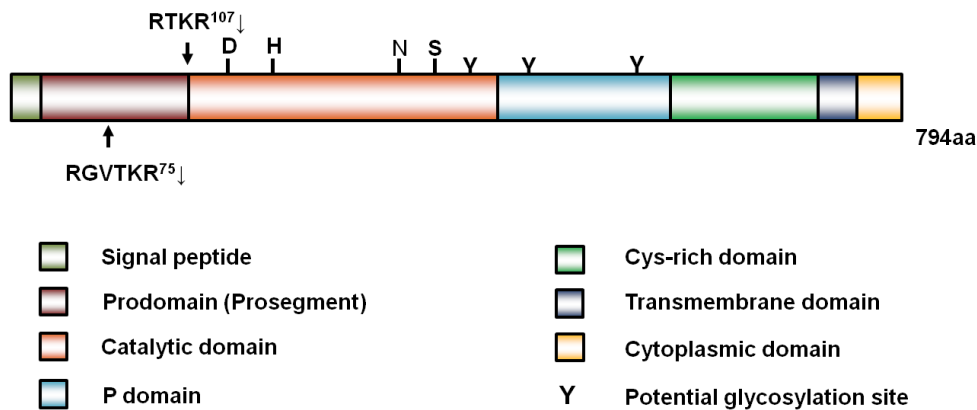


Fig. 1.7: Scheme of the furin structure. Various domains are presented in different colored bars and N-glycosylation sites are indicated by Y. The catalytic triad, aspartic acid (D153), histidine (H194), and serine (S368) are labeled by bold D, H and S, respectively. The asparagine (N295), which is the part of the oxyanion, is labelled by N. It is conserved in all members of the PCs family, except for the PC2, where it is replaced by aspartic acid. The primary autocatalytic motif RTKR and secondary autocatalytic motif RGVTKR are highlighted. The arrows indicate the cleavage sites. Figure is modified from Seidah & Prat, 2012.

Furin recognizes substrate with a consensus sequence Arg-X-Arg/Lys-Arg↓ (R-X-R/K-R, X is any amino acid) and efficiently cleaves at the C-terminal arginine residue of this motif. Furin has a broad substrate spectrum and cleaves various important cellular protein precursors, such as β -nerve growth factor (β -NGF) (Bresnahan et al., 1990) and insulin-like growth factor I (IGF-I) (Duguay et al., 1997). It is also responsible for proteolytic activation of glycoproteins or fusion proteins of enveloped viruses and bacterial toxins (Fig. 1.8 and Table 5.2). Moreover, furin is expressed in many human cancer cells, such as non-small cell lung carcinomas, head and neck squamous-cell carcinomas and glioblastomas (Thomas, 2002; Seidah & Prat, 2012).

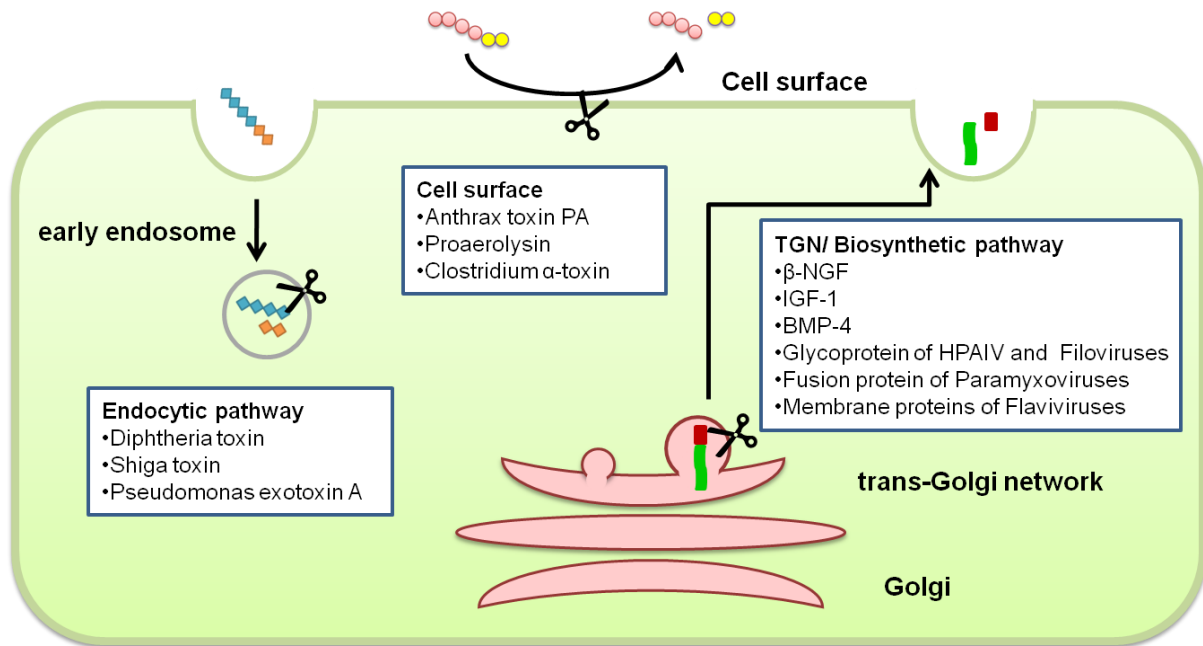


Fig. 1.8: Sites of substrates activation by furin. Precursors of β -nerve growth factor (β -NGF), bone morphogenetic protein-4 (BMP-4), the insulin-like growth factor 1 (IGF-1), glycoproteins of highly pathogenic avian influenza virus (HPAIV), filoviruses, including Ebola virus (EBOV) and Marburg virus (MBGV), membrane protein of flaviviruses, including Dengue virus (DENV) and West Nile virus (WNV) and fusion protein of paramyxoviruses, including measles virus (MV), Newcastle disease virus (NDV) and respiratory syncytial virus (RSV) are all cleaved in the TGN/biosynthetic pathway. Substrates such as Anthrax toxin protective antigen (PA), proaerolysin and *Clostridium* α -toxin are cleaved by furin at the cell surface. In mildly acidic early endosomes, furin cleaves substrates, such as *Diphtheria* toxin, Shiga toxin and *Pseudomonas* exotoxin A. Figure is taken from Gary Thomas, 2000 and Kornelia Harges, Institute of Pharmaceutical Chemistry, Philipps University Marburg, and modified.

1.4 Prevention and treatment of influenza

1.4.1 Vaccination

Vaccination is one of the most effective ways to control seasonal epidemics and pandemics of influenza. Since the first influenza vaccines became available in the late 1940s, many efforts have been made to develop safer and more efficacious influenza vaccines. Influenza continuously undergoes antigenic drift and shift in HA and NA antigens (see 1.1.3.1), once antigenically novel strains appear, vaccines containing formerly prevalent strains cannot provide protection against the novel strains. Therefore, the composition of the influenza vaccine must be changed every year based on recommendations made by the WHO.

There are two basic types of influenza vaccines available. One is the inactivated influenza vaccine that was first developed in 1940s and is administered via intramuscular injection. It is composed of either whole virus or viral fractions, of which the virions are disrupted or split with detergents and then the soluble viral envelope proteins are purified. Inactivated vaccine is recommended for children over 6 months of age and people with chronic medical conditions as well as pregnant women (CDC¹). The live attenuated influenza vaccine was approved for use in USA in 2003. It is administered via nasal spray. In comparison with the inactivated vaccine, the live attenuated vaccine is easier to administer and more effective in young children (Ambrose et al., 2008). However, attenuated viruses are still living viruses that are able to replicate *in vivo*. Thus, the live attenuated vaccine may cause mild symptoms such as rhinorrhea, nasal congestion, fever, or sore throat. Therefore, it is recommended only for people aged 2-49 years, but is not recommended for pregnant women, for people who have a weakened immune system, or for people with certain chronic diseases (CDC¹).

Both inactivated and live attenuated vaccines are produced from embryonated egg or cell cultures, containing three strains of influenza viruses: influenza A (H3N2) virus, influenza A (H1N1) virus and one influenza B viruses. For the 2013-2014 flu season quadrivalent vaccine, containing two influenza A strains and two influenza B strains is available and is given as a nasal spray (CDC¹).

Although vaccine is the primary method for influenza prophylaxis, it has several disadvantages. Vaccination cannot provide complete protection, as the efficacy of the influenza vaccine is related to the age immune competence of the individual receiving it and also depends on the match of antigenicity between the vaccine and circulating strains. Importantly, it cannot be timely produced to protect people from infection of a new pandemic influenza, because current technology requires at least six months to develop sufficient amounts of vaccine to meet the worldwide need (Tosh et al., 2010).

1.4.2 Approved antiviral agents

Anti-influenza drugs play an indispensable role for non-vaccinated people and for certain high-risk populations who are not recommended for vaccination, including the very young or the very old, immunocompromised individuals and people with cardiac or pulmonary disease. Currently, two classes of anti-influenza drugs are available: adamantane derivatives and neuraminidase inhibitors, which target the functional

domains of viral proteins and thus provide an inhibitory effect against different strains of influenza A viruses.

1.4.2.1 Adamantane derivatives

The adamantane derivatives, amantadine (1-adamantanamine hydrochloride) and rimantadine (alpha-methyl-1-adamantane-methylaminehydrochloride) have been long used for influenza A virus infection treatment (Fig. 1.9). Amantadine was first approved for treatment of Asian influenza virus (H2N2) infection in 1966, and in 1976 was approved for treatment of influenza A virus infection (De Clercq, 2006). Adamantanes have antiviral properties against all subtypes of influenza A virus, but not influenza B or C virus, because neither possesses M2 proteins. They inhibit virus replication by blocking the flow of protons from the acidified endosome into the interior of the virus through the M2 ion channel, and thus prevent dissociation of RNPs from M1 proteins (uncoating). However, the worldwide rapid emergence of fully pathogenic and transmissible adamantane-resistant viruses has discouraged the use of amantadine and its analogs. Up to approximately 30% patients may shed resistant viruses when treated with amantadine or rimantadine (Shiraishi et al., 2003). And the work of Suzuki *et al.* showed that a sensitive virus became resistant when passaged more than three times in the presence of amantadine (Suzuki et al., 2003). Therefore, since 2010 only neuraminidase inhibitors are recommended by WHO for treatment of influenza A and B virus infection.

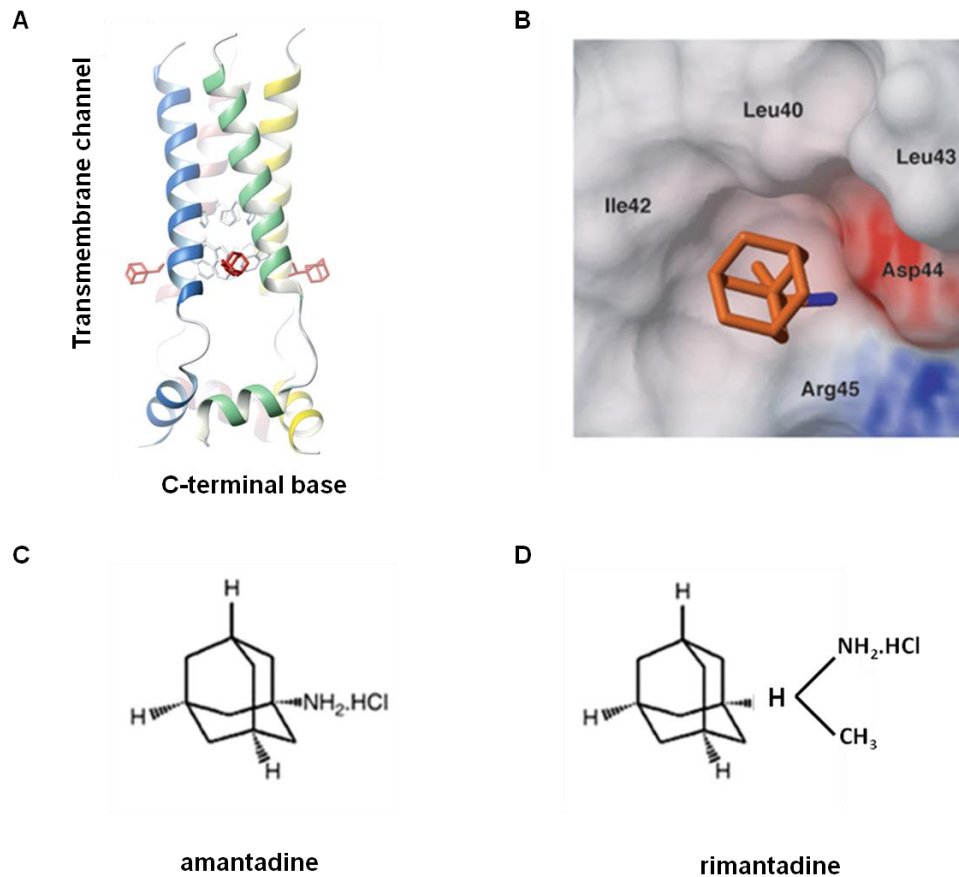


Fig. 1.9: M2 protein inhibitors. (A) A ribbon representation of the proposed transmembrane domain of M2 protein. The rimantadine is colored in red. (B) Surface representation of the rimantadine-binding pocket in M2 protein. (C) amantadine and (B) rimantadine are two M2 protein inhibitors, which can block the proton channel protein M2. Figure A and B are taken from Schnell & Chou, 2008. Figure C and D are taken from De Clercq, 2006.

1.4.2.2 Neuraminidase inhibitors

Neuraminidase inhibitors are structurally similar to sialic acid. They block the neuraminidase activity by competitively binding to the enzymatic active site and thereby prevent the release of progeny virions and the further spread of virus throughout the upper respiratory tract. Currently, two neuraminidase inhibitors, oseltamivir (Tamiflu; ethyl(3R,4R,5S)-4-acetamido-5-amino-3-(1-ethylpropoxy)-1-cyclohexene-1-carboxylate) and zanamivir (Relenza; 4-guanidino-Neu5Ac2en), have been licensed for therapeutic and prophylactic treatment against both influenza A and influenza B viruses since 1999 (Fig. 1.10). Oseltamivir is a prodrug, which can be administered orally and it is rapidly converted into the active form, oseltamivir

carboxylate, by hepatic esterases. Zanamivir is administered by oral inhalation as a dry powder (De Clercq, 2006).

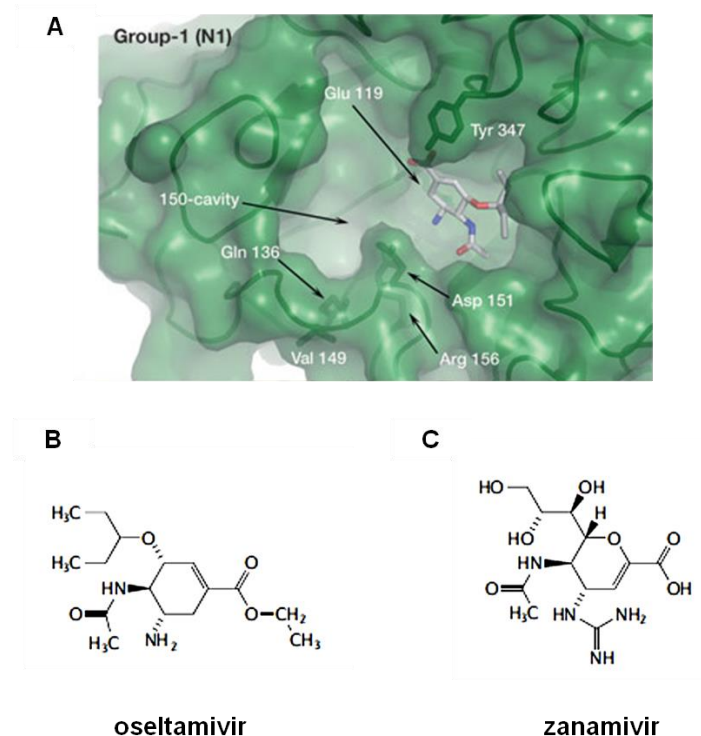


Fig. 1.10: Neuraminidase inhibitors. (A) The neuraminidase of group N1 is shown in surface representation. Oseltamivir is shown in sticks. Figure A is taken from Russell et al., 2006. Figure B and C are taken from De Clercq, 2006.

Neuraminidase inhibitor-resistant viruses have been isolated in neuraminidase inhibitor treated patients and through serial passage in the presence of a neuraminidase inhibitor in *in vitro* studies (McKimm-Breschkin, 2000). Oseltamivir-resistant viruses were detected at a very low frequency in comparison with amantadine-resistant viruses. However, since 2007 they have spread worldwide. Almost all the tested A/Brisbane/59/2007-like H1N1 influenza strains that circulated worldwide in the influenza season 2008-2009 contained the H275Y NA mutation that conferred the resistance to oseltamivir. And 1% tested pandemic 2009 H1N1 viruses were resistant to oseltamivir (CDC²).

1.4.3 Other antiviral agents

Ribavirin has long been known as a broad-spectrum antiviral agent. Aerosolized ribavirin has been approved for treatment of RSV infection. Oral ribavirin is also used

in combination with peginterferon- α for treatment of chronic hepatitis C virus (HCV) infection. The intravenous form of ribavirin has been registered for the treatment of haemorrhagic fever with renal syndrome (HFRS). The main target of ribavirin is inosine 5'-monophosphate (IMP) dehydrogenase, a cellular enzyme which is responsible for the conversion of IMP to xanthosine 5'-monophosphate, a key enzyme involved in the biosynthesis of guanosine triphosphate (GTP) and viral RNA synthesis (Fig. S1 in supplementary) (De Clercq, 2006). A triple combination of amantadine, oseltamivir and ribavirin has been reported to have synergistic activity against influenza A viruses in vitro and in vivo, including against amantadine- and oseltamivir-resistant viruses (Nguyen et al., 2009; 2010).

Global circulation of drug-resistant influenza variants is the major challenge of present antiviral therapeutics. Based on the pre-existing antiviral drugs, new antiviral targets and strategies need to be exploited for prevention and control of influenza. Several new anti-influenza agents have just entered or are expected to enter clinical development. Some target the virus, including novel neuraminidase inhibitors, laninamivir (Ikematsu & Kawai, 2011) and peramivir (Shetty & Peek, 2012) as well as RNA polymerase inhibitor (Favipiravir, T-705) (Furuta et al., 2002). Others target host cellular mechanisms, such as the sialidase fusion protein DAS181 (Malakhov et al., 2006; Moss et al., 2012), which can remove the influenza virus receptor, sialic acids from the airway epithelium. Moreover, furin inhibitor is also considered to be a promising antiviral agent (Watanabe et al., 1995; Hallenberger et al., 1992; Jean et al., 2000; Seidah & Prat, 2012; Becker et al., 2010, 2012) (Fig.1.12).

1.4.3.1 Proprotein convertase inhibitors

1.4.3.1.1 Furin inhibitors

The first furin inhibitors based on peptidyl chloromethyl ketones were reported in 1989 (Garten et al., 1989). These inhibitors, such as dec-RVKR-cmk (Stieneke-Gröber et al., 1992; Garten et al., 1994) possess a peptidyl segment and a reactive head. The peptidyl part is responsible for targeting the enzyme, and the reactive group irreversibly labels the enzyme by forming a covalent bond. And in 1992 it was the first time suggested as an antiviral therapeutic agent (Hallenberger et al., 1992). Since then, many efforts have been made to develop more efficient and potent furin inhibitors. Several peptide inhibitors were developed either from the furin recognition sequence (Anglikier, 1996) or from the furin prodomain (Basak & Lazure, 2003). Another potent

furin inhibitor is a polyarginine compound, nona-D-arginine. It inhibits furin with a K_i value of 1.3nM (Cameron et al., 2000; Kacprzak et al., 2004). However, its toxicity and poor ability to cross the cell membrane may cause big problems for its therapeutic use *in vivo* (Cameron et al., 2000). Recently, several highly potent substrate analogues, peptidomimetic furin inhibitors with the K_i values in nanomolar range were synthesized. They contain a furin recognition motif and a C-terminal 4-amidinobenzylamide mimicking a decarboxylated arginine (Fig. 1.11) (Becker et al., 2010, 2012). These inhibitors were examined *in vitro* and some showed promising inhibitory efficacies against the infection of HPAIV subtype H7N1. Another peptide based furin inhibitor, AC-[aza β^3 R]ARRRKK[aza β^3 R]T-NH₂ with the K_i value of 33nM showed potent inhibitory activity against the activation of HA of HPAIV and Shiga toxin (Gagnon et al., 2014). In addition to these peptide based inhibitors, several other nonpeptide inhibitors were designed. The first reported nonpeptic compounds are neoandrographolide, a diterpene lactone extracted from the medicinally active plant *Andrographis paniculata*, and its succinoyl ester derivatives (Basak et al., 1999). However, to date most nonpeptide furin inhibitors exhibit only moderate activity against furin in the micromolar to millimolar range. An exception is a series of small molecules. They are the guanidinylated aryl 2,5-dideoxystreptamine derivatives (GADDs), which were derived from 2,5-dideoxystreptamine. One of these derivatives inhibits furin with a K_i value of 6nM (Jiao et al., 2006). Some macromolecular compounds also show excellent potency against furin, which include naturally occurring human serine protease inhibitor 8 (PI8 or Serpin B8) (Dahlen et al., 1998) and genetically modified variants of α 1-antitrypsin (α 1-PDX) (Jean et al., 1999), turkey ovomucoid third domain (Bontemps et al., 2007; Lu et al., 1993) and eglin C (Bontemps et al., 2007; Liu et al., 2004) (Table 5.1).

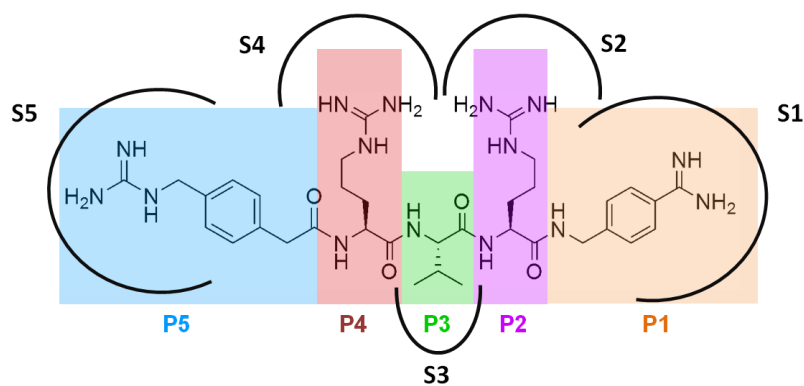


Fig. 1.11: Structure of furin inhibitor MI-701. MI-701 (4-guanidinomethyl-phenylacetyl-Arg-Val-Arg-4-amidinobenzylamide, 4-Guame-Phac-RVR-Amba) is a substrate analogue inhibitor, consisting of residues P1, P2, P3, P4 and P5, which bind in the complementary furin subsites (S1 to S5). Figure is taken from the PhD thesis of Kornelia Hardes, Institute of Pharmaceutical Chemistry, Philipps University Marburg, with modification.

1.4.4 Combination therapy

Combination therapies for treatment with human immunodeficiency virus (HIV), chronic hepatitis C virus (HCV), influenza virus and *Mycobacterium tuberculosis* infections have shown greater therapeutic efficacy than monotherapy (Langebeek et al., 2014; Maruyama et al., 2013; Govorkova & Webster, 2010; Mitchison, 2012). Benefits of combination therapy over monotherapy include the possibility of reducing emergence of drug-resistance and enhanced inhibitory efficacy with low concentration of each drug, which is thereby dose-sparing and reduces dose-related drug toxicity and side effects (Govorkova & Webster, 2010; Hayden, 2013).

1.5 Aim of the study

The aim of this study is to evaluate the inhibitory efficacy of furin inhibitors for the treatment of highly pathogenic influenza virus (HPAIV) infection. The most efficacious furin inhibitor was thereafter combined with one or two antiviral drugs to achieve enhanced therapeutic effects against HPAIV infection.

A series of peptidomimetic furin inhibitors were screened for their cytotoxicity at different concentrations. Compounds that were toxic to the cells at the given concentrations were not included in this study. The inhibitory effects of furin inhibitors on proteolytic activation of HA, on virus spread from infected cells to their neighboring cells, and on multicycle replication were examined. Moreover, the most efficacious furin inhibitor was combined with oseltamivir and ribavirin for treatment of infection caused by HPAIVs A/chicken/fowl plaque virus/Rostock/1934 (H7N1) and A/Thailand/1(KAN-1)/2004 (H5N1). The effect of the furin inhibitor on the development of oseltamivir-resistance has also been analyzed.

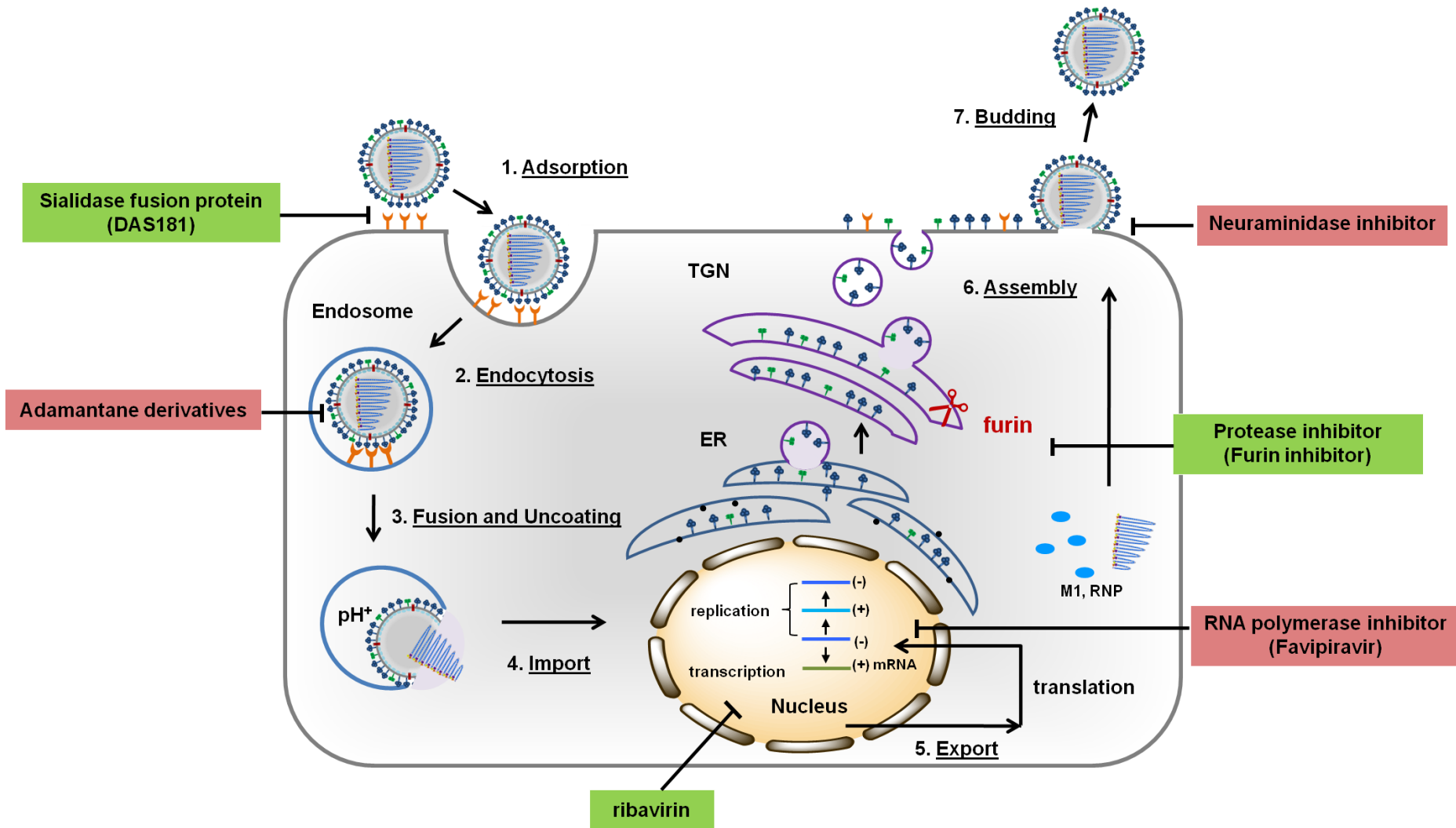


Fig. 1.12: Antiviral agents target different steps during influenza virus replication. Inhibitors in red boxes target viral protein. Inhibitors in green boxes target host factors.

2. Materials

2.1 Chemicals

Acetic acid	Riedel-de-Haën, Seelze
Acrylamide Rotiphorese Gel 30	Roth, Karlsruhe
ε-Aminocaproic acid	Merck Eurolab, Darmstadt
Ammonium peroxodisulphate (APS)	Biorad, Richmond (USA)
Agarose, Ultrapure	Invitrogen, Darmstadt
Avicel	FMC BioPolymer
Bovine serumalbumin (BSA)	Serva, Heidelberg
Bromophenol blue	Serva, Heidelberg
Dimethyl sulfoxide (DMSO)	Merck Eurolab, Darmstadt
Disodium hydrogen phosphate (Na ₂ HPO ₄)	Merck Eurolab, Darmstadt
dNTP mix	Stratagene, Heidelberg
Ethanol	Riedel-de-Haën, Seelze
Ethidium bromide	Roche, Mannheim
Ethylenediaminetetra acetic acid (EDTA)	Merck Eurolab, Darmstadt
Fetal calf serum (FCS)	Gibco, Karlsruhe
Formaldehyde	BDH, England
L-Glutamine 200mM (100x)	Gibco, Karlsruhe
Glycerin	Roth, Karlsruhe
Glycine	Roth, Karlsruhe
HEPES buffer (1M)	Gibco, Karlsruhe
Horse serum	Sigma-Aldrich, Steinheim
Hydrochloric acid (HCl)	Merck Eurolab, Darmstadt
Isopropanol	Merck Eurolab, Darmstadt
Magnesium chloride (MgCl ₂ x 6 H ₂ O)	Merck Eurolab, Darmstadt
β-Mercaptoethanol	Sigma-Aldrich, Steinheim
Methanol (MeOH)	Riedel-de-Haën, Seelze
4-Methylumbelliferone sodium salt (4-MUSS)	Sigma-Aldrich, Steinheim
MUNANA = 2'-(4-Methylumbelliferyl)-α-D-N-acetylneuraminic acid	Sigma-Aldrich, Steinheim
Milk powder	Töpfer, Dietmannsried

Monopotassium dihydrogen phosphate (KH_2PO_4)	Merck Eurolab, Darmstadt
MTT = (3-(4,5-dimethylthiazol-2-yl)-2,5-diphenyltetrazolium bromide)	Sigma-Aldrich, Steinheim
Neutral red	Merck Eurolab, Darmstadt
Oseltamivir	F. Hoffmann-La Roche, Nutley, USA
Paraformaldehyde (PFA)	Sigma-Aldrich, Steinheim
Penicillin/Streptomycin 5000 IU/ml	Gibco, Karlsruhe
Potassium chloride (KCl)	Merck Eurolab, Darmstadt
β -Propiolactone	Sigma-Aldrich, Deisenhofen
Ribavirin	Sigma-Aldrich, Steinheim
Seakem LE agarose	Rockland, Maine USA
Sodium acetate	Merck Eurolab, Darmstadt
Sodium carbonate (Na_2CO_3)	Merck Eurolab, Darmstadt
Sodium chloride (NaCl)	Merck Eurolab, Darmstadt
Sodium dodecyl sulphate (SDS)	Merck Eurolab, Darmstadt
Sodium hydroxide (NaOH)	Merck Eurolab, Darmstadt
Sucrose	Merck Eurolab, Darmstadt
N, N, N', N' -Tetramethylethylenediamine (TEMED)	Biorad, Richmond (USA)
Tris(hydroxymethyl)aminomethane (Tris)	Roth, Karlsruhe
Triton X-100	Serva, Heidelberg
True Blue peroxidase substrate	KPL Protein reasearch Products, Gaithersburg, USA
Tween-20	Serva, Heidelberg

2.2 Consumed materials

Cell culture microplates (6-, 24- und 96-well)	Greiner, Nürtingen
Cell scraper	Greiner, Nürtingen
Microreaction tubes, 1.5ml and 2ml	Eppendorf, Hamburg
Microreaction tubes (1.5ml, 2ml)	Eppendorf, Hamburg
Microreaction tubes 1.5ml for ultracentrifuge	Beckman, USA
Nitrocellulose transfermembrane	Whatman, New Jersey (USA)
Parafilm	Pechiney Plastic Packaging, Neenah (USA)
PCR tubes, 0.2ml	Biozym, Hess. Oldendorf
Polypropylen reaction flask (15ml, 50ml)	Greiner, Nürtingen

Scalpel	Feather BLDG, Osaka, Japan
Sterile needle (0.55 x 25mm)	Becton Dickinson, Fraga (ESP)
Syringe (1ml)	Becton Dickinson, Fraga (ESP)
Tissue Culture Flasks (25cm ² , 75cm ²)	Greiner, Nürtingen

2.3 Instruments

Centrifuge micro 22R	Hettich
Centrifuge 5417R	Eppendorf
Electrophoresis equipment	Keutz, Reiskirchen
Epoch Microplate Spectrophotometer	Biotek, USA
Epoch Microplate Fluorescence photometer	Biotek, USA
Illuminated magnifier	Eschenbach, Nürnberg
Incubator for cell cultures	Thermo, USA
L7-55 Ultracentrifuge	Beckman, USA
Multifuge 3 S-R	Thermo Fisher Scientific, Langenselbold
Nanodrop ND-100	Thermo Fisher Scientific, Langenselbold
Peristaltic pump P-3	Pharmacia fine chemicals
Odyssey™ <i>Infrared Imaging System</i> LI-COR®	Biosciences, Bad Homburg
Optima L-100K Ultracentrifuge	Beckman, USA
Sonifier Branson 102 C	Branson, Danbury, USA
UV/Visible Spectrophotometers (in BSL3)	Biochrom, England

2.4 Kits

One-step RT-PCR kit	Qiagen, Hilden
QIAquick Gel Extraction kit	Qiagen, Hilden
QIAquick PCR Purification kit	Qiagen, Hilden
RNeasy Mini kit	Qiagen, Hilden
QIAamp Viral RNA Mini kit	Qiagen, Hilden

2.5 Protein markers

Page Ruler Prestained Protein Ladder	MBI-Fermentas, St.Leon-Rot
DNA-marker GeneRuler™ 1kb DNA ladder	MBI-Fermentas, St.Leon-Rot

2.6 Antibodies

2.6.1 Primary antibodies

Anti-FPV serum from rabbit (10.03.92)	provided by Prof. Dr. Wolfgang Garten Institute of Virology, Philipps University Marburg, Germany
Anti-H5N1 serum from rabbit (04.05.88)	provided by Prof. Dr. Wolfgang Garten Institute of Virology, Philipps University Marburg
Anti-VSV serum from rabbit	provided by Prof. Dr. Georg Herrler Institute of Virology, University of Veterinary Medicine, Hannover

2.6.2 Secondary antibodies

Anti-rabbit serum (goat), IRDye 800	Rockland, Gilbertsville, USA
Anti-mouse serum (donkey) Alexa Fluor 680	Molecular Probes, Karlsruhe
Anti-tubulin (mouse)	Sigma-Aldrich, Deisenhofen
Anti-rabbit from sheep, HRP	DAKO, Dänemark
Anti-mouse from sheep, HRP	DAKO, Dänemark

2.7 Enzymes

Phusion High-Fidelity DNA polymerase	Thermo, Scientific
Reverse transcriptase (RevertAid H Minus)	Fermentas, St.Leon-Rot
RiboLock RNase inhibitor (Ribolock)	Fermentas, St.Leon-Rot
Trypsin-TPCK	Sigma-Aldrich, Deisenhofen

2.8 Primers

Primer (oligonucleotides) was synthesized by Eurofins MWG Operon (Ebersberg).

Primers for RT-PCR and sequencing (5'-3')

NA uni forward primer: TATTGGTCTTCAGGGAGCAAAGCAGGAGT

NA uni reverse primer: ATATGGTCTCGTATTAGTAGAAACAAGGAGTTTTT

Bm-HA-1_forward primer: TATTCGTCTCAGGGAGCAAAGCAGGGG

Bm_NS-890_reverse primer: ATATCGTCTCGTATTAGTAGAAACAAGGGTGT

H7-400 reverse primer: CATGCACTAGTTGTTCCG

H7-700 forward primer: CATTGGTTGATCTTGGATCC

H7-1300 forward primer: GCTGTATGAGCGAGTGAG

FPV_NA_Seq_forward primer: GCATGGGTTGGCTAAC

FPV_NA_Seq_reverse primer: CTCTTGCGTTCTCAATAT

2.9 Viruses

Institute of Virology, Phillips university Marburg, Germany

Prof. Dr. Hans-Dieter Klenk and Prof. Dr. Wolfgang Garten

A/chicken/fowl plague virus /Rostock/1934 (H7N1), FPV

FPV_mutant_HA_{mono} viruses

Vesicular stomatitis virus, VSV

Institute of Virology, Phillips University Marburg, Germany

Dr. Mikhail Matrosovich

A/Thailand/1(KAN-1)/2004 (H5N1), KAN-1

2.10 Consumed materials for cell cultures

Dulbecco's Modified Eagle Medium (DMEM)	Gibco, Karlsruhe
2 x Modified Eagle Medium (2xMEM)	Gibco, Karlsruhe
Glutamine (100x)	Gibco, Karlsruhe
Penicillin/Streptomycin (P/S)	Gibco, Karlsruhe
Fetal calf serum (FCS)	Gibco, Karlsruhe
Trypsin/EDTA	Gibco, Karlsruhe

2.10.1 Cell culture medium

DMEM growth medium	DMEM 10% FCS 1% glutamine 1% Penicillin/Streptomycin
DMEM medium (w/o FCS)	DMEM 1% glutamine 1% Penicillin/Streptomycin
Avicel suspension, 2.4% (w/v)	2.4g Avicel dissolved in 100ml dH ₂ O
Overlay medium	2xMEM and 2.4% Avicel solution (1:1) 1% glutamine 1% Penicillin/Streptomycin 2% FCS

2.10.2 Cell lines

MDCK	a subclone derived from the heterogenous parent Madin-Darby canine kidney cells, which was kindly provided by Prof. Dr. Wolfgang Garten, virology, Marburg
Vero E6	isolated from kidney epithelial cells from an African green monkey, which was kindly provided by Prof. Dr. Wolfgang Garten, virology, Marburg

2.11 Buffers

PBS _{def} (pH 7.0) (Phosphate buffer deficient)	NaCl	8.00g
	KCl	0.20 g
	Na ₂ HPO ₄	1.15g
	KH ₂ PO ₄	0.20g
	dH ₂ O	ad 1l
PBS ⁺⁺	MgCl ₂	0.1g
	CaCl ₂	0.13g
	PBS _{def}	ad 1l
Anode buffer I (pH9.0)	1M Tris-HCl pH9.0	300ml
	ethanol	200ml
	dH ₂ O	ad 1l
Anode buffer II (pH7.4)	1M Tris-HCl pH7.4	25ml
	ethanol	200ml
	dH ₂ O	ad 1l
Cathode buffer (pH9.0)	1M Tris-HCl pH9.0	25ml
	ε-Aminocaproic acid	5.25g
	Ethanol	200ml
	dH ₂ O	ad 1l

Western Blot transfer buffer	Tris	
	Glycine	5.8g
	Ethanol	2.9g
	dH ₂ O	200ml
		ad 1l
10 x Running buffer pH 8.8 (for SDS-PAGE)	SDS	10g
	Tris	30g
	Glycine	144g
	dH ₂ O	ad 1l
4x SDS-sample buffer	0.5M Tris/HCl pH6.8	4ml
	SDS	0.4 g
	Glycerin	4ml
	2% bromphenol blue	0.1ml
	β-mercaptoethanol dH ₂ O	0.4ml
Neutral red stock solution	Neutral red dye	40mg
	PBS _{def}	10ml
Neutral red medium	Neutral red stock solution	100µl
	DMEM medium (w/o FCS)	10ml
Neutral red destain solution	96% ethanol	50% (v/v)
	dH ₂ O	49% (v/v)
	Acetic acid	1% (v/v)
Calcium-TBS- buffer (MUNANA assay)	NaCl	0.85%
	Tris pH 7.0	0.02M
	CaCl ₂	4mM
Stop buffer pH 10.7 (MUNANA assay)	Ethanol	25%
	Glycine	0.1M

10 x TBE buffer, pH 8.0	Tris-base	108g
	Boric acid	55g
	0.5M EDTA, pH 8.0	40ml
	dH ₂ O	ad 1l
ELISA buffer (Immunostaining)	Horse serum	10%
	Tween-20	1%
	PBS _{def}	ad 1l
0.05% Tween (Immunostaining)	Tween-20	500µl
	PBS _{def}	ad 1l
0.3% Triton-X (Immunostaining)	Triton-X	3ml
	PBS _{def}	ad 1l

2.12 Others

SPF chicken eggs

Chicken erythrocytes

Lohmann GmbH, Cuxhaven

Animal house, Philipps University Marburg

3. Methods

3.1 Molecular and biological methods

3.1.1 Antiviral compounds

The neuraminidase inhibitor, oseltamivir carboxylate (GS4071), ribavirin, furin inhibitor dec-RVKR-cmk and synthetic peptidomimetic furin inhibitors were prepared as 10mM stock solutions in PBS_{def}. The trypsin protease inhibitor aprotinin was dissolved in H₂O as 10mM stock solution. All inhibitors were stored at -20°C until use. Oseltamivir carboxylate is referred to as oseltamivir (Os) in this thesis (Structures of inhibitors are shown in Fig. S1 and Table S3).

3.1.2 MTT viability assay

The effect of inhibitors on the viability of MDCK cells was investigated by the MTT assay. MTT, 3-(4,5-dimethylthiazol-2-yl)-2,5-diphenyltetrazolium bromide, is a yellow substrate that can be reduced to purple formazan in living, metabolically active cells, but not in dead cells (Mosmann, 1983).

MDCK cells were seeded in 96-well plates and grown to 100% confluence. Cells were incubated with inhibitor-containing Dulbecco's Modified Eagle (DMEM) medium of different concentrations at 37°C. As a control, mock cells were incubated in medium without inhibitors. After a 24 or 48 hour-incubation, the inhibitor-containing medium was removed. Cells were washed with PBS_{def} and incubated with MTT solution (0.5mg/ml in PBS_{def}) for 2h at 37°C. After removal of the MTT solution, the formazan crystals were solubilised in 100µl dimethyl sulfoxide (DMSO) for 10min at room temperature. The absorbance of formazan solution in each well was quantified at 570nm by an Epoch Microplate Spectrophotometer (Biotek, USA). For quantification, the MTT data was normalized against the untreated mock cells, of which the viability was set to 100%.

3.1.3 Stability measurements of furin inhibitors with high performance liquid chromatography

The stability of furin inhibitors was measured by high performance liquid chromatography (HPLC). The stocks of furin inhibitors were diluted in DMEM medium without FCS to final concentration of 30µM or 10µM and then incubated in the presence

or absence of MDCK cells at 37°C. At different time points after incubation, 0h, 24h, 48h, 72h and 96h, 200µl cultured medium was collected and centrifuged at 30,000 rpm for 15min, of which 100µl were analyzed by analytical reverse phase HPLC. Quantitative determination of the inhibitor peak area yielded the amount of inhibitor remaining at each time point. The HPLC analyses were conducted by Prof. Dr. Torsten Steinmetzer, Institute of Pharmaceutical Chemistry, Philipps University Marburg (Becker et al., 2012).

3.1.4 Sodium dodecyl sulfate polyacrylamide gel electrophoresis

Sodium dodecyl sulfate polyacrylamide gel electrophoresis (SDS-PAGE) is one of the most efficient methods for separating proteins by their electrophoretic mobility after binding of SDS to the proteins. The polyacrylamide gel was prepared according to the gel recipes. Protein samples were suspended in SDS sample buffer, containing sodium dodecyl sulfate (SDS) and β-mercaptoethanol, sonically treated for 30 to 60s and heated at 95°C for 5min. Insoluble material was removed by centrifugation at 13000rpm for 10min (Laemmli, 1970). The gel was run at 150V (constant voltage) at room temperature until the bromophenol blue dye just ran off of the gel, which took about 1.5h. After electrophoresis, the gel was subjected to Western blot.

Gel recipes (enough for 2 mini-gels):

Separating gel	10%	12%
dH ₂ O	3.9ml	3.3ml
1.5M Tris, 0.4% SDS, pH 8.8	2.6ml	2.6ml
30% Acrylamide (Rotiphorese-Gel 30 (37.5:1))	3.33ml	4ml
10% APS	70µl	70µl
TEMED	17µl	17µl

Stacking gel	4.5%
dH ₂ O	2.9ml
0.5M Tris, 0.4% SDS, pH 6.8	1.3ml
30% Acrylamide (Rotiphorese-Gel 30 (37.5:1))	750μl
10% APS	70μl
TEMED	17μl

3.1.5 Western blots

Western blot (WB) analysis is a 'semi-dry' blotting technique used for detecting a protein of interest from a great number of proteins (Kyhse-Andersen, 1984). After electrophoresis, proteins separated by SDS-PAGE were transferred from within the gel onto a nitrocellulose (NC) membrane (pore size 0.45μm) under a constant current of 0.8mA/cm² for about 1h. The membrane, gel and filter papers were soaked with WB-transfer buffer and placed as showed below.

Anode (+)

3 x Whatman-filter paper soaked with WB-transfer buffer

NC membrane

SDS-PAGE gel

3 x Whatman-filter paper soaked with WB-transfer buffer

Cathode (-)

To detect the bound proteins the unspecific protein-binding sites on the NC membrane were saturated by shaking in 7% milk buffer for 30min at room temperature. After, the membrane was incubated with the primary antibody for 1h at room temperature or overnight at 4°C. Before incubation with the secondary antibody, the membrane was washed with PBS_{def} three times. The secondary antibody was coupled with a Fluorophor (Alexa 680 or IRDye 800). After 1h incubation at room temperature, the membrane was again washed with PBS_{def} three times. Finally, the protein bands were visualized and quantified by the program Odyssey 2.01 (LI-COR Biosciences, USA).

3.1.6 Viral RNA extraction

Viral RNAs were isolated from the supernatants of infected cells using the QIAamp viral RNA Kit (Qiagen) according to the manufacturer's instructions. 140μl virus

suspension was added to 560µl lysis buffer (buffer AVL from QIAamp viral RNA Kit containing 1% carrier RNA) and followed by 15s pulse-vortexing. Lysis of viral particles was completed after 10-minute incubation at room temperature and then it was mixed thoroughly with 560µl ethanol (100%). Afterwards, this homogeneous solution was subjected to the QIAamp Mini column, where the viral RNA was bound. After several wash steps, viral RNA was eluted with 50µl elution buffer (Buffer AVE from QIAamp viral RNA Kit) and stored at -80°C until use. The concentration of RNA was measured by photometer (NanoDrop ND-100).

3.1.7 One-step reverse transcription polymerase chain reaction

RNA samples were amplified by one-step reverse transcription polymerase chain reaction (one-step RT-PCR), which was conducted using the QIAamp One-step RT-PCR Kit (Qiagen) according to the manufacturer's instructions. The RNA template was first transcribed into complementary DNA (cDNA) by using a reverse transcriptase. The cDNA was then used as a template for PCR to amplify specific segments. The entire reaction from cDNA synthesis to PCR amplification was performed in one tube.

RT-PCR mix (total volume 50µl):

RT-PCR mix:

Template RNA	200ng-2µg
sense primer (10pmol/µl)	1µl
antisense primer (10pmol/µl)	1µl
dNTP (10mM each)	2µl
5x One-step RT-PCR buffer	10µl
RiboLock RNase inhibitor (40u/µl, 2500u)	0.5µl
One -step RT-PCR enzyme mix	2µl
dH ₂ O (RNase free)	23.5µl

RT-PCR program:

Temperature	Time	
50°C	30min	
95°C	15min	
94°C	1min	} 35 cycles
58°C	1min	
72°C	2min	
72°C	10min	
8°C	until abort	

3.1.8 Two-steps reverse transcription polymerase chain reaction

3.1.8.1 Reverse transcription

Extracted RNAs (800ng-2µg) were incubated with 1µl Uni influenza primer and dH₂O (RNase free water) to a total volume of 12.5µl at 65°C for 5min then followed by a 10min incubation on ice. After that, 4µl 5x RevertAid H Minus-buffer, 2µl dNTP, 0.5µl RevertAid H Minus reverse transcriptase and 0.5µl RibLock RNase inhibitor were added to this mixture and incubated at 25°C for 10min, 42°C for 60min and 70°C for 10min. Synthesized cDNA was stored at -20°C before use.

3.1.8.2 Polymerase chain reaction

Polymerase chain reaction (PCR) was developed by Kary Mullis in 1983 (Mullis & Faloona, 1987). The PCR reaction was prepared as the following recipe in a total volume of 50µl.

PCR mix (total volume 50µl):

cDNA	150ng
sense primer (10pmol/µl)	1µl
antisense primer (10pmol/µl)	1µl
dNTP (10mM each)	1.5µl
Phusion polymerase (2u/µl)	0.5µl
5x Phusion HF reaction buffer	10µl
dH ₂ O	31µl

PCR program:

Temperature	Time	
98°C	30s	
98°C	10s	} 40 cycles
58°C	30s	
72°C	2.5min	
72°C	5min	
8°C	until abort	

3.1.9 DNA electrophoresis

Agarose gel electrophoresis is a commonly used analytical technique for DNA fragments separation. Agarose was dissolved to in 0.5% TBE buffer to a final concentration of 1%. Electrophoresis was performed in 0.5% TBE buffer at 120V for analysis and at 100V for DNA extraction. After incubation of the gel with ethidium bromide (EB), DNA fragments were visualized under the UV light (360nm).

3.1.10 DNA fragment extraction and purification

DNA fragments were extracted from an agarose gel using the QIAquick Gel Extraction Kit (Qiagen) according to the manufacturer's instructions. DNA fragments were excised from the agarose gel and dissolved in solubilisation buffer (buffer QG from QIAquick Gel extraction kit). DNA-containing QG buffer was loaded to a QIAquick spin column to bind DNA. After several washing steps, DNA was eluted in 50µl H₂O. The concentration of eluted DNA was determined by photometer (NanoDrop ND-100).

3.1.11 DNA purification

DNA purification was performed using the QIAquick PCR Purification Kit (Qiagen) according to the manufacturer's instructions. DNA samples were thoroughly mixed with binding buffer (buffer PBI from QIAquick PCR purification Kit), then samples were added to a QIAquick spin column to bind DNAs. After several wash steps, DNA was eluted in 50µl dH₂O.

3.1.12 DNA-sequencing

DNA sequencing was performed by the company Seqlab (Göttingen).

Sequencing mix:

Plasmid-DNA or PCR product	300-400ng
Primer (forward or reverse) (10pmol/μl)	1μl
H ₂ O	add to 15μl

3.2 Cell culture methods

To study the effects of synthesized furin inhibitors *in vitro*, MDCK and Vero E6 cells were used and cultured in DMEM growth medium supplemented with 1% penicillin/streptavidin (Pen/Strep, P/S), 1% glutamine and 10% fetal calf serum (FCS). Cells were grown in an incubator at 37°C with 5% CO₂ and 80% humidity.

Both MDCK and Vero E6 cells were grown in DMEM growth medium in T-75 flasks and were split twice a week. The growth medium was carefully poured off from the flasks and cells were washed once with 10ml PBS_{def}. Afterwards 3ml trypsin/EDTA was added to the cells and incubated with the cells in the incubator at 37°C until the cells were completely detached from the flasks. Detached cells were then resuspended as single cells in 7ml fresh DMEM growth medium. The required amount of cell suspension was pipetted out of the flask and added into a new flask or cell culture plates.

3.3 Virological methods**3.3.1 Virus propagation in eggs**

Influenza virus, A/fowl plague virus/Rostock/1934 (FPV), A/Thailand/1(KAN-1)/2004 (KAN-1) and FPV_mutant_HA_{mono} were propagated in the allantoic cavity of 11-day-old pathogen-free embryonated chicken eggs. The viability of each chicken embryo was checked before infection using an illuminator. To infect embryos, the blunt end of the egg was first disinfected with iodine and then a small hole was punched into the shell on the top of the egg. 200μl virus dilutions (virus stock 1:1000 diluted in PBS_{def}) were injected into the allantoic cavity using a 1ml syringe fitted with a 1 inch (dimension: 0.55 x 25mm) sterile needle and the hole in the shell was sealed with glue. Infected eggs were kept at 37°C in an egg incubator and checked daily to monitor the viability of each embryo until they were dead (24h to 48h p.i.). Eggs with dead embryos were kept at 4°C overnight. To harvest the virus, eggs were opened with forceps at the blunt end, and the allantoic fluids were collected using a 5ml syringe fitted with a 1.5 inch, 21-gauge needle. Cell debris was removed by centrifugation at 4600 rpm for

20min. The virus-containing allantoic fluids were frozen in aliquots and stored at -80°C . The virus was titrated by plaque assay (see 3.3.4).

3.3.2 Virus propagation in cell cultures

Vesicular stomatitis virus (VSV) was propagated in Vero E6 cells. Confluent Vero E6 in T-75 flask were washed with PBS⁺⁺ and infected with VSV at a multiplicity of infection (MOI) of 0.1 (0.1 PFU/cell). This means 9.4×10^6 cells were infected with 9.4×10^5 virions. After 1h of virus adsorption, the virus dilutions were removed and infected cells were washed with PBS⁺⁺. 10ml DMEM medium (w/o FCS) was added to the flask. Infected cells were incubated at 37°C until more than 90% cytopathic effects (CPE) of cells appeared. Virus-containing supernatants were collected and cell debris was removed by centrifugation at 4600 rpm for 10min. The supernatants were frozen in aliquots and stored at -80°C , and virus titer was determined by plaque assay.

3.3.3 Hemagglutination assay

The hemagglutination assay (HA assay) is a simple, rapid method to quantify the influenza virus particles. In contrast to a plaque assay which only detects infectious viruses, both infectious and non-infectious viruses are detected by HA assay (Hirst, 1942).

V-bottomed 96-well plates were used in this assay. $50\mu\text{l}$ PBS_{def} was pipetted into each well and $50\mu\text{l}$ of virus sample was added to the first one. Virus was serially diluted 2-fold in PBS_{def} from 1:2 to 1:2¹² and mixed with an equal volume of 0.5% chicken RBCs. Plates were incubated at 4°C for about 30min. As the HA protein of influenza virus is able to bind to sialic acid receptors on the surface of erythrocytes. The non-agglutinated erythrocytes, which were not bound by viruses, sank to the bottom of the wells and formed distinct red buttons, whereas the virus-bound, agglutinated erythrocytes formed a lattice that coats the well. Virus titer was given in HAU/ml. The HA titer was the last dilution that showed complete hemagglutination activity.

3.3.4 Plaque assay

Plaque assay is a standard method used to determine the number of infectious virus in cell cultures. Infected cells are covered with a semi-solid medium, such as agar, carboxymethyl cellulose (CMC) or Avicel, which prevents the virus from spreading indiscriminately and thus causes a local infection. Each infectious virus particle forms a plaque (Matrosovich et al., 2006).

Cells were seeded in 24-well plates and grown to 100% confluence (MDCK cells for influenza virus and Vero E6 cells for VSV). Virus suspensions were serially diluted 10-fold in DMEM medium (w/o FCS) and 200µl of virus dilution was added to each well. Infected cells were incubated at 37°C for 1h and then were washed once with PBS_{def}, before 400µl of 1.2% Avicel overlay-medium was added to each well. It should be noted that 1µg/µl trypsin-TPCK must be added to the overlay-medium for cells infected with FPV_mutant_HA_{mono} viruses. After incubation at 37°C for 2 days, the overlay-medium were removed and cells were washed once with PBS_{def}. At 48h post infection (p.i.) 500µl 4% paraformaldehyde (PFA) was added to each well. Plaque visualization was performed by immunostaining (3.3.6). Plaques were counted after staining and the virus titer was given in PFU/ml by using the following formula.

$$\text{virus titer (PFU/ml)} = N \times \text{df} \times 5$$

N: number of plaques in each well

df: dilution factor

3.3.5 Plaque reduction assay

A plaque reduction assay was used to determine the drug sensitivity of influenza viruses and was performed according to the protocol from Matrosovich *et al.* with modification (Matrosovich *et al.*, 2006). Cells in 24-well or 6-well plates were inoculated with virus diluted to 50/70PFU. After 1h of virus adsorption, viral inoculums were replaced with 500µl (24-well plates) or 3ml (6-well plates) Avicel overlay medium containing serially diluted drugs. Plaque calculations were performed after incubation at 37°C for 2 (24-well plates) or 3 days (6-well plates).

3.3.6 Immunostaining

Infected cells were fixed with 4% PFA and permeabilized with 0.3% Triton X-100 in PBS_{def} at room temperature for 20min. Afterwards, cells were incubated with primary antibody for 1h followed by incubation with HRP-conjugated secondary antibody for 1h. Plaques or infected cells were visualized by incubating with peroxidase substrate TrueBlue (KPL) for 5-10min. Stained cells were washed with H₂O to stop the reaction and then dried. Antibodies were diluted in freshly prepared ELISA buffer (see 2.11).

After incubation with primary and secondary antibody, cells were washed 3 times with 0.05% Tween 20 buffer (Matrosovich et al., 2006).

3.3.7 Cleavage of HA0 protein in the presence of furin inhibitors

MDCK cells in a 24-well plate were infected with FPV at a high MOI of 100. After 1h incubation at 37°C, virus dilutions were removed and cells were washed with PBS_{def}. DMEM media (w/o FCS) containing different inhibitors at indicated concentrations were then added to each well. At 16 or 24h p.i., virus-containing supernatants and infected cells were collected and analyzed. Infected cells were scraped in PBS_{def} and pelleted by centrifugation at 13000 rpm for 10min. Cell pellets were resuspended in 4x SDS sample buffer and prepared before subjection to the SDS-PAGE and Western blot (see 3.1.4 and 3.1.5).

Virus-containing supernatants were centrifuged at 10000 rpm for 10min to remove the cell debris. The released virus in the supernatant (after initial centrifugation) was then concentrated by ultracentrifugation at 450000 rpm at 4°C for 1h. Virus pellets were resuspended in 4 x SDS sample buffer and prepared before subjected to the SDS-PAGE and Western blot (3.1.4 and 3.1.5).

3.3.8 Virus spread in the presence of inhibitors

MDCK cells were seeded in 24-well plates and grown to 100% confluence. Cells were infected with FPV or KAN-1 virus at a low MOI of 0.001 for 1h at 37°C. After infection, virus dilutions were removed and unbound viruses were washed off with PBS_{def}. Fresh DMEM medium (w/o FCS) containing a furin inhibitor at indicated concentrations was added to the cells. For combination treatment, infected cells were treated with furin inhibitor, oseltamivir and ribavirin at various concentrations. As a control, infected cells were incubated in DMEM medium (w/o FCS) without inhibitors. 24h after infection, infected cells were washed once with PBS_{def}, fixed with 4% PFA and immunostained with anti-FPV antiserum (see 3.3.6).

3.3.9 HPAIV multicycle replication in the presence of a single inhibitor

MDCK cells in 24-well plates were infected with FPV or KAN-1 virus at an MOI of 0.0001. Viral inoculums were removed 1h after virus adsorption and then unbound virus particles were washed off with PBS_{def}. DMEM medium (w/o FCS) containing furin inhibitor MI-701, oseltamivir or ribavirin at different concentrations, were added to each

well, respectively. At 18h, 24h, 48h, 72h and 96h p.i. virus-containing supernatants were collected and titrated by plaque assay (see 3.3.4).

3.3.10 Control inhibition assay using FPV mutant

MDCK cells were seeded in 24-well plates and grown to more than 90% confluency. Cells were infected with FPV_mutant_HA_{mono} at an MOI of 0.0001. After 1h of virus adsorption, unbound viruses were washed off with PBS_{def}. To support the FPV_mutant_HA_{mono} virus multicycle replication, infected cells were incubated in DMEM medium (w/o FCS) containing 1µg/ml Trypsin-TPCK. For inhibition assay, stocks of furin inhibitor MI-701, trypsin inhibitor aprotinin and oseltamivir were diluted in DMEM medium (w/o FCS) containing 1µg/ml Trypsin-TPCK and added to infected cells. As a control, infected cells were incubated in the absence of inhibitors. At 24h, 48h and 72h p.i., viral supernatants were collected and viral titer was determined by plaque assay.

3.3.11 Combination treatment of HPAIV infection

To investigate the inhibitory efficacy of furin inhibitor MI-701 in combination with oseltamivir and ribavirin, MDCK cells were infected with FPV or KAN-1 virus at an MOI of 0.0001. After 1h of virus adsorption, unbound viruses were washed off and cells were treated with furin inhibitor MI-701 and oseltamivir in combination or together with ribavirin in triple combination at different concentrations. Virus-containing supernatants were collected at 18h, 24h, 48h, 72h and 96h p.i. and virus titer was determined by plaque assay (see 3.3.4).

3.3.12 Time of inhibitor addition

The influence of therapeutic time on the inhibitory activity of a drug against HPAIV was investigated by a time-based approach. MDCK cells in 24-well plates were grown to 100% confluence and infected with FPV at an MOI of 0.001. Virus inoculums were left on the cells for 1h. Cells were then washed with PBS_{def} and treated with furin inhibitor MI-701 as a single drug or together with oseltamivir and ribavirin in triple combination. Inhibitor treatment was conducted immediately after infection (0h p.i.) or at 6h, 14h, 20h or 30h p.i.. At 48h p.i., cell culture supernatants were collected for virus titration and cells were fixed with 4% PFA. Infected cells were visualized by immunostaining using anti-FPV anti-sera (see 3.3.6).

3.3.13 Neutral red uptake assay

Neutral red uptake assay (NR assay) is widely used for determination of viral cytopathogenicity and treatment effectiveness, as it provides a quantitative estimation of the number of viable cells in a culture. Neutral red (NR) dye penetrates the cell membrane by non-ionic passive diffusion and concentrates in lysosomes, where the pH is lower than in the cytoplasm. When the cells are damaged or dead, the lysosomes can no longer bind the dye. Therefore, the retained amount of dye is proportional to the number of viable cells.

The NR assay was modified from the protocol from Repetto *et al.* (Repetto et al., 2008). Medium was removed from the cells in 96-well plates and 100µl NR medium, which was prepared one day in advance from 4mg/ml NR stock solution, was carefully added to each well. After incubation for 2h at 37°C with 5% CO₂, NR medium was removed and cells were washed with PBS_{def}. To extract the dye from living cells, 100µl NR destain solution was added to each well and the plate was incubated on a shaking device for 10min. The amount of NR taken up by cells was quantified at 562nm using a spectrophotometer.

3.3.14 Inhibitor efficiency calculation

To access the 50% effective concentration (EC₅₀) of inhibitors, MDCK cells were confluent grown in 96-well plates and infected with FPV at an MOI of 0.0001. After 1h, virus inoculums were removed and cells were washed with PBS_{def}. A stock of furin inhibitor MI-701 was serially diluted in DMEM medium (w/o FCS) and was then added to the cells. The plates were incubated at 37°C. Virus control cells were left untreated and mock cells were not infected with virus. At 48h p.i. the extent of CPE in each well was determined by neutral red uptake assay (3.3.13). The EC₅₀ calculations were conducted by normalizing the NR data for each well against the mock control and virus control, which were set to 100% and 0, respectively. Normalized NR data were plotted as percent virus infection inhibition versus inhibition concentration. The data points were then fitted using five-parameter curve fitting in Graphpad Prism (Graphpad Software, La Jolla, CA) to obtain the EC₅₀.

3.3.15 Synergistic inhibition analysis

To investigate the interactions of MI-701 and oseltamivir and ribavirin, MDCK cells were seeded in 96-well plates and infected with FPV at an MOI of 0.0001. After 1h for virus adsorption, 100µl DMEM medium (w/o FCS) containing furin inhibitor MI-701 and

oseltamivir in combination or together with additional ribavirin in triple combination was added to each well (experimental design in 96-well plate see Fig. S6 in supplementary). 48h after infection the extent of virus caused CPE in each well was determined NR assay (see 3.3.13).

The synergy analysis was calculated using the MacSynergy III program, which is an Excel worksheet. It was developed by Prichard and Shipman based on the MacSynergy II program (Prichard & Shipman, 1990; Prichard et al., 1993). Data were presented as contour plots. The theoretical additive interactions were calculated from the concentration-response curves of single inhibitor and subtracted from the experimentally determined inhibition to reveal different drug-drug interactions: additive, no differences between theoretical additive interactions and observed inhibition; synergy, the theoretical additive interactions is less than the experimental inhibition; or antagonism, which indicates the experimentally determined inhibition was greater than expected. All the values were derived from the mean of 3 replicates and presented at 95% confidence, which eliminates insignificant deviations from the additive surface.

3.3.16 Vesicular Stomatitis Virus control infection experiment

Vero E6 cells in 24-well plate were infected with VSV at an MOI of 0.0001. After 1h of virus adsorption, viral inoculums were removed and unbound viruses were washed off. Fresh DMEM medium (w/o FCS) containing furin inhibitor MI-701, oseltamivir alone or in combination at indicated concentration was added to cells. As a control, infected cells were incubated with DMEM medium (w/o FCS) in the absence of inhibitors. At different time points, released viruses were titrated by plaque assay using Vero cells (see 3.3.4).

3.3.17 Control infection experiment with apathogenic influenza virus

MDCK cells were infected with FPV_mutant_HA_{mono} at an MOI of 0.0001. After 1h of virus adsorption, unbound virus particles were washed off. DMEM medium (w/o FCS) containing 1µg/ml Trypsin-TPCK and different inhibitors, furin inhibitor MI-701, aprotinin or oseltamivir, at indicated concentrations were added to the cells. As a control infected cells were incubated without inhibitor treatment. At 24h, 48h and 72h p.i. virus-containing supernatants were collected and titrated by plaque assay (see 3.3.4).

3.3.18 Serial propagation of FPV in the presence and absence of antivirals

FPV was serially passaged in the presence or absence of antivirals to determine the development of drug-resistant variants. The protocol was conducted according to Ilyushina *et al.* with modification (Ilyushina *et al.*, 2006) (Fig. 3.1). MDCK cells in T-25 flasks were infected with FPV at a low MOI of 0.001 in DMEM medium (w/o FCS). The virus was allowed to adsorb for only 30min at 37°C to minimize the probability of selecting virus with weak affinity for host receptors. The inoculums were removed after virus adsorption and the cells were washed with PBS_{def.} After that, fresh DMEM medium (w/o FCS) containing furin inhibitor MI-701 and oseltamivir alone or in combination was added to the cells. Cells were then incubated at 37°C until greater than 90% CPE appeared. At that time, the virus-containing supernatants from drug treated infected cells were collected, clarified of cellular debris by centrifugation at 1800 rpm for 5min at 4°C and stored at -80°C. Virus titer of each sample was determined by plaque assay in MDCK cells after each passage. For subsequent passages, cells were infected with the supernatant from the previous passage at an MOI of 0.001. The concentration of oseltamivir and furin inhibitor MI-701 in the first round of selection was chosen at a low level, at which virus replication in cell cultures was about 50% inhibited. The concentrations of both inhibitors were doubled in the each subsequent passage. Every few passages, plaque reduction assay were performed to examine the susceptibility of virus to the correspondent inhibitor.

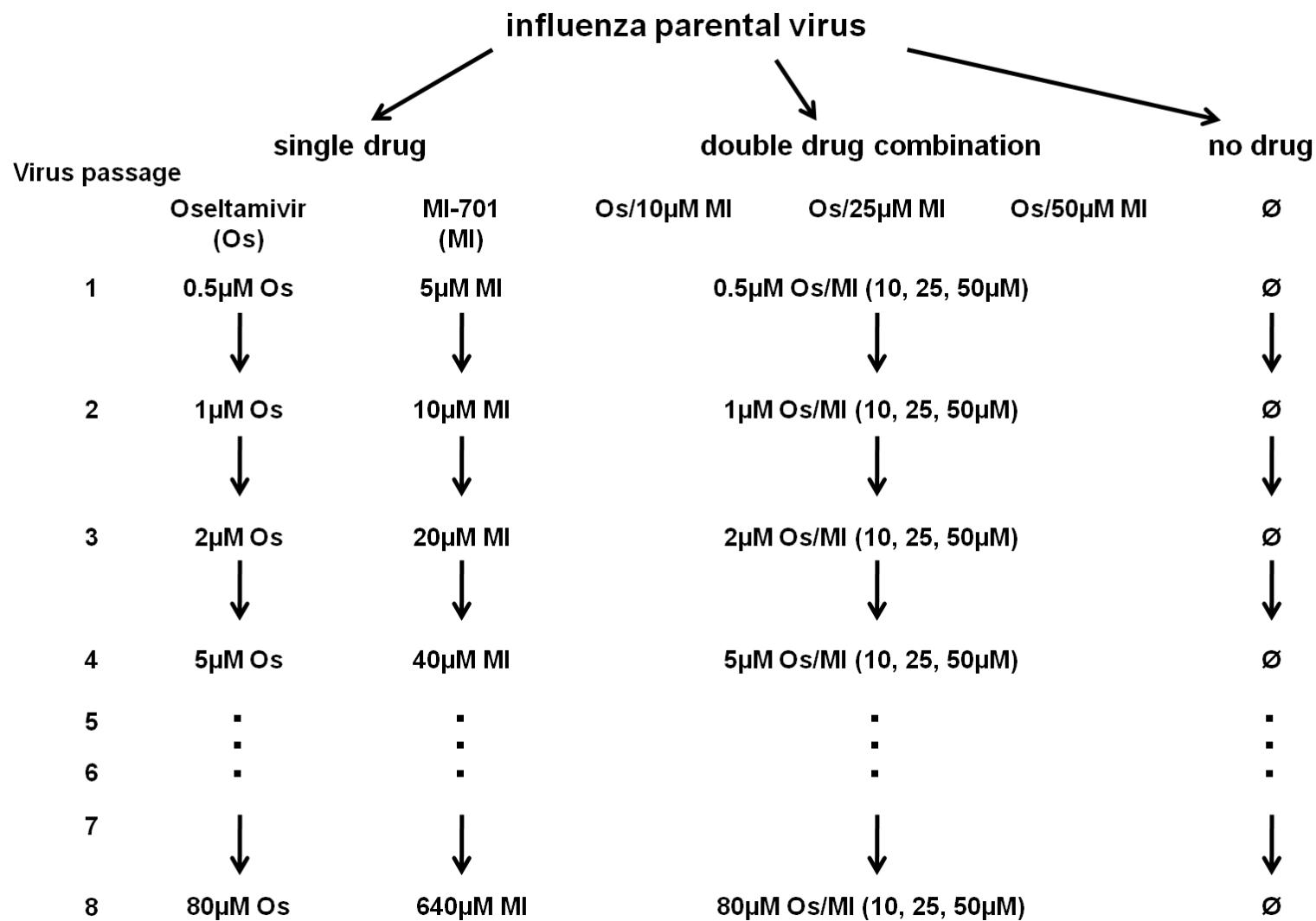


Fig.3.1: Scheme of propagation of FPV in the presence and absence of antivirals in MDCK cells. MI=MI-701; Os=oseltamivir; ∅ = no drug.

3.3.19 Virus inactivation

Research on highly pathogenic influenza virus must be conducted under biosafety level 3 (BSL-3) containment conditions. The limited working condition under BSL-3 hampers the timely characterization of such viruses. β -Propiolactone inactivation allows for better and more efficient studies on such viruses under biosafety level 2 (BSL-2) conditions (Jonges et al., 2010).

Both egg- and cell-grown viruses were incubated with 0.05% β -propiolactone at 4°C for 2 days. 2% HEPES buffer was extra added to cell-grown viruses. After incubation, inactivated viruses were subjected to blind passages in MDCK cells twice. As a control, viruses without treatment with β -propiolactone were passaged parallel in MDCK cells. For blind passage, confluent MDCK cells in T-25 flasks were incubated with DMEM medium (w/o FCS) containing 10% β -propiolactone treated viruses at 37°C. After one week, 500 μ l the culture supernatants was used as inoculums for the second passage on MDCK cells and the cells were incubated at 37°C for one week. Harvested culture supernatants were titrated by plaque assay to confirm inactivation. After confirmation, these viruses were allowed to be exported out of BSL-3.

3.3.20 Determination of neuraminidase activity

To compare the susceptibility of FPV variants to oseltamivir, 2'-(4-methylumbelliferyl)- α -D-N-acetylneuraminic acid (MUNANA)-based enzyme inhibition assay was used. MUNANA is a fluorometric substrate, which is cleaved by NA to yield free 4-methylumbelliferone (4-MU). The fluorescence of released 4-MU is expressed in relative fluorescence units (RFU) for NA activity determination (Potier et al., 1979; Marathe et al., 2013).

FPV wild type and variants were diluted in calcium-TBS buffer. The viral dilution, which generates an equivalent RFU to that generated by 10 μ M of 4-methylumbelliferone sodium salt (4-MUSS) was selected for NA enzyme inhibition assay and can be evaluated by a 4-MUSS standard curve.

To generate a 4-MUSS standard curve, 100 μ M 4-MUSS working solution was prepared from 0.1mM stock solution and then serially diluted in 2-fold dilution in stop buffer. 200 μ l of each dilution of 4-MUSS was added to a black, flat-bottomed 96-well plate. The fluorescence activity of each dilution of 4-MUSS was measured with an Epoch Microplate Spectrophotometer (Biotek, USA), using an excitation wavelength of 360nm, an emission wavelength of 460nm and was plotted against 4-MU concentrations.

To determine the NA activity, FPV wild type and mutants were serially diluted 2-fold in MUNANA buffer and 40µl of each dilution of viruses were added to a black, flat-bottomed 96-well plate. Wells containing only calcium-TBS buffer acted as blank control. After that 1mM MUNANA substrate was prepared from 4mM stock solution in MUNANA buffer and 10µl of MUNANA substrate was added to each well, including blank control wells. The buffer was mixed with the virus dilutions by pipetting up and down several times. The plates were then sealed with parafilm and incubated at 37°C for 60min. To stop the reaction, 150µl of stop buffer was added to each well and the released 4-MU was measured with an Epoch Microplate Spectrophotometer (Biotek, USA), using an excitation wavelength of 360nm and an emission wavelength of 460nm. The RFU was plotted against virus dilutions, in which the mean of blank controls value was subtracted. The virus dilution which produced the equal level of RFU to 10µM of 4-MUSS was determined and was used in NA enzyme inhibition assay.

3.3.21 Virus susceptibility to oseltamivir

FPV viruses were diluted in MUNANA buffer. This dilution produced an equal level of RFU to 10µM 4-MUSS (3.3.21). Then 4000nM oseltamivir was prepared from 10mM stock solution and was diluted four-fold in MUNANA buffer. 20µl of each dilution was added to each well and mixed thoroughly. Wells contained virus dilutions or only MUNANA buffer as blank or virus control, respectively. The plate was sealed and incubated at 37°C for 30min, then 10µl of 1mM MUNANA substrate was added to each well and the plate was resealed and incubated at 37°C for 60min. The reaction was terminated by adding 150µl stop buffer to each well. Released 4-MU was measured with Epoch Microplate Spectrophotometer (Biotek, USA), using an excitation wavelength of 360nm and an emission wavelength of 460nm. The 50% inhibitory concentration (IC₅₀) of the NA inhibitor was the concentration of oseltamivir that produced 50% RFU of virus control value. This was determined by plotting the dose-response curve of inhibition of NA against RFU. Values were the means of four independent determinations.

3.3.22 Growth kinetic of FPV mutants

The growth kinetic of FPV wild type and FPV_{NA} mutants, FPV_{NA}^{H275Y}, FPV_{NA}^{N295S} and FPV_{NA}^{I223M/P272H} viruses were evaluated using MDCK cells in 6-well plates. Confluent MDCK cells were infected with virus at an MOI of 0.0001. After 1h incubation

at 37°C, viral inoculums were replaced with 3ml fresh DMEM medium (w/o FCS). At 14h, 24h, 48h, 72h p.i., virus-containing supernatants were collected for virus titer determination using plaque assay (see 3.3.4).

3.3.23 Effect of MI-701 on replication of FPV mutants

MDCK cells were infected with FPV wild type and FPV mutants, FPV_NA^{H275Y}, FPV_NA^{N295S} and FPV_NA^{I223M/P272H}, at an MOI of 0.0001. After 1h, virus dilutions were removed and cells were washed with PBS_{def}. Infected cells were treated with 50µM MI-701 or left untreated. At 18h, 24h, 48h and 72h p.i. released viruses were titrated by plaque assay (see 3.3.4).

4. Results

4.1 Screening of furin inhibitors

The emergence of drug-resistant viruses is a big challenge for the treatment of influenza infection with antivirals. Therefore, searching for novel antiviral targets is urgently needed to control and prevent annual influenza epidemics or pandemics.

Since the cleavage of HA of HPAIV by furin is a prerequisite for virus replication (see 1.3.1), furin inhibitors emerged to be potential therapeutic agents for treatment of HPAIV infection. In this chapter, more than 20 synthesized peptidomimetic furin inhibitors were examined for their cytotoxicity and potential inhibitory efficiency against HPAIV in cell culture.

4.1.1 Determination of cytotoxicity

Before analyzing antiviral efficacy of these compounds, their cytotoxicity was examined by MTT assay (data is shown in Table S4 in supplementary). MDCK cells were grown to 100% confluency and incubated with inhibitors at two different concentrations, 25 μ M and 50 μ M. The viability of treated cells was measured at 24h and 48h after incubation. Most compounds, both at the lower concentration of 25 μ M and at the higher concentration of 50 μ M proved to be non-toxic for the cells, except the compounds MI-232 and MI-233. The addition of these compounds caused 40% and 80% loss of viability at the concentration of 25 μ M and 50 μ M, respectively. Compounds MI-259 and MI-283 exhibited no cytotoxic effects at the concentration of 25 μ M, but caused more than 50% viability reduction at the concentration of 50 μ M (Fig. 4.1).

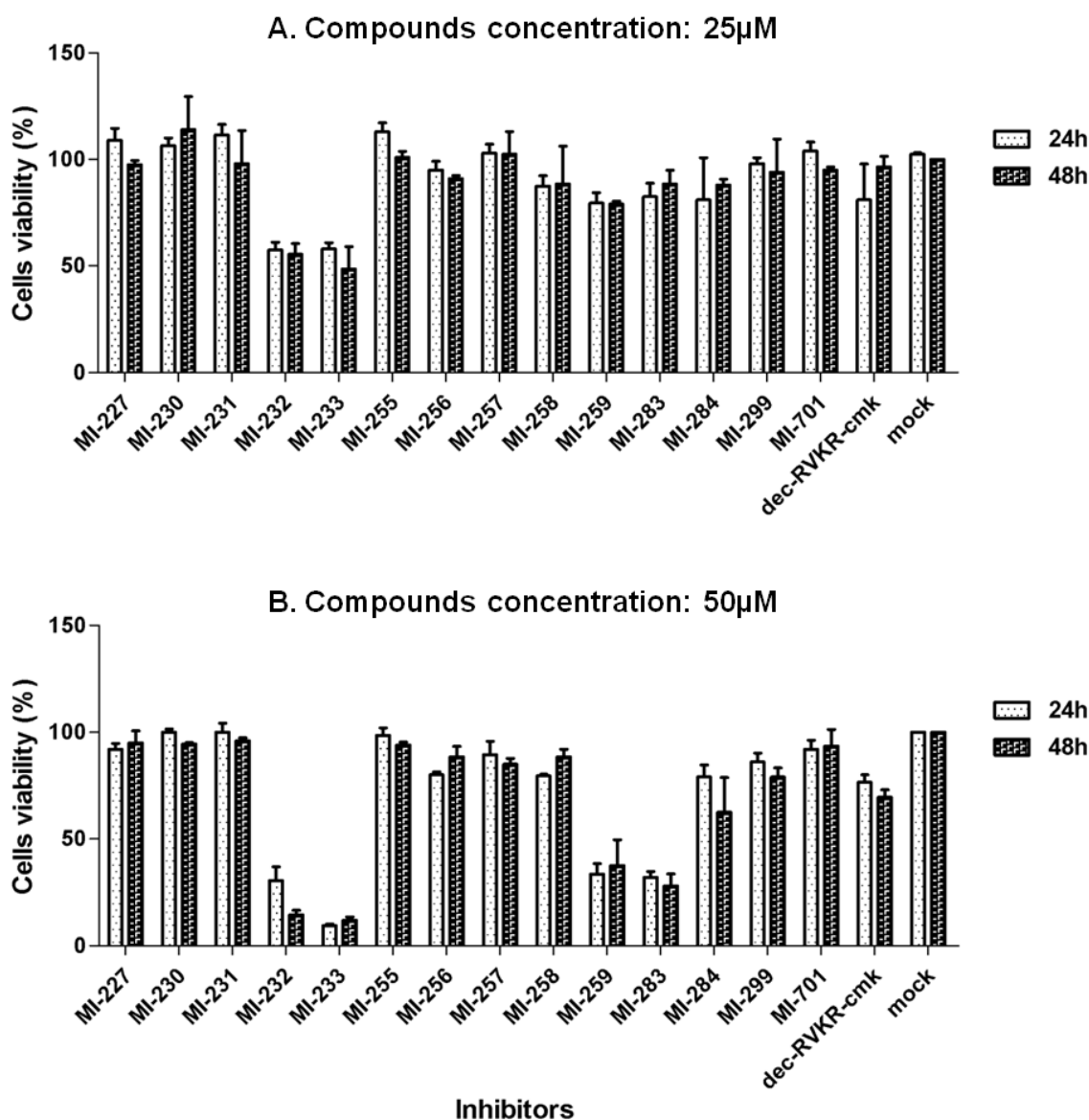


Fig. 4.1: Cytotoxicity determination of different furin inhibitors *in vitro*. The cytotoxic effects of synthesized furin inhibitors were determined by MTT assay. MDCK cells were treated with different compounds at 25 μ M (A) or 50 μ M (B), respectively. Mock cells were incubated in the absence of inhibitors. After incubation at 37°C for 24h or 48h, cells were further incubated with 0.5mg/ml MTT for 2h at 37°C. The produced formazan was eluted in DMSO and quantified by measuring at wavelength 570nm by a spectrophotometer. Structure of each inhibitor is shown in Table S3 in supplementary.

Compound MI-701 was well tolerated by the MDCK cells up to 400 μ M (Fig. 4.2). As expected, presence of oseltamivir did not affect the viability of the cells, even at the concentration of 400 μ M, whereas cells which were incubated with more than 100 μ M of ribavirin for 48h lost approximately 30% viability. Moreover, the furin inhibitor dec-RVKR-cmk (Stieneke-Gröber et al., 1992; Garten et al., 1994), which was used as a

reference inhibitor, also induced a slightly cytotoxic effect at 50 μ M (ca. 10%) when compared with untreated cells.

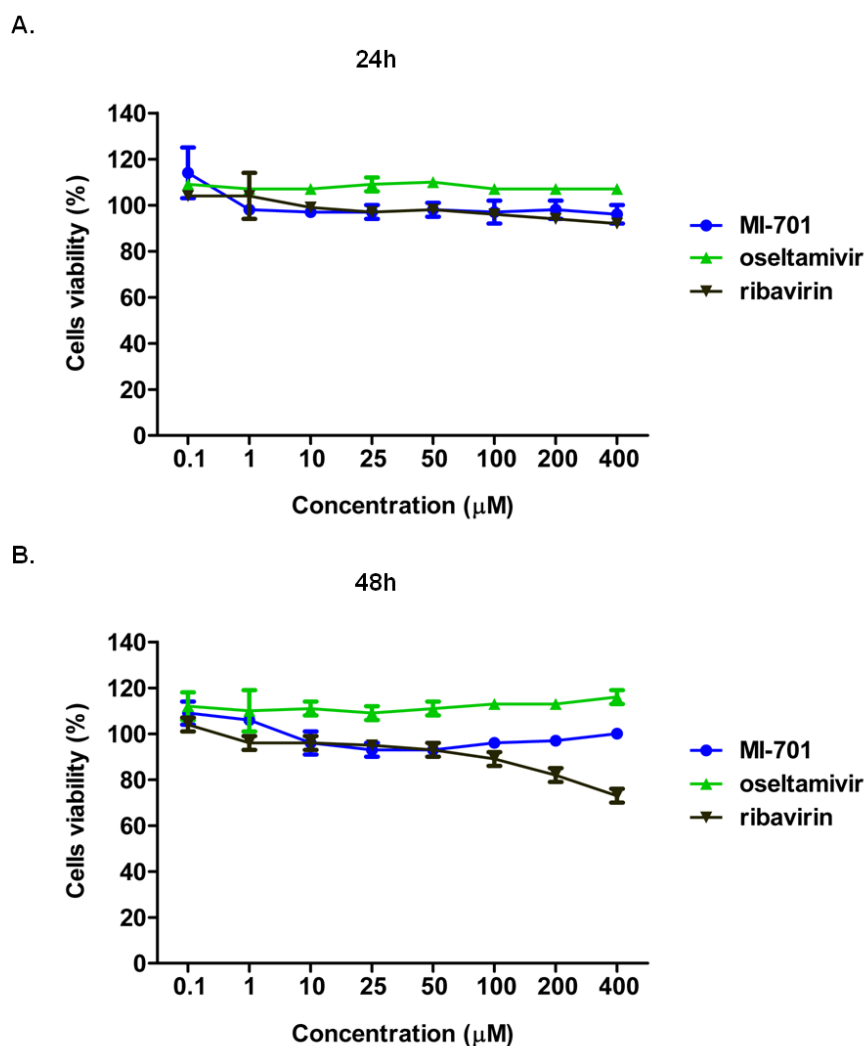


Fig. 4.2: Dose-dependent cytotoxicity of different inhibitors. The cytotoxic effects of oseltamivir and ribavirin were determined by MTT assay in parallel. MDCK cells were treated with different inhibitors at indicated concentrations, ranging from 0.1 to 400 μ M, respectively. Control cells were incubated in pure DMEM medium (w/o FCS) in the absence of inhibitors. After incubation at 37°C for 24h (A) or 48h (B), cells were further incubated with 0.5mg/ml MTT for 2h at 37°C. Produced formazan was dissolved in DMSO and quantified by measuring at wavelength 570nm by a spectrophotometer. For quantification, the viability of control cells was set to 100%. (n = 4).

4.1.2 Determination of stability

To determine the stability of selected furin inhibitors, compounds MI-701 and MI-299 were selected and prepared in DMEM medium (w/o FCS) at the concentrations of

10 μ M and 30 μ M. Compounds at indicated concentrations were incubated at 37°C in the presence or absence of MDCK cells for 24h, 48h, 72h and 96h. After incubation, the supernatant of each sample was collected and cell debris was removed. Samples were then analysed by *Prof. Dr. Torsten Steinmetzer* using analytical HPLC at the *Institute of Pharmaceutical Chemistry, Philipps University Marburg*.

Both compounds were stable in pure medium up to 96h (Fig. 4.3), whereas in the presence of MDCK cells the amount of both compounds decreased in a time dependent manner. The amount of compound MI-701 was reduced by approximately 30% and 50% when its initial concentration was 30 μ M and 10 μ M, respectively, while compound MI-299 was reduced to 40% and 50%.

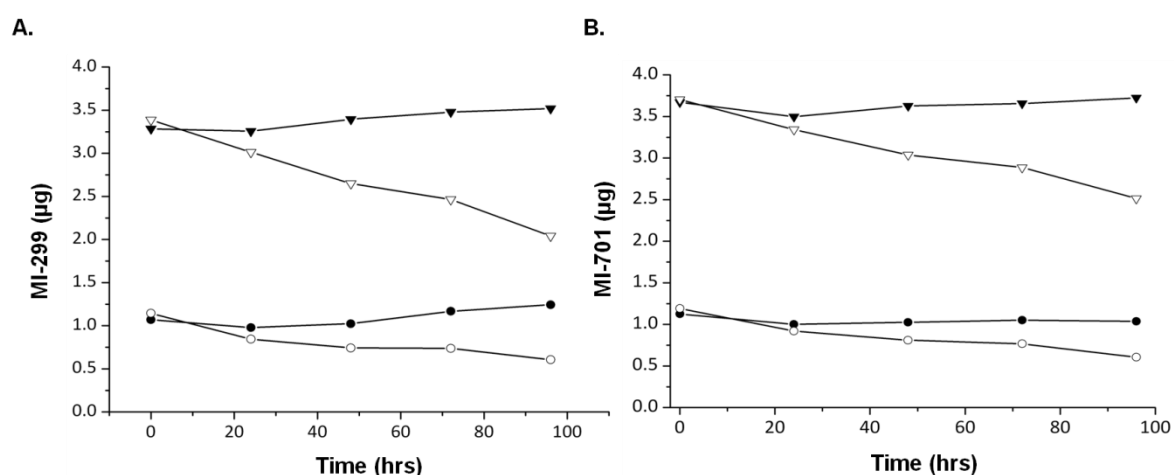


Fig. 4.3: Stability measurement of furin inhibitors. Compound MI-299 (A) and MI-701 (B) at 10 and 30 μ M were incubated in the presence or absence of MDCK cells in DMEM medium (w/o FCS) or in pure DMEM medium (w/o FCS) at 37°C. 24h, 48h, 72h and 96h after incubation, medium that contained MI-701 was collected and cleared by centrifugation at 30,000rpm at 4°C for 15min. Supernatants were stored at -80°C before being analyzed by HPLC, which corresponds to approximately 3.7 μ g for the 30 μ M solution and to 1.2 μ g for the 10 μ M solution. Δ = 30 μ M in MDCK cell cultures; \blacktriangle = 30 μ M in pure medium; \circ = 10 μ M in MDCK cell cultures; \bullet = 10 μ M in pure medium. Figures were taken from Becker et al., 2012 with modification.

4.1.3 Cleavage of HA0 in the presence of furin inhibitors

In order to analyze the cleavage of HA of HPAIV in the presence of furin inhibitors, MDCK cells were infected with A/chicken/fowl plague virus/Rostock/1934 (H7N1) (FPV) at a high MOI of 100. Infected cells were treated with different furin inhibitors at the concentration of 50 μ M. As a control, infected cells were left untreated. At 16h p.i.

approximately 90% cytopathic effect (CPE) was detected and infected cells were collected and suspended in SDS sample buffer containing β -mercapthoethanol. Viral protein samples were loaded onto an SDS-PAGE gel and were analyzed by Western blot (Fig. 4.4).

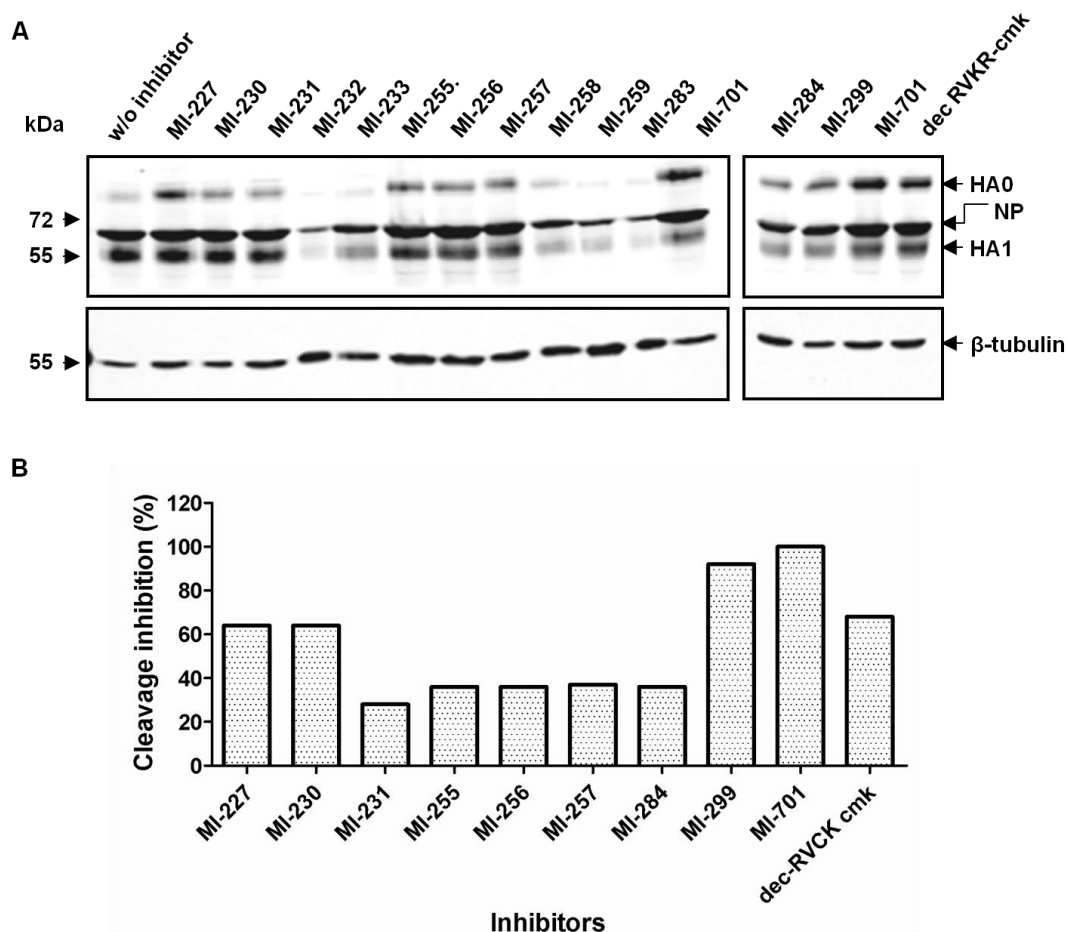


Fig. 4.4: Cleavage of HA in the presence of different furin inhibitors (A) and quantification of HA cleavage inhibition (B). MDCK cells were infected with FPV at an MOI of 100. After virus adsorption, infected cells were treated with different furin inhibitor at a concentration of 25 μ M or without inhibitor treatment. At 16h p.i. cell lysates were collected and subjected to SDS-PAGE under reducing conditions and Western blot analysis using antiserum against FPV and an anti-tubulin antibody as a loading control. Furin inhibitor dec-RVCR-cmk was used as a reference inhibitor in this experiment. (B) For quantification, the intensity of each HA0 band was standardized against that of the β -tubulin bands. The normalized intensities of HA0 obtained in cells treated with 50 μ M MI-701 were set to 100%. The intensities of protein bands were measured by the program Odyssey 2.1. Toxic inhibitors were not quantified.

Viral HA0 proteins were almost completely cleaved into HA1 and HA2 subunits in the absence of furin inhibitor (Fig. 4.4). Treatment of cells with 50 μ M compounds MI-232,

MI-233, MI-258, MI-259 and MI-283 led to less production of viral proteins (structures in Table S3 in supplementary). This indicated that these compounds were toxic for cells and thus affected the growth of FPV in cells. After quantification (Fig. 4.4B) it was observed that treatment with furin inhibitors resulted in detection of more than 20% precursor HA0, and the compounds MI-227, MI-230, dec-RVCR-cmk MI-299 as well as MI-701 significantly inhibited the cleavage of HA0 from 60% to 90%, among which compound MI-701 was the most potent.

4.2 Inhibitory efficacy of furin inhibitor MI-701 against HPAIV infection

4.2.1 Cleavage of HA0 in the presence of inhibitor MI-701

The inhibitory effect of the compound MI-701 on the cleavage of HA protein was the most potent and therefore was further studied. MDCK cells were infected with FPV at a high MOI and treated with different concentrations of furin inhibitor MI-701. Cell lysates and virus-containing supernatants were collected at 24h p.i. and then subjected to SDS-PAGE and Western blot (Fig. 4.5). In comparison with untreated cells, treatment with MI-701 not only resulted in accumulation of uncleaved HA0 proteins in cell lysates but also led to release of non-infectious virus particles, which contains inactivated HA proteins. The amount of HA0 in both cell lysates and supernatants increased with increasing concentrations of inhibitor MI-701, ranging from 0.5 μ M to 50 μ M. The inhibitory effects of MI-701 at the different concentrations were quantified as described in Fig. 4.5. The inhibitory effects of MI-701 on HA cleavage was obviously dose-dependent. The HA cleavage of HPAIV KAN-1 virus in the presence of MI-701 was also investigated, which was strongly inhibited in the presence of MI-701, ranging from 0.1 μ M to 50 μ M. Treatment of 1 μ M of MI-701 resulted in detection of more than 50% of the uncleaved form of HA (Fig. S2 in supplementary).

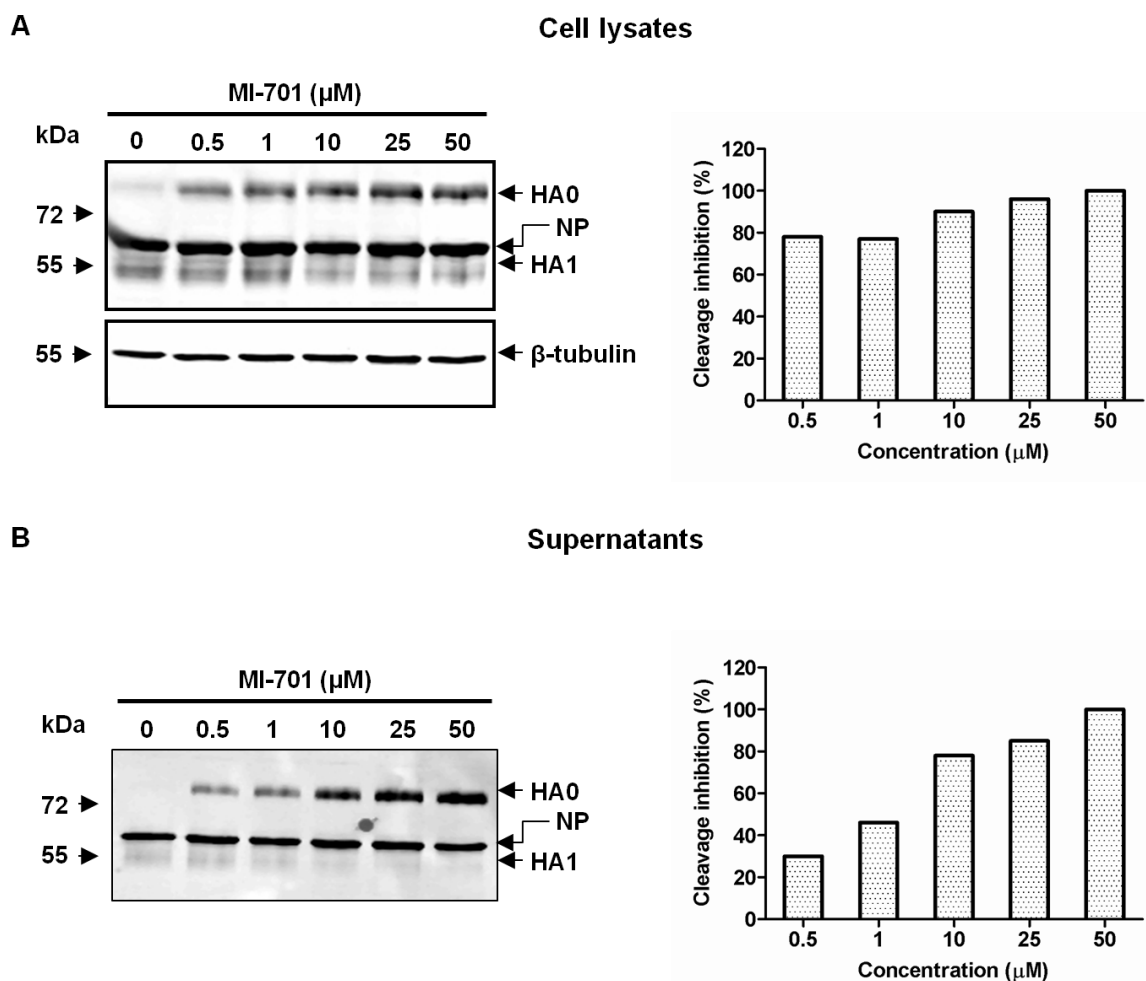


Fig. 4.5: Cleavage of HA0 in the presence of inhibitor MI-701 at various concentrations. MDCK cells were infected with FPV at an MOI of 100. After virus adsorption, infected cells were treated with MI-701 at concentrations of 0.5, 1, 10, 25 and 50 μ M, respectively, or without inhibitor treatment. At 24h p.i. cell lysates (A) and virus-containing supernatants (B) were collected and subjected to SDS-PAGE and Western blot. Viral protein bands were visualized using antiserum against FPV and anti-tubulin antibody as loading control. For quantification, the intensity of each HA0 band was standardized correlating to the β -tubulin bands (A) or NP bands (B) and the normalized intensity of HA0 obtained in cells treated with 50 μ M MI-701 was set to 100%. The intensities of protein bands were performed by the program Odyssey 2.1.

4.2.2 Virus spread in the presence of inhibitor MI-701

It has been shown in the last chapter that treatment with compound MI-701 efficiently inhibited the cleavage of HA0 of FPV. The inhibitory potency of the compound MI-701 against the secondary infection of non-infected neighbouring cells was examined. MDCK cells were infected with FPV or KAN-1 virus at a low MOI. Infected cells were

incubated with an increasing concentration of inhibitor MI-701. Infected cells were fixed at 24h p.i. and were visualized by immunostaining (Fig. 4.6).

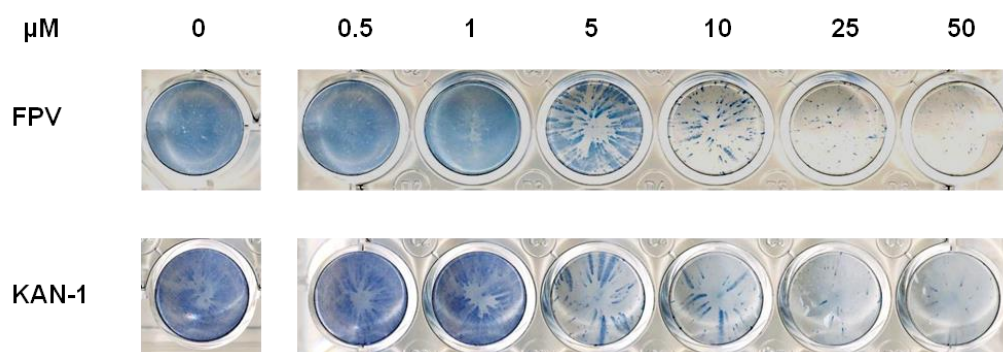


Fig. 4.6: Virus spread in the presence of furin inhibitor MI-701. MDCK cells were infected with FPV or KAN-1 virus at an MOI of 0.001. Infected cells were treated with compound MI-701 at concentration of 0.5 μ M, 1 μ M, 5 μ M, 10 μ M, 25 μ M or 50 μ M or incubated without inhibitor treatment. At 24h p.i. cells were fixed with 4% PFA and then infected cells were immunostained against anti-FPV antibody and HRP-conjugated anti-rabbit secondary antibody.

Without treatment of MI-701 almost all the cells were infected due to the secondary infection, whereas treatment of MI-701, ranging from 5 μ M to 50 μ M, protected the neighbouring non-infected cells from secondary infection, especially in cells treated with 25 μ M and 50 μ M MI-701, where only slight spread of infections was observed. However, treatment with MI-701 less than 5 μ M was not able to suppress the spread of infection.

4.2.3 Inhibitory efficacy of inhibitor MI-701 on HPAIV multicycle replication

HPAIV FPV and KAN-1 virus were employed to explore the inhibitory efficacy of MI-701 on virus replication in cell cultures. Two additional antivirals, oseltamivir and ribavirin, were examined in parallel in this experiment. The neuraminidase inhibitor oseltamivir inhibits virus release by inhibiting the activity of neuraminidase. Ribavirin interferes with virus replication by inhibiting a key enzyme inosine 5'-monophosphate (IMP) dehydrogenase that is involved in viral RNA synthesis (De Clarcq, 2006).

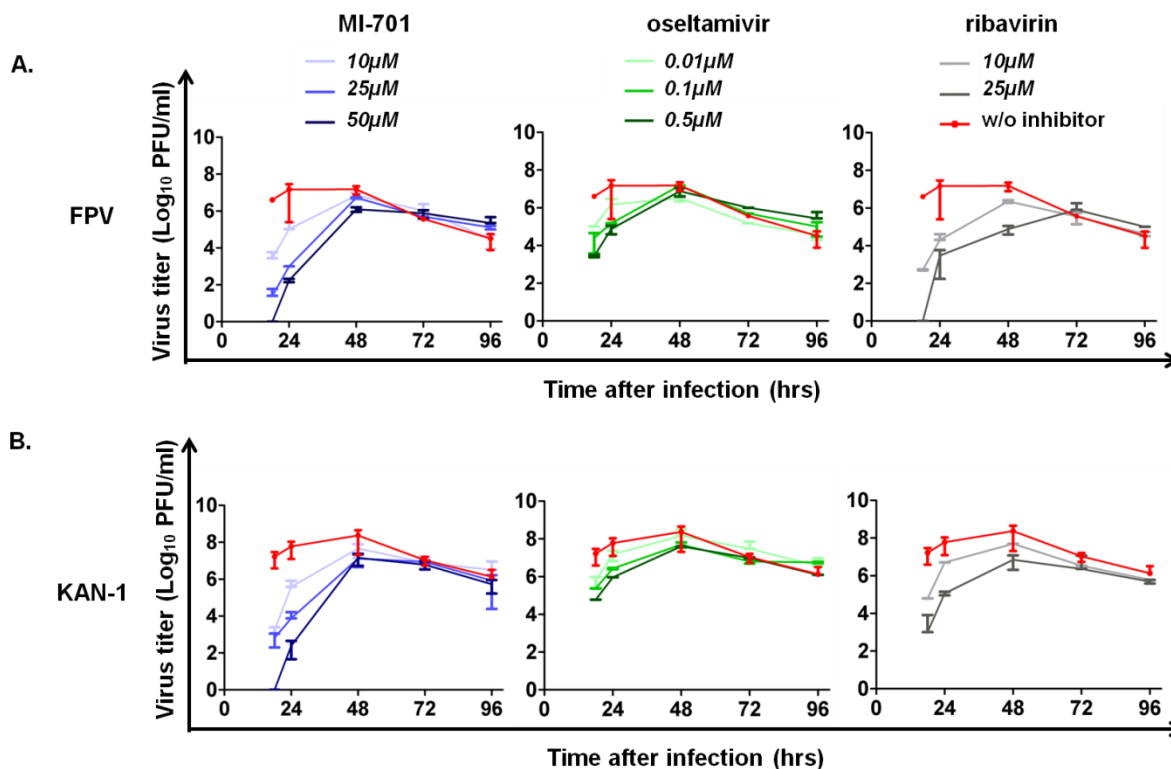


Fig. 4.7: Inhibition of HPAIV multicycle replication in cell cultures. MDCK cells were infected with FPV (A) or KAN-1 virus (B) at an MOI of 0.0001. Virus inoculum was removed after 1h and then cells were washed with PBS_{def} and incubated with inhibitor MI-701 at the concentration of 10µM, 25µM and 50µM, or oseltamivir at the concentration of 0.01µM, 0.1µM and 0.5µM or ribavirin at the concentration of 10µM and 25µM, respectively. As a control, infected cells were incubated in infection medium without inhibitor. At indicated time points, 18h, 24h, 48h, 72h and 96h p.i., virus-containing supernatants were collected and virus titer was determined by plaque assay. (n ≥ 3)

MDCK cells were infected with FPV or KAN-1 virus at a low MOI of 0.0001 and then treated with inhibitor MI-701, oseltamivir or ribavirin at indicated concentrations, respectively (Fig. 4.7 A and B). Virus titer at indicated time points was determined by plaque assay. As shown in Fig. 4.7 both FPV and KAN-1 virus rapidly replicated in untreated cells and reached highest titer of 10^7 and 10^8 PFU/ml at 24h p.i. and 48h p.i. respectively. As expected, oseltamivir and ribavirin efficiently inhibited FPV and KAN-1 virus propagation. Inhibitor MI-701 suppressed the virus replication in a dose-dependent manner (Fig. 4.7 A and B). Treatment with 10µM MI-701 resulted in approximately 100-fold virus titer reduction in FPV- and KAN-1 virus-infected cells at 24h p.i.. In the presence of 50µM of inhibitor MI-701 the release of both viruses were delayed for 18h and virus yields at 24h p.i. were reduced approximately 1,000,000-fold.

4.2.4 Specificity of furin inhibitor MI-701

The FPV_mutant_HA_{mono} virus was derived from FPV with the HA cleavage site PSR↓GLF, which is proteolytic activated by trypsin or trypsin-like proteases. Thus, the replication of FPV_mutant_HA_{mono} virus should be inhibited by addition of the trypsin inhibitor aprotinin and neuraminidase inhibitor oseltamivir, but not by a furin inhibitor. MDCK cells were infected with FPV_mutant_HA_{mono} virus at a low MOI. Cells were then incubated with furin inhibitor MI-701, oseltamivir and aprotinin at indicated concentrations, respectively. At indicated time points, virus samples were collected and titrated by plaque assay (Fig. 4.8).

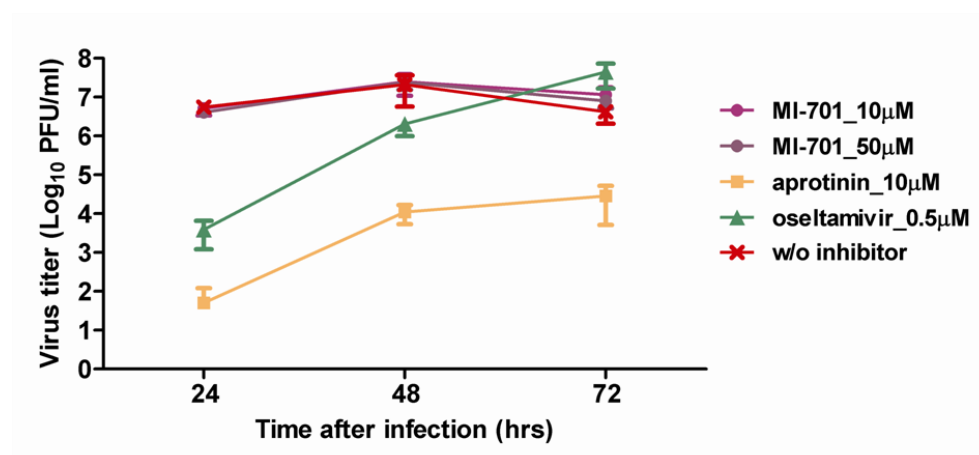


Fig. 4.8: Inhibition of FPV_mutant_HA_{mono} multicycle replication in cell cultures. MDCK cells were infected with FPV_mutant_HA_{mono} virus at an MOI of 0.0001. After 1h, viral inoculums were removed and unbound virus particles were washed off with PBS_{def}. Infected cells were incubated DMEM medium (w/o FCS) containing 1μg/ml trypsin-TPCK and different inhibitors: 10μM and 50μM MI-701, 10μM aprotinin and 0.5μM oseltamivir. At 24h, 48h and 72h p.i. virus-containing supernatants were collected and the virus titer was determined by plaque assay. (n = 2)

As expected, the virus yields in aprotinin- and oseltamivir-treated cells were one million- and thousand-fold reduced, respectively, at 24h p.i. in comparison with those in cells without treatment and treatment of MI-701 did not inhibit the replication of FPV_mutant_HA_{mono} virus. The virus titer in cells treated with either 10μM MI-701 or 50μM MI-701 was comparable to that of non-treated cells. It demonstrated that the compound MI-701 was specific furin-targeting inhibitor (Fig. 4.8).

4.3 Combination therapy against HPAIV

Combination chemotherapy has been well studied and developed to treat cancer and diseases caused by infectious pathogens, such as human immunodeficiency virus type 1 (HIV-1). Combination of two or more drugs that achieve the same effects through different mechanisms may enhance the therapeutic efficiency more than treatment with single drug. In chapter 4.1, furin inhibitor MI-701 was proved to be a promising anti-influenza agent, which potently inhibited the cleavage of HA0 and hence resulted in poor virus spread and replication in cell cultures. Therefore, it is of great interest to know, if the anti-HPAIV efficacy would be further enhanced when furin inhibitor MI-701 is combined with other antivirals.

Furin inhibitor MI-701 was combined with neuraminidase inhibitor oseltamivir in or together with ribavirin in triple combination for treatment the infection of HPAIV in cell cultures. Drug-drug interaction was evaluated by using the MacSynergy III program (Prichard & Shipman, 1990). Oseltamivir used in this thesis is its active form oseltamivir carboxylate.

4.3.1 Cell viability in the presence of different drugs

The combination of multi-drugs with different functions may induce additional toxicity that is not observed by using either drug alone (Pirrone et al., 2011). Therefore, it is important to evaluate the toxicity of combined MI-701, oseltamivir and ribavirin to the cells. MDCK cells were treated with a combination of MI-701 and oseltamivir or together with ribavirin in triple combination for 24h and 48h, respectively (Fig. 4.9). All treated cells preserved similar viability to untreated cells, indicating that treatment with MI-701, oseltamivir and ribavirin in combination at indicated concentrations did not induce toxic effects to the cells.

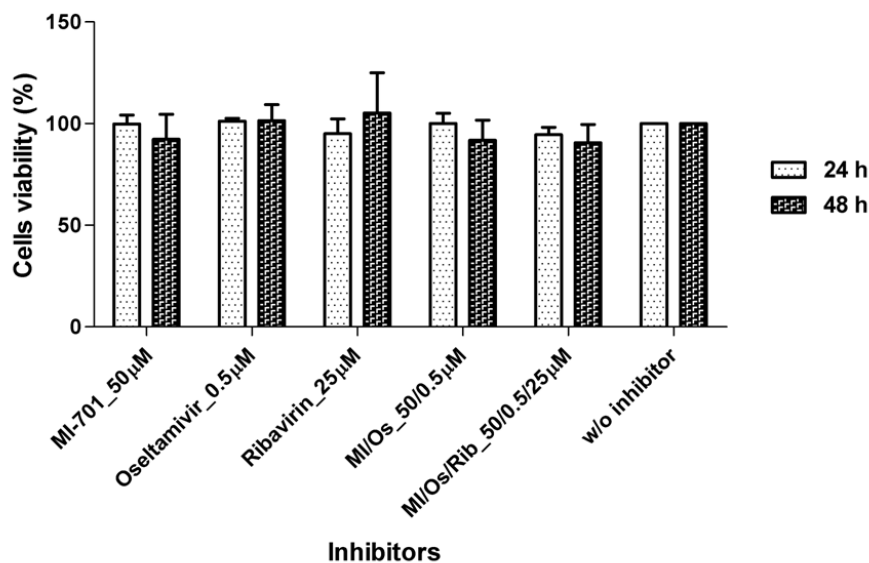


Fig. 4.9: Cytotoxicity of MI-701 in combination with antiviral agents. The cytotoxic effects in the presence of drugs in combinations were determined by MTT assay. MDCK cells were incubated with 50µM MI-701 (MI) alone, in combination with 0.5µM oseltamivir (Os) or together with 0.5µM oseltamivir and 25µM ribavirin (Rib). As a control, cells were incubated in DMEM medium (w/o FCS) in the absence of inhibitor. After incubation at 37°C for 24h or 48h, cells were further incubated with 0.5mg/ml MTT for 2h at 37°C. The produced formazan was eluted in DMSO and quantified by measuring at wavelength 570nm by a spectrophotometer. (n = 2)

4.3.2 Virus spread in the presence of double drugs

The spread of HPAIV in the presence of combined MI-701 and oseltamivir was first examined. MDCK cells were infected with FPV at a low MOI and were incubated with 10µM, 25µM and 50µM MI-701, 0.01µM, 0.1µM and 0.5µM oseltamivir alone or in combination. Infected cells were immunostained using anti-FPV antibody at 48h p.i.. Single drug treatment with MI-701 at the concentration $\geq 25\mu\text{M}$ or oseltamivir at the concentration of 0.5µM strongly suppressed virus propagation, whereas 10µM MI-701 and oseltamivir $\leq 0.1\mu\text{M}$ were not sufficient to inhibit virus replication at 48h p.i. (Fig. 4.10). Combination treatment with 10µM MI-701 and 0.1µM oseltamivir remarkably suppressed the comet-like foci of virus spread in MDCK cells, and combination of 50µM MI-701 and 0.5µM oseltamivir completely blocked the virus spread in MDCK cells. Therefore, it was demonstrated that combination treatment of furin inhibitor MI-701 and oseltamivir could achieved more efficient inhibitory efficacy than treatment with a single drug (monotreatment).

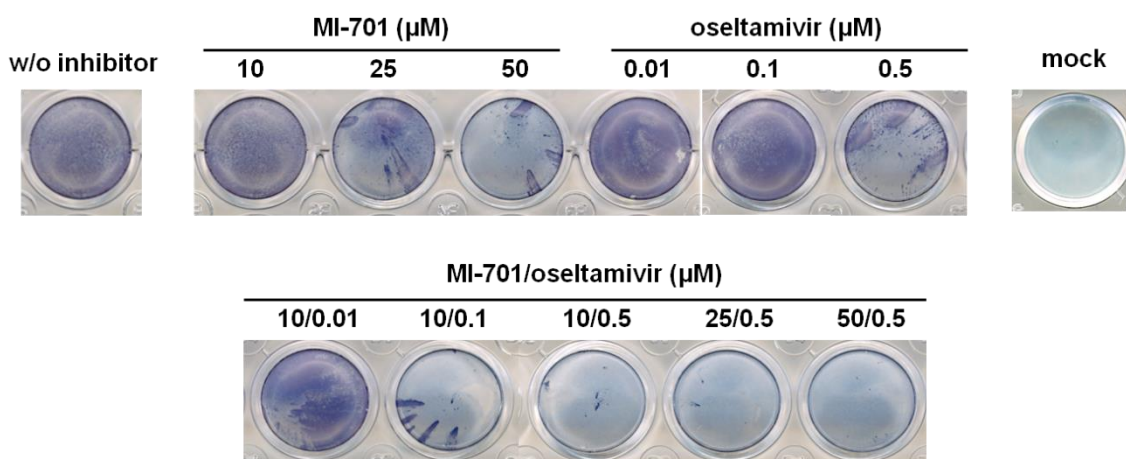


Fig. 4.10: Virus spread in the presence of MI-701 and oseltamivir. MDCK cells were infected with FPV at an MOI of 0.001. Infected cells were treated with inhibitor MI-701 at 10, 25 or 50 μ M, and oseltamivir at the concentration of 0.01, 0.1 or 0.5 μ M respectively, or in combination. As controls, both uninfected cells and infected cells were incubated in pure medium in the absence of inhibitor. At 24h p.i. cells were fixed with 4% PFA and infected cells were immunostained using anti-FPV antibody and HRP-conjugated anti-rabbit secondary antibody. Microscopic images of infected cells are shown in Fig. S3 in supplementary.

4.3.3 Virus replication in the presence of double drugs

In order to better evaluate the inhibitory efficacy of combined inhibitors for treatment the HPAIV infection, the replication of HPAIV in the presence of MI-701 and oseltamivir was examined. MDCK cells were infected with FPV or KAN-1 virus at an MOI of 0.0001 and treated with inhibitor MI-701 and oseltamivir in combination (Fig. 4.11). Treatment with 10 μ M MI-701 and 0.1 μ M oseltamivir in conjunction completely blocked the FPV virus propagation at 18h p.i. and thereby caused about 10000-fold virus titer reduction at 24h p.i.. When the concentration of oseltamivir was increased to 0.5 μ M, no virus was detected at 24h p.i. and resulted in ten thousand-fold virus titer reduction at 48h p.i. (Fig. 4.11A). In comparison with the data of FPV, 10 μ M MI-701 in combination with different concentrations of oseltamivir, 0.01 μ M, 0.1 μ M and 0.5 μ M, did not completely inhibit replication of KAN-1 virus at 18h p.i.. Virus replication was totally blocked at 48h p.i. in the presence of 50 μ M MI-701 and 0.5 μ M oseltamivir (Fig. 4.11B, left). All the data above demonstrated that the double combination with MI-701 and oseltamivir remarkably enhanced antiviral activity against the HPAIV infection in comparison with monotreatment with either MI-701 or oseltamivir.

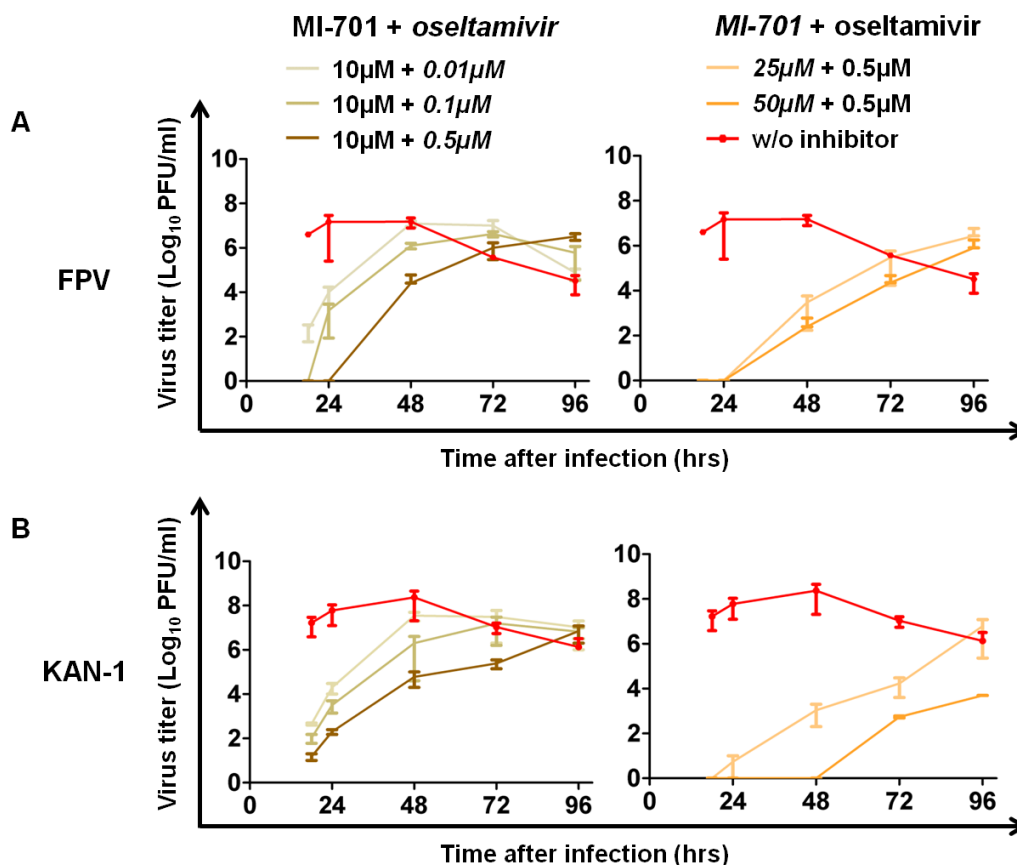


Fig. 4.11: HPAIV multicycle replication in the presence of double drugs. MDCK cells were infected with FPV (A) or KAN-1 (B) virus at an MOI of 0.0001. Virus dilution was removed after 1h. Infected cells were washed with PBS_{def} and treated with MI-701 (MI) at the concentration of 10μM, 25μM or 50μM in combination with 0.01μM, 0.1μM or 0.5μM oseltamivir (Os). As a control, infected cells were incubated in DMEM medium (w/o FCS) without inhibitors. At 18h, 24h, 48h, 72h and 96h p.i., virus-containing supernatants were collected for virus titer determination using plaque assay. (n ≥ 3)

4.3.4 Virus replication in the presence of triple drugs

Subsequently, the MI-701 was combined with oseltamivir and ribavirin for treatment of the infection of HPAIV. MDCK cells were infected with FPV or KAN-1 virus at a low MOI and treated with MI-701, oseltamivir and ribavirin in combination at indicated concentrations. In comparison with double treatment, virus titer in triple drugs-treated cells was further reduced. Some combinations completely inhibited virus release by 96h (Fig. 4.12). Presence of MI-701, oseltamivir and 10μM ribavirin maximally inhibited the release of FPV by 48h, whereas when cells treated with 50μM MI-701, 0.5μM oseltamivir and 25μM ribavirin, the release of FPV was blocked completely by 96h (Fig. 4.12A). As for the KAN-1 virus, triple combination with MI-701, oseltamivir and 10μM

ribavirin also maximally blocked virus production by 48h (Fig. 4.12B), and when the concentration of ribavirin was increased from 10 μ M to 25 μ M, their inhibitory efficacy was significantly enhanced. Virus yield was completely blocked by 96h in cells treated with 10 μ M MI-701, 0.5 μ M oseltamivir and 25 μ M ribavirin or treated with MI-701 \geq 25 μ M, oseltamivir > 0.01 μ M and 25 μ M ribavirin.

In addition, the viability of infected cells with or without treatment was examined at 96h p.i. by NR assay (Fig. 4.13). Infected cells without inhibitor treatment lost almost all viability at 96h p.i., whereas cells treated 50 μ M MI-701, 0.5 μ M oseltamivir and 25 μ M ribavirin, which completely blocked the virus yield at 96h p.i., still preserved approximately 70% viability. The loss of 30% viability was likely due to the virus infection, because combination treatment of uninfected cells did not result in any loss of viability (Fig. 4.9).

Altogether, it is demonstrated that infected cells benefited from the triple combination treatment. The inhibitory efficacy of triple combination treatment with MI-701, oseltamivir and ribavirin is greater than that of the double combination treatment or monotreatment. Importantly, triple combinations, which are capable to completely block the virus release by 96h, did not induce any toxic effects to the treated cells.

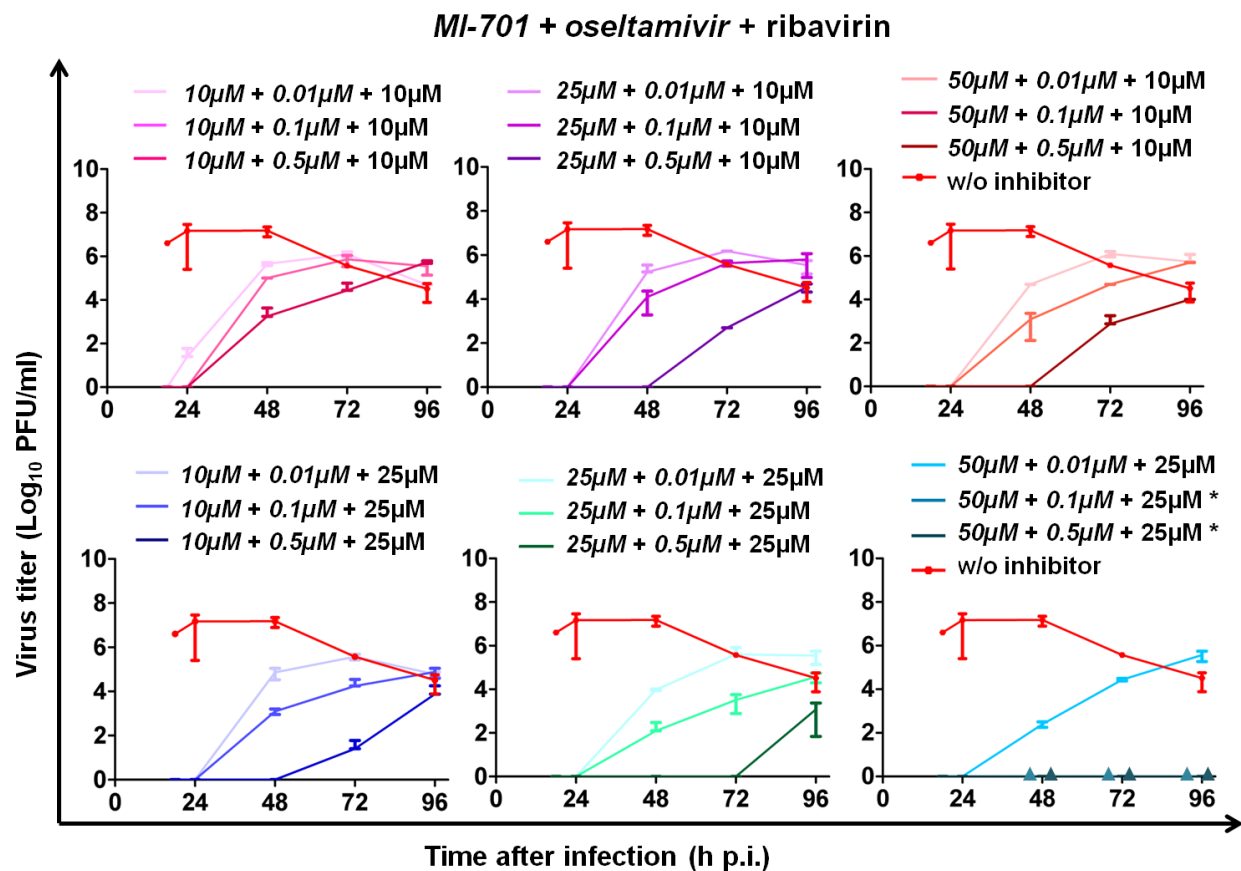


Fig. 4.12A: Multicycle replication of HPAIV subtype H7N1 in the presence of triple drugs. MDCK cells were infected with FPV at an MOI of 0.0001. After virus adsorption for 1h, unbound viruses were quickly washed off with PBS_{def} and cells were treated with MI-701 (MI) (10 μ M, 25 μ M or 50 μ M), oseltamivir (Os) (0.01 μ M, 0.1 μ M or 0.5 μ M) and ribavirin (10 μ M or 25 μ M). Control cells were infected and incubated in medium in the absence of inhibitor. At time points, 18h, 24h, 48h, 72h and 96h p.i., virus-containing supernatants were collected and the virus titer was determined by plaque assay. (n \geq 3). * Virus yield was completely blocked in cells treated with 50 μ M MI-701, 0.1 μ M/0.5 μ M oseltamivir and 25 μ M ribavirin and was shown as \blacktriangle in indicated colour.

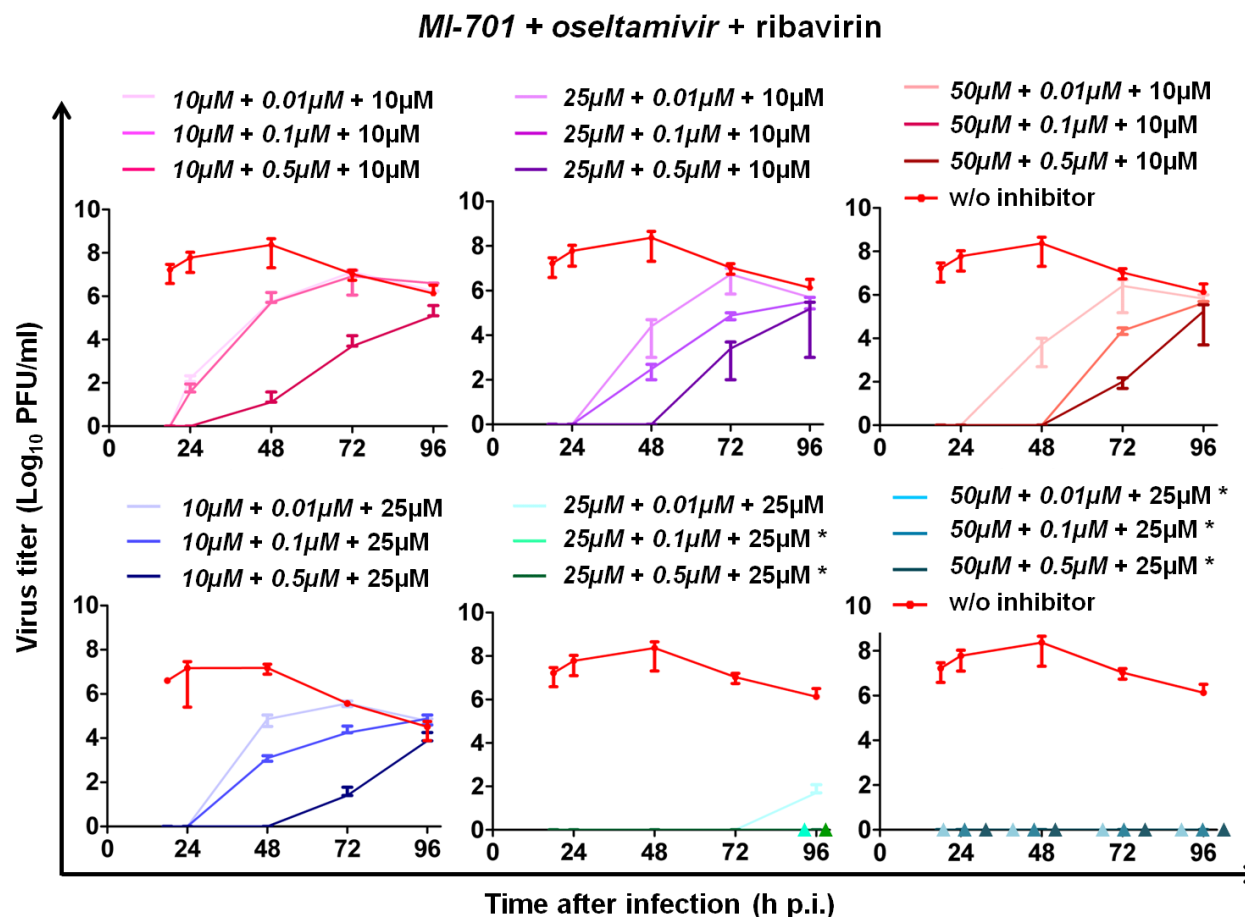


Fig. 4.12B: Multicycle replication of HPAIV subtype H5N1 in the presence of triple drugs . MDCK cells were infected with KAN-1 virus at an MOI of 0.0001. After virus adsorption for 1h, unbound viruses were quickly washed off with PBS_{def} and cells were treated with MI-701 (MI) (10µM, 25µM or 50µM), oseltamivir (Os) (0.01µM, 0.1µM or 0.5µM) and ribavirin (10µM or 25µM). Control cells were infected and incubated in medium in the absence of inhibitor. At time points, 18h, 24h, 48h, 72h and 96h p.i., virus-containing supernatants were collected and the virus titer was determined by plaque assay (n ≥ 3). * Virus yield was completely blocked in cells treated with 25µM/50µM MI-701, 0.1µM/0.5µM oseltamivir and 25µM ribavirin and was shown as ▲ in indicated colour.

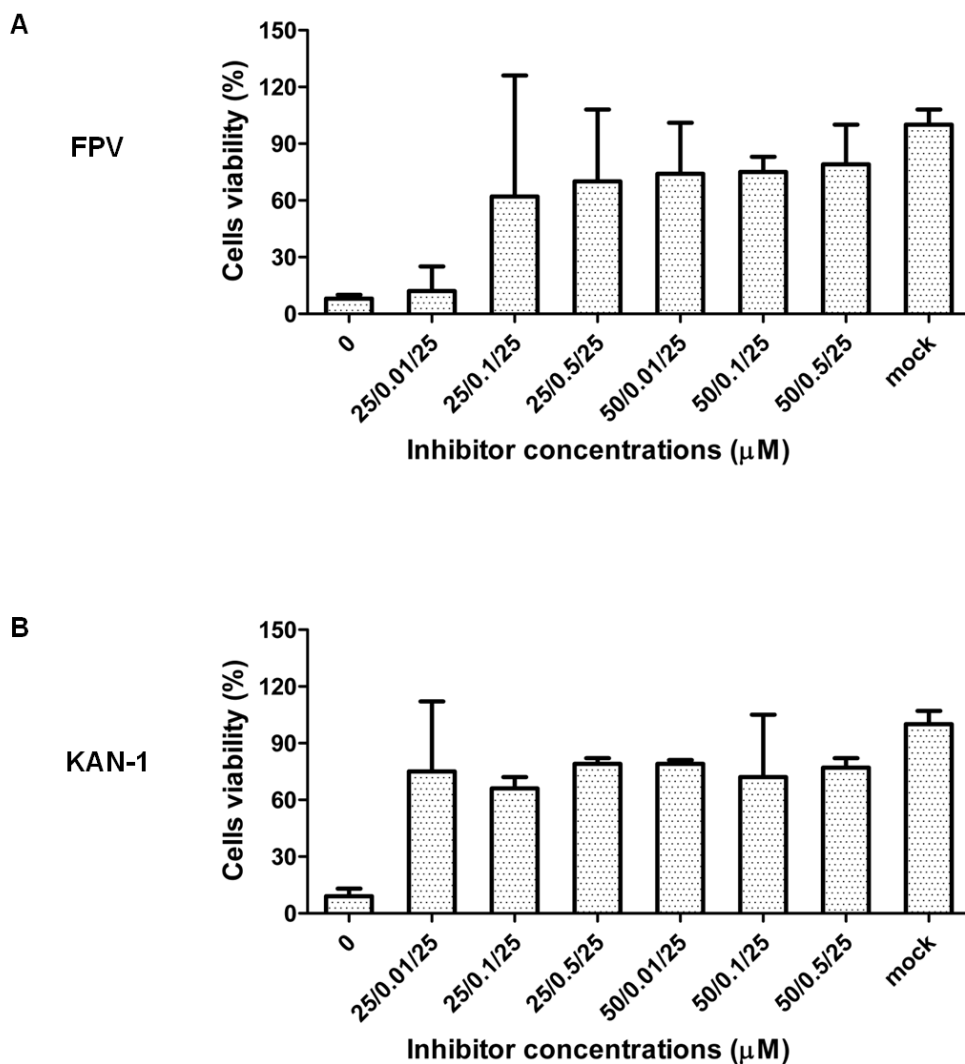


Fig. 4.13: Viability of inhibitor treated infected cells at 96h p.i.. The viability of treated cells at 96h p.i. was determined by neutral red assay. MDCK cells were infected with FPV or KAN-1 virus at MOI of 0.0001. 1h after virus adsorption, infected cells were treated with triple drugs, MI-701 (MI), oseltamivir (Os) and ribavirin (rib) at indicated concentrations. MI/Os/rib: 25/0.01/25 μM , 25/0.1/25 μM , 25/0.5/25 μM , 50/0.01/25 μM , 50/0.1/25 μM and 50/0.5/25 μM . As controls, infected cells and uninfected cells (mock) were incubated in DMEM medium (w/o FCS) in the absence of inhibitors. At 96h p.i. cells were stained with neutral red and quantified by measuring at wavelength 562nm by a spectrophotometer. For quantification, the viability of infected cells was normalized against that of the control mock cells, which was set to 100%. (n = 3)

Furthermore, the vesicular stomatitis virus (VSV) was used to examine the possible toxic effects of combined furin inhibitor MI-701 and oseltamivir on virus itself. Ribavirin was not tested in this experiment, presence of it can inhibit the growth of VSV (Toltzis & Huang 1986), and is therefore not suitable for this control test.

Vero E6 cells were infected with VSV at a low MOI 0.0001. Infected cells were then incubated in DMEM medium (w/o FCS) containing MI-701 and oseltamivir alone or in combination. Since VSV does not contain neuraminidase and its replication is not dependent on efficient cleavage of its glycoprotein, presence of furin inhibitor and neuraminidase inhibitor should not have influences on the replication of VSV in cell cultures. As expected, replication of VSV was not affected in the presence of either MI-701, oseltamivir alone or in combination, indicating that the MI-701 and oseltamivir in combination did not induce any toxic effects to the cells (Fig. 4.14).

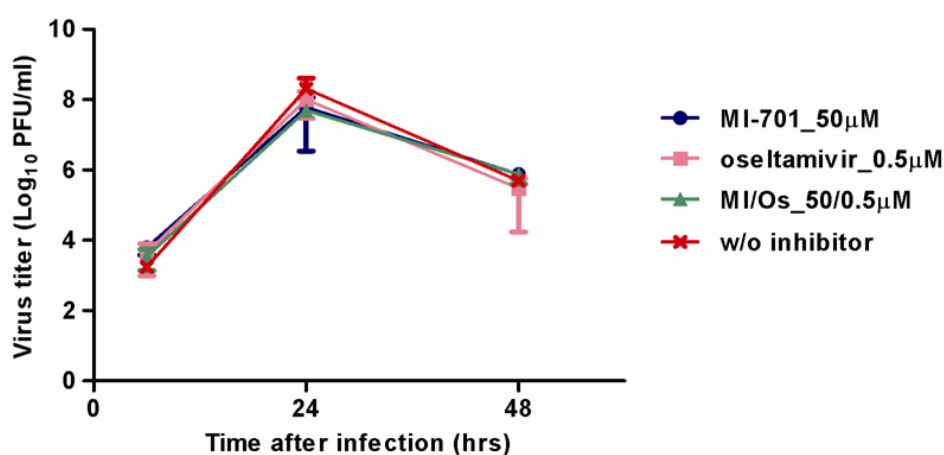


Fig. 4.14: Vesicular stomatitis virus control infection. Vero E6 cells were infected with vesicular stomatitis virus (VSV) at an MOI of 0.0001. After virus adsorption for 1h, infected cells were treated with 50µM MI-701 (MI), 0.5µM oseltamivir (Os) alone or in combination. Control cells were infected with VSV without treatment. At different time points, 6h, 24h and 48h p.i. virus-containing supernatants were collected and the virus titer was determined by plaque assay. (n = 2)

4.3.5 Determination of the 50 percentage effective concentration of MI-701, oseltamivir and ribavirin as single drugs or in combination

The 50% effective concentration (EC_{50}) is defined as the concentration of a drug that can inhibit virus replication up to 50% and is an important pharmacological parameter for drug development. MDCK cells in 96-well plates were infected with FPV at an MOI of 0.0001. Infected cells were then treated with serially diluted MI-701, oseltamivir and ribavirin alone or in combinations. The EC_{50} of each drug was determined by measuring the extent of virus-induced CPE in MDCK cells at 48h p.i. using neutral red assay (NR assay) (Table 4.1).

Table 4.1: Reduction of EC₅₀ for MI-701 as single agent or in double and triple combinations¹.

Inhibitor	EC ₅₀ (μM)	95% Confidence interval ²	Reduction fold of EC ₅₀ ³
MI-701 (MI)	2.8	1.1-2.9	
Oseltamivir (Os)	0.08	0.05-0.1	
Ribavirin (rib)	16.8	13.2-21.3	
MI + 0.01μM Os	1.2	0.6-2.2	2.3
MI + 0.1μM Os	0.6	0.3-1.3	4.7
MI + 0.5μM Os	0.001	0.0003-0.007	2800
MI + 0.01μM Os + 1μM rib	0.8	0.4-1.7	3.5
MI + 0.1M Os + 1μM rib	0.06	0.02-0.2	46.7
MI + 0.5μM Os + 1μM rib	0.0002	0-0.006	14000

¹ The NR data was plotted as percent inhibition versus compound concentration and shown in Fig. S4 in supplementary.

² A confidence interval can tell how precisely the value is determined. 95% confidence interval means a range of values that is 95% certain contains the true value.

³ The reduction fold of EC₅₀ is calculated by dividing the EC₅₀ of MI-701 by the EC₅₀ of combined drugs.

As shown in Table 4.1, the EC₅₀ for MI-701 and ribavirin were in micromolar range, whereas oseltamivir was in nanomolar range. The potency of MI-701 was enhanced when it was combined with oseltamivir. The EC₅₀ for MI-701 was 2.1-fold reduced in the presence of 0.01μM oseltamivir and 2800-fold reduced when the concentration of oseltamivir was increased from 0.01μM to 0.5μM. Moreover, the EC₅₀ for MI-701 was further reduced in triple combination with oseltamivir and ribavirin. The highest reduction, 14000-fold reduction, was seen in the presence of 0.5μM oseltamivir and 1μM ribavirin compared to that of the MI-701 used as a single agent. Therefore, the antiviral activity of MI-701 was greater in triple combination than in double combination or as a single agent. This observation indicated that lower dose of each drug were required in combination to achieve the same inhibitory effect caused by single-drug treatment.

4.3.6 Synergy analysis

When two or more drugs are used in combination to inhibit virus replication, they can produce drug-drug interactions defined as “synergistic,” “additive,” or “antagonistic”

when their combined effect exceeds, equals, or less than that of the sum of the effects of the individual drugs, respectively (Govorkova & Webster, 2010).

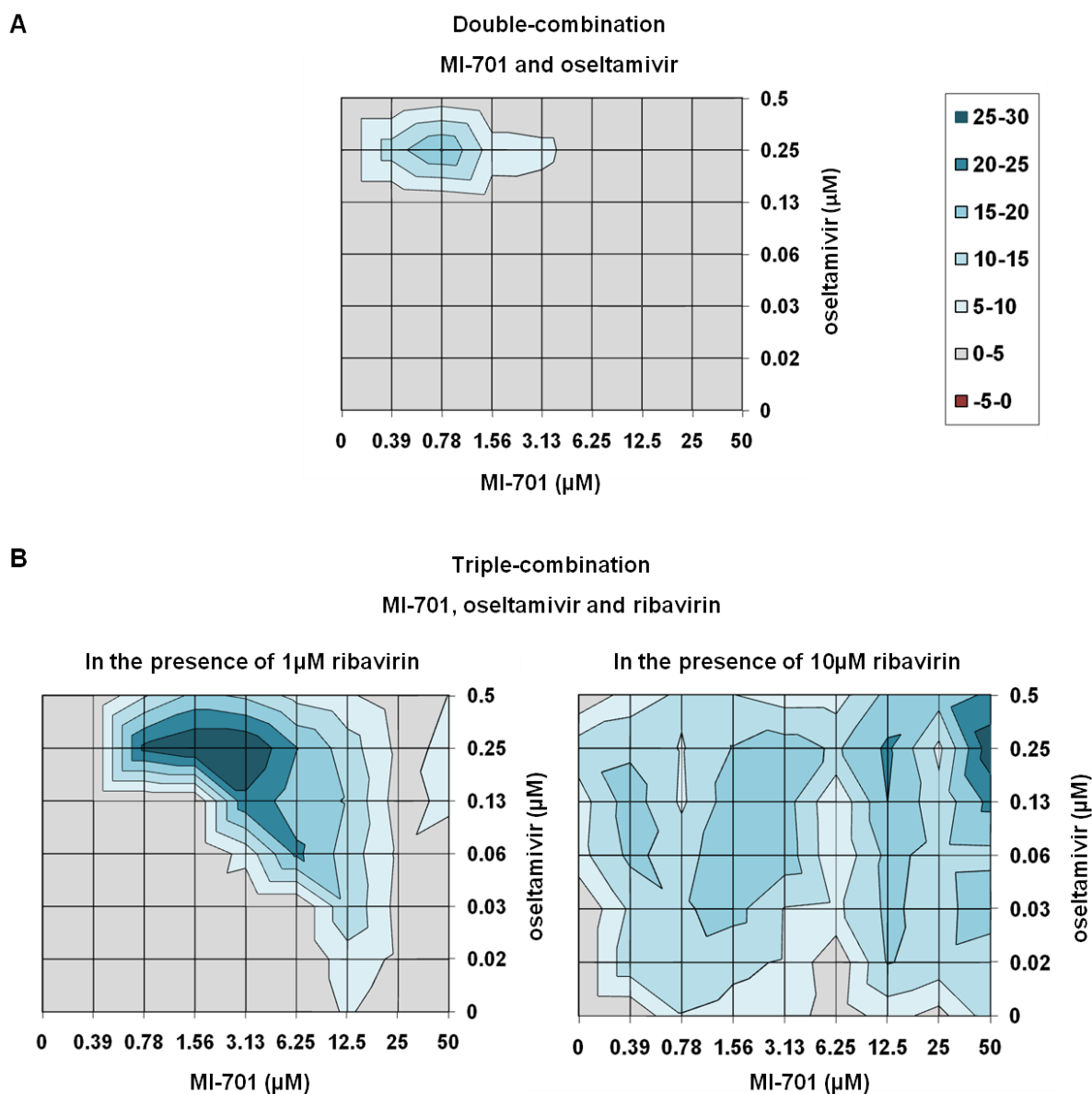


Fig. 4.15: Synergistic inhibition of MI-701 in double combination and triple combination against FPV. MDCK cells in 96-well plates were infected with FPV at an MOI of 0.0001 and then treated with serially diluted MI-701 and oseltamivir in combination (A) or plus 1 μM or 10 μM ribavirin in triple combination (B). 48h after infection the extent of virus-induced CPE in each well was determined by neutral red (NR) staining. Grey areas indicated the interaction was additive, blue areas indicated the synergistic interaction and red areas indicated the antagonistic interaction. The intensity of the color corresponded to the percent inhibition above (synergistic) or below (antagonistic) the expected level. Data are presented as the mean values of 3 replicates with 95% confidence intervals. NR data are shown in Fig. S6 in supplementary.

To access the possible interaction between MI-701, oseltamivir and ribavirin in combinations, MDCK cells were seeded in 96-well plates and treated with serially diluted MI-701 in combination with oseltamivir or together with 1µM or 10µM ribavirin. At 48h p.i. the CPE of cells were measured by NR staining (experimental design in 96-well plate see Fig. S6 in supplementary). The theoretical calculated additive inhibition is generated from the dose-dependent curve of single inhibitor using specific equations (for double combination: $Z = X + Y(1-X)$, X, Y represent that inhibition produced by inhibitor X or Y, respectively, Z refers to the total inhibition produced by inhibitor X and Y in combination; the equation for calculating the total inhibition produced by triple drugs has not been published) (Prichard & Shipman, 1990). The calculated additive inhibition is then subtracted from the experimentally determined inhibition to reveal different drug-drug interactions (all the calculations were generated after entering the NR data manually in the Excel worksheet of the MacSynergy III program). The data were presented as contour plots, in which the experimental inhibition effect was equal to, greater or less than the theoretical calculated additive inhibition, and are shown in grey, blue and red, respectively. As shown in Fig. 4.15A the MI-701 and oseltamivir in double combination was largely additive; synergy was observed within the concentration range from about 0.39µM to 1.5µM for MI-701 and 0.2µM to 0.4µM for oseltamivir. No antagonism was found. Triple-combination of MI-701, oseltamivir and ribavirin was synergistic against the replication of FPV across a wide range of concentrations, and the synergy area was expanded along with the increasing concentration of ribavirin from 1µM to 10µM. Triple combination with ribavirin at the concentration 10µM reached the limits of NR assay, thus the EC₅₀ of MI-701 in triple combination with oseltamivir and 25µM ribavirin was not determined.

4.4 Effects of treatment initiation on antiviral activity

The antiviral efficiency of a drug is related to the life cycle of the treated viruses and the time of drug-application. MDCK cells were infected with FPV at a low MOI. Inhibitors were added to the cells at given time points. Cells were fixed at 48h p.i. and immunostained using anti-FPV antiserum (Fig. 4.16A). Under the low-MOI conditions a larger number of cells were not initially infected with the FPV. Without treatment almost all the cells were infected with FPV at 48h p.i. due to the secondary infection. Triple treatment with MI-701, oseltamivir and ribavirin immediately after virus adsorption efficiently protected the neighbouring uninfected cells. The FPV usually

starts to release progeny viruses at 6h to 8h p.i., and treatment initiated at 6h p.i. was still capable to efficiently suppressed virus spread. However, treatment started at 14h p.i. or later no longer prevented infection (Fig. 4.16B).

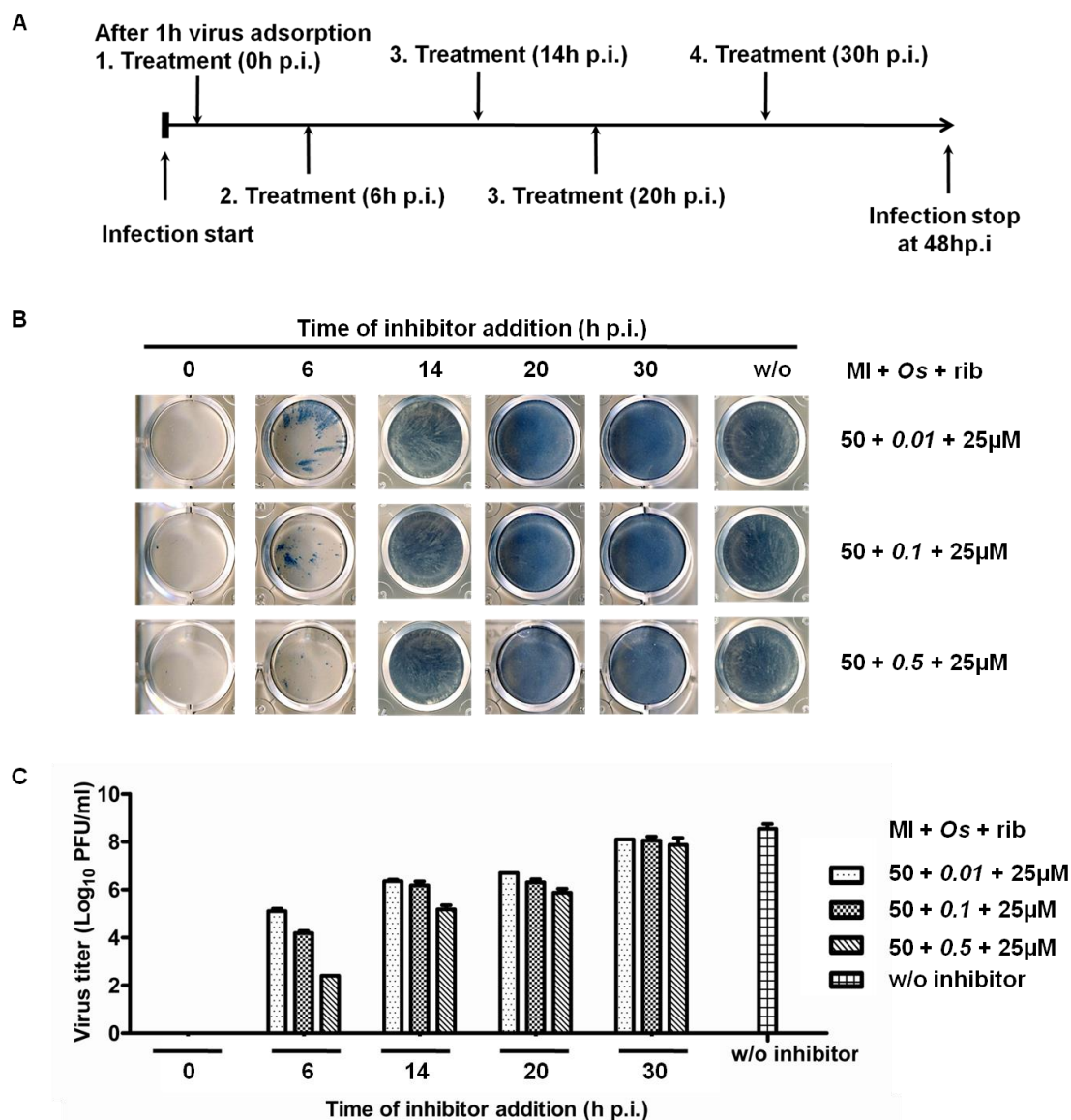


Fig. 4.16: Time of inhibitor addition. (A) Schematic image of experiment build up. MDCK cells were infected with FPV at an MOI of 0.001. Infected cells were treated immediately or 6h, 14h, 20h, 30h after infection with 50µM MI-701(MI), 25µM ribavirin (rib) and together with oseltamivir (Os) at different concentration, 0.01, 0.1 and 0.5µM, respectively. Control cells were infected with FPV without inhibitor treatment. Mock cells were not infected with FPV. At 48h p.i. cells were fixed with 4% PFA and then infected cells were immunostained against anti-FPV antibody and HRP-conjugated anti-rabbit secondary antibody (B). Virus-containing supernatants of each well were collected and titrated by plaque assay (C).

Released viruses were quantified by plaque assay (Fig. 4.16C). Complete inhibition was observed when treatment was initiated immediately after infection (0h p.i.). Treatment at 6h p.i. led to up to one million reduction of virus yield when compared with untreated cells. Although a larger amount of virions were released into the supernatants, initiation of triple combination treatment at this time point resulted in up to 1000-fold virus titer reduction. Initiation of triple combination treatment after 30h p.i. was insufficient to inhibit virus replication.

Taken together this experiment showed that triple treatment with MI-701, oseltamivir and ribavirin exerted their antiviral effects during the early stage of virus replication cycle, suggesting that triple treatment should be conducted as early as possible but not later than 2 days after infection to obtain an optimal antiviral activity.

4.5 Development of drug-resistant FPV

Challenger of the current anti-influenza therapy is the worldwide rapid emergence and circulation of drug-resistant viruses. The potent furin inhibitor MI-701 was proven to be an efficient anti-influenza agent, either used for a mono-treatment or for combination treatment with oseltamivir and ribavirin. However, the potential of furin inhibitor MI-701 to develop resistant influenza is unclear. Previous studies showed that combinatorial therapy using different virus-targeting antivirals reduced the emergence of drug-resistant influenza variants (Ilyushina et al., 2006). In this chapter FPV was used to examine whether treatment with oseltamivir and furin inhibitor MI-701 alone would lead to occurrence of resistant FPV mutants and whether combination treatment with both inhibitors would suppress the development of drug-resistant FPV mutants.

4.5.1 Propagation of FPV in the presence of MI-701

To investigate the possible development of MI-701-resistant viruses, FPV was serially passaged in MDCK cells under an increasing concentration of MI-701 for eight times. The concentration of MI-701 was doubling in each subsequent passage. Virus susceptibility to MI-701 was controlled by plaque reduction assay. By the seventh passage there was still no significant susceptibility changes detected between viruses that propagated in medium in the absence of inhibitor MI-701 and viruses, which were passaged under an increasing concentration of inhibitor MI-701 (Fig. 4.17).

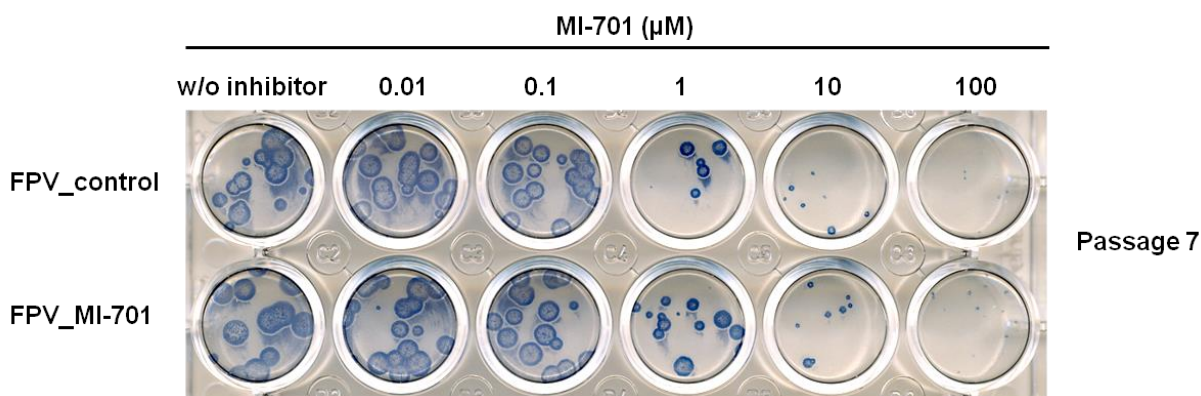


Fig. 4.17: Susceptibility of passaged FPV to furin inhibitor MI-701. Plaque reduction assay was used to monitor the susceptibility of FPV to furin inhibitor MI-701. MDCK cells were infected with 50 PFU of FPV viruses that were passaged in the infection medium in the absence of inhibitors (FPV_control) or in the presence of MI-701 (FPV_MI-701). After incubation at 37°C for 1h, the virus inoculum was removed and fresh 1.2% avicel overlay medium containing 2% FCS and desired concentration of MI-701 was added to the cells. 48h after incubation overlay medium was removed and cells were fixed by 4% PFA. Infected cells were immunostained against anti-FPV antibody and HRP-conjugated anti-rabbit secondary antibody.

Therefore, it was concluded that propagation of FPV under the pressure of furin inhibitor MI-701 did not result in development of drug-resistant viruses. This result was confirmed by sequence analysis. No mutations were found in either HA or NA protein of FPV_MI-701 viruses (Table 4.2).

4.5.2 Propagation of FPV in the presence of oseltamivir

FPV wild type, which is not resistant to oseltamivir, was passaged in MDCK cells under an increasing concentration of oseltamivir. Virus titer of each passaged FPV was determined by plaque assay. Every three to four passages, the susceptibility of passaged virus to oseltamivir was monitored by plaque reduction assay.

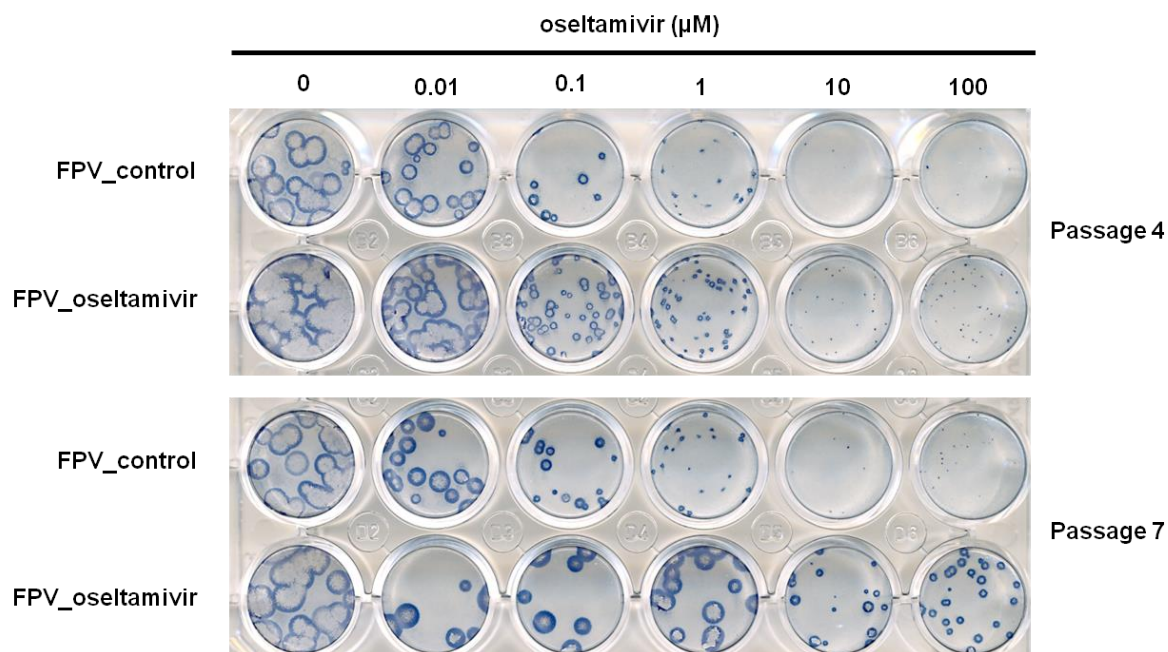


Fig. 4.18: Susceptibility of passaged FPV to oseltamivir. Plaque reduction assay was used to monitor the susceptibility of FPV to oseltamivir. MDCK cells were infected with 50 PFU of FPV, which was passaged in the absence of oseltamivir (FPV_control) or in the presence of oseltamivir (FPV_oseltamivir). After incubation at 37°C for 1h, virus inoculum was removed and fresh 1.2% avicel overlay medium containing 2% FCS and 0.01 μ M, 0.1 μ M, 1 μ M, 10 μ M and 100 μ M oseltamivir was added to the cells, respectively. 48h after incubation overlay medium was removed and cells were fixed by 4% PFA. Infected cells were immunostained against anti-FPV antibody and HRP-conjugated anti-rabbit secondary antibody.

After four passages, the susceptibility of FPV_oseltamivir that was passaged in the presence of increasing concentration of oseltamivir, was slightly decreased in comparison with FPV that was passaged in medium in the absence of oseltamivir (Fig. 4.18). FPV_oseltamivir formed more plaques in the presence of 0.1 μ M and 1 μ M oseltamivir than FPV control virus that was passaged in the absence of inhibitors. Many small plaques with a diameter less than 1mm were found in FPV_oseltamivir infected cells in the presence of 10 μ M and 100 μ M oseltamivir, but not in FPV_control virus-infected cells. The FPV was further passaged under the concentration of oseltamivir and by the seventh passage the susceptibility of FPV_oseltamivir virus to oseltamivir was distinctly decreased. Bigger plaques were formed in the presence of 10 μ M and 100 μ M oseltamivir, while no plaques were formed in cells infected with FPV control viruses in the presence of 10 μ M or 100 μ M oseltamivir. After sequence analysis of the NA gene of the FPV control virus and FPV_oseltamivir viruses from the fourth and

seventh passage, a histidine to tyrosine substitution mutation at amino acid 275 (in N1 numbering) in NA was confirmed. The H275Y mutation was a well known oseltamivir-resistant mutation, which has been found in many oseltamivir-resistant influenza A isolates, including pandemic 2009 H1N1 and human pathogenic H5N1 (de Jong et al., 2005; van der Vries et al., 2010). The NA gene of FPV and FPV_oseltamivir virus from selected passages were also sequenced and results are showed in Table 4.2. The NA^{H275Y} mutation first appeared in the third passage and was continually identified in subsequent passages. The H275Y mutation was the only mutation that the FPV developed under the pressure of oseltamivir. In repeated experiment a mixture of H275H and H275Y in NA were detected in the FPV_oseltaviri virus in the third passage (data not shown).

4.5.3 Propagation of FPV in the presence of oseltamivir and furin inhibitor MI-701

FPV was passaged eight times in the presence of oseltamivir and MI-701. The concentration of oseltamivir was doubled in the subsequent passage, whereas the concentration of MI-701 was constant at 10µM, 25µM or 50µM. To determine the possible appearance of mutations, the NA and HA genes of viruses were fully sequenced from indicated passages (Fig. 4.19 and Table 4.2).

Table 4.2: Sequence analysis of FPV variants in the presence of drugs *in vitro*

Passage	no drug ^a	Oseltamivir alone ^b	Oseltamivir + MI-701 ^b			MI-701 alone ^c
			10µM MI-701	25µM MI-701	50µM MI-701	
1	NO	NO				
2		NO	NO			
3	NO	H275Y	I223M/P272H		NO	NO
4		H275Y	I223M/P272H	NO	N295S	
5	NO	H275Y	I223M/P272H		N295S	NO
6		H275Y	I223M/P272H	NO	N295S	
7				NO		
8	NO	H275Y		H275Y		NO

a: only NA full gene was sequenced

b and *c*: both NA and HA full genes were fully sequenced

By the fourth passage, another mutation was detected. An amino acid substitution at position 295, asparagines to serine (N295S), in NA was detected in FPV that was passaged in the presence of oseltamivir and 50 μ M MI-701. As for FPV that was passaged in the presence of oseltamivir and 25 μ M MI-701, the mutation H275Y in NA appeared in the eighth passage. This was five passages later than the mutations that occurred in FPV passaged in the presence of oseltamivir alone. A double mutation (I223M/P272H) with amino acid substitution at position 223, isoleucine to methionine (I223M), and proline to histidine at position 272, was detected in FPV that passaged in the presence of oseltamivir and 10 μ M MI-701 in the third passage.

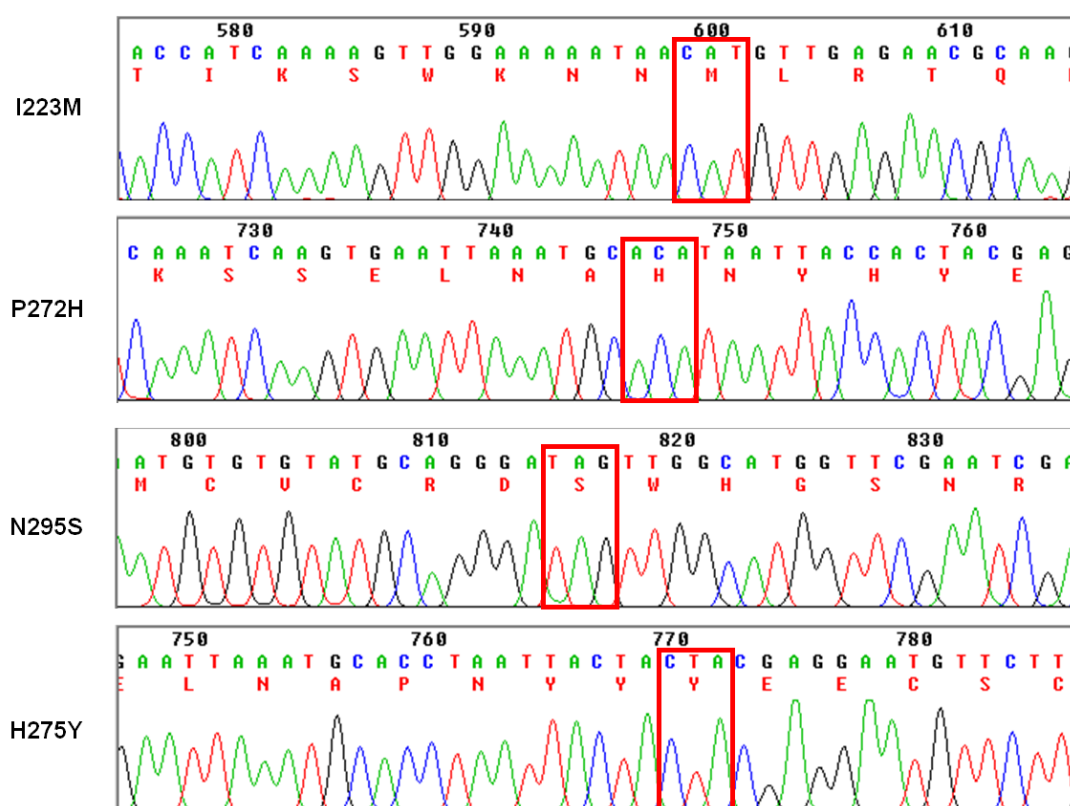
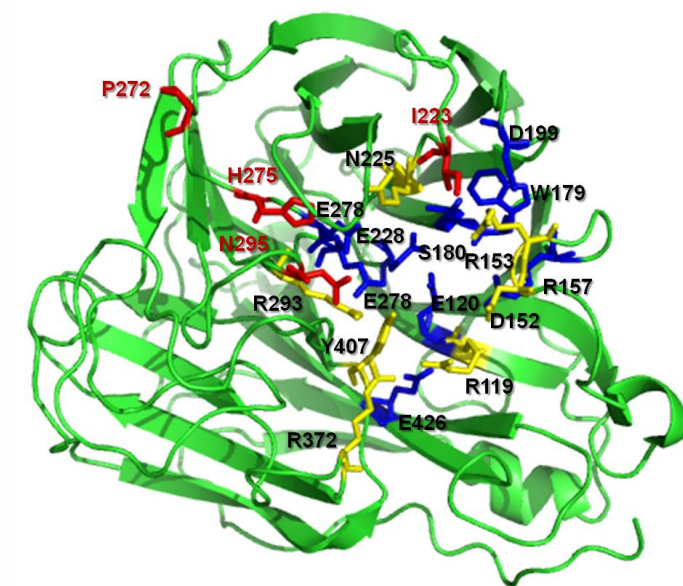


Fig. 4.19: Sequence analysis is represented in chromatogram. Four mutations, I223M, P272H, N295S and H275Y in NA are indicated using red box.

A



B

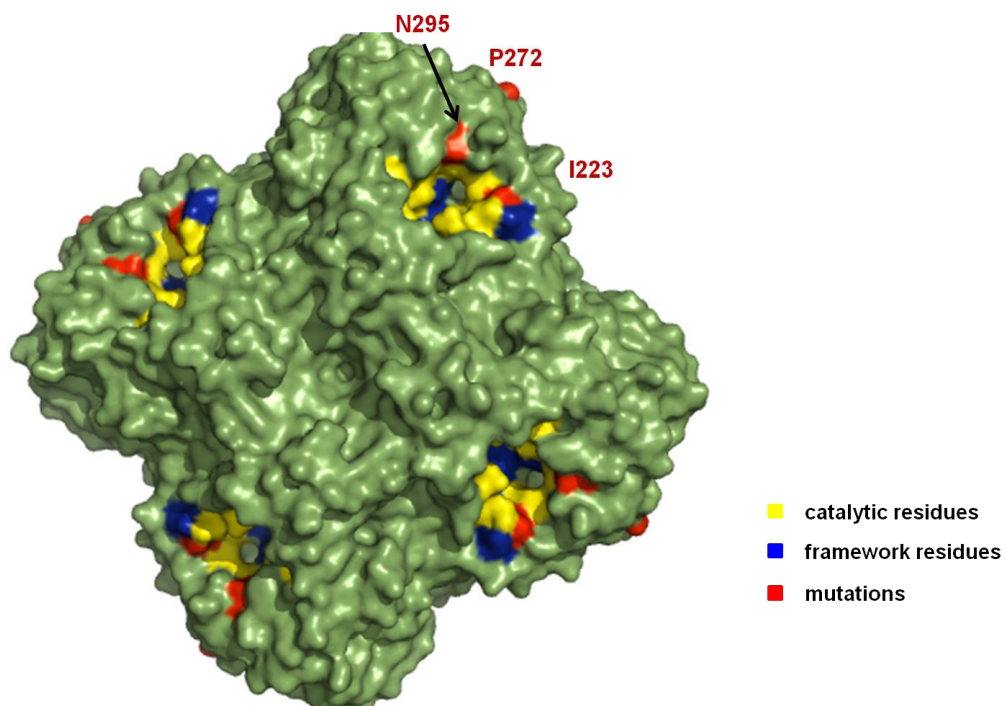


Fig. 4.20: Crystal structure of group-1 (N1) NA monomer in ribbons representation (A) and NA tetramer in surface representation (B). Catalytic residues in NA are shown in yellow, the framework residues in NA are shown in blue and the NA residues, I223, P272, H275 and N295 are shown in red. The H275 residue, which was located inside the active site, was not indicated in (B).

PDB accession codes. The crystal structure is available from the RCSB PDB under accession codes 2HTY for the avian influenza H5N1. (www.rcsb.org/pdb/explore/explore.do?structureId=2hty)

The four mutations on the virus, the four mutated residues, H275Y, I223M, P272H and N295S, together with critical residues in NA active site were projected onto the three-dimensional structure of NA derived from avian H5N1 (Fig. 4.20). The active site of influenza virus NA contains nine conserved catalytic residues: R119, D152, R153, R225, E277, R293, R372, and Y407 that directly interact with the substrate and 11 conserved framework residues: E120, R157, W179, S180, D/N199, I223, E228, H275, E278, N295, and E426 that support the catalytic residues. As shown in Fig. 4.20A, the three mutations at the positions 223, 275 and 295 were in the framework residues surrounding the catalytic residues, while the mutation at the position 272 was distal to the active site. Residues at the positions, 223, 295 and 272 were surface exposed, whereas the residue at position 275 was located inside of the active site, which could not be detected on the surface of NA.

4.5.4 Virus susceptibility to oseltamivir *in vitro*

An NA enzyme inhibition assay was used to characterize the susceptibilities of FPV variants to oseltamivir (Fig. 4.21).

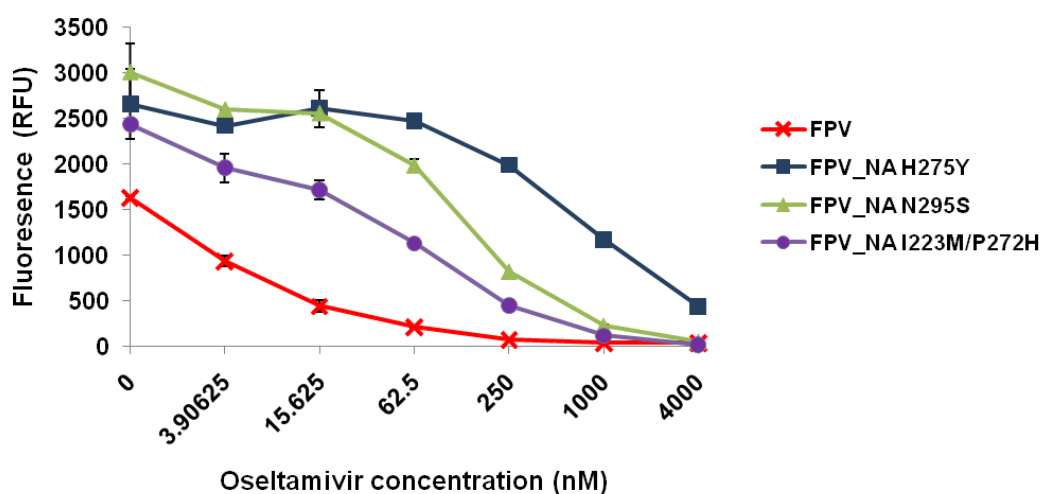


Fig. 4.21: NA enzyme inhibition assay of FPV mutants. The susceptibility of FPV variants to oseltamivir was determined by MUNANA-based enzyme inhibition assay. Viral dilution, which emits an equivalent RFU generated by 10 μ M 4-methylumbelliferone sodium salt (4-MUSS) was selected afterwards for NA enzyme inhibition assay. Viruses were incubated at 37°C for 30min with 4mM of oseltamivir and then 30min with fluorogenic MUNANA substrate at a final concentration of 200 μ M. The fluorescence of released 4-methylumbelliferone (4-MU) was measured with an Epoch microplate spectrophotometer. (n = 3)

The concentration of oseltamivir that was required to inhibit 50% (IC₅₀) of NA enzymatic activity of FPV and FPV mutants was calculated and shown in Table 4.3. The oseltamivir IC₅₀ of FPV was 5.57nM, 50.69nM for the FPV_NA^{I223M/P272H} virus, 112.11nM for the FPV_NA^{N295S} virus and 784.23nM for the FPV_NA^{H275Y} virus. The single mutation H275Y in NA remarkably reduced the susceptibility to oseltamivir. The IC₅₀ of FPV_NA^{H275Y} virus to oseltamivir was 140-fold increased, whereas the IC₅₀ of virus with single mutation N295S in NA and double mutations I223M/P272H in NA to oseltamivir were moderately increased, approximately 20-fold and 9-fold, respectively.

Table 4.3: Susceptibility of FPV mutants to oseltamivir.

Virus	NA enzymatic inhibition	
	Oseltamivir IC ₅₀ ± SD (nM)*	Fold increase**
FPV	5.57 ± 1.12	
FPV_NA ^{H275Y}	784.23 ± 275.24	140.8
FPV_NA ^{N295S}	112.11 ± 15.63	20.13
FPV_NA ^{I223M/P272H}	50.69 ± 0.35	9.1

* Mean±SD was derived from two independent measurements.

** The reduction fold in IC₅₀ was calculated by dividing the IC₅₀ of FPV mutant by the IC₅₀ of FPV wild type.

4.5.5 Biological characterization of FPV variants

The effects of the NA mutations H275Y, N295S and I223M/P272H on the fitness of the viruses were determined by comparing their growth kinetics with those of FPV wild type viruses.

4.5.5.1 Growth kinetics of FPV variants in cell cultures

The growth kinetic of FPV variants in MDCK cells was examined to further analyze the impact of these NA mutations. As shown in Fig. 4.22, wild type FPV replicated efficiently in MDCK cells and rapidly reached approximately 10⁵ PFU/ml at 14h p.i., whereas FPV_NA^{N295S} and FPV_NA^{I223M/P272H} produced approximately 1000-fold less virus particles. Virus titer was 10-fold reduced in FPV_NA^{H275Y}-infected cells.

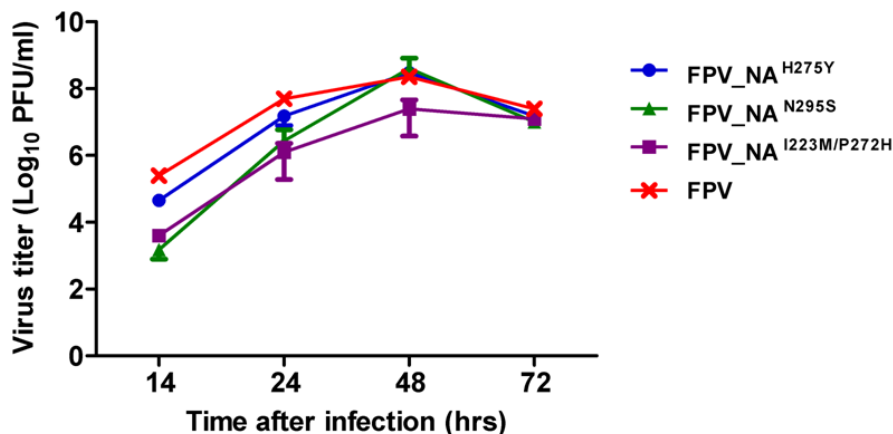


Fig. 4.22: Growth FPV wild type and FPV mutants in cell cultures. MDCK cells were infected with FPV wild type or FPV_NA^{H275Y}, FPV_NA^{N295S}, FPV_NA^{I223M/P272H} viruses at an MOI of 0.0001, respectively. Infected cells were incubated in DMEM infection medium at 37°C. At indicated time points, 14h, 24h, 48h and 72h p.i., virus-containing supernatants were collected and released viruses were titrated by plaque assay. (n=2)

48h after infection, all variants reached a comparable titer (approximately 10^8 PFU/ml) to that of the wild type virus, except for the FPV_NA^{I223M/P272H} virus, which produced 100-fold less progeny viruses.

4.5.5.2 Effect of furin inhibitor MI-701 on replication of FPV mutants

Although the presence of MI-701 did not prevent the development of oseltamivir-resistant mutations in FPV virus, no mutation related to the resistance to MI-701 was found. To investigate the effect of MI-701 on oseltamivir-sensitive and -resistant viruses, MDCK cells were infected with FPV wild type virus, FPV_NA^{H275Y}, FPV_NA^{N295S} or FPV_NA^{I223M/P272H} virus at a low MOI, respectively and infected cells were treated with MI-701 at a concentration of 50 μ M (Fig. 4.23).

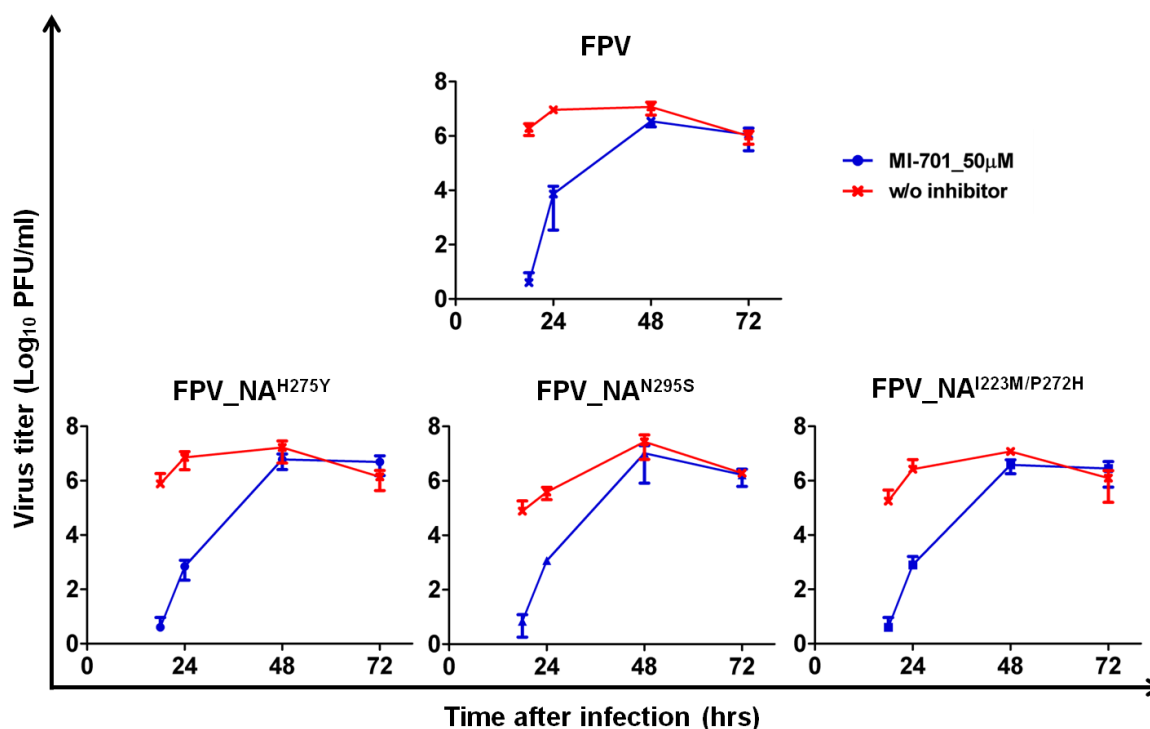


Fig. 4.23: Inhibitory efficacy of MI-701 on FPV mutants replication. MDCK cells were infected with FPV wild type virus (FPV) or FPV_NA^{H275Y}, FPV_NA^{N295S} or FPV_NA^{I223M/P272H} viruses at an MOI of 0.0001, respectively. Infected cells were treated with 50μM MI-701 or incubated in DMEM medium (w/o FCS) in the absence of inhibitor. At indicated time points, 18h, 24h, 48h and 72h p.i., virus-containing supernatants were collected and released viruses were titrated by plaque assay.

As shown in Fig. 4.23, treatment with 50μM MI-701 significantly inhibited the replication of both FPV wild type virus and its mutant viruses FPV_NA^{H275Y}, FPV_NA^{N295S}, FPV_NA^{I223M/P272H} at 18h p.i., which indicated that furin inhibitor MI-701 could be a potential drug against the infection of oseltamivir-resistant HPAIV.

Above all, it was demonstrated that the presence of oseltamivir and 25μM furin inhibitor MI-701 suppressed the development of an oseltamivir-resistant mutation. In the presence of oseltamivir and furin inhibitor MI-701, a mutation N295S and a double mutation I223M/P272H were detected in NA in the early virus passages. However, they exhibited mild reduction of susceptibility to oseltamivir and reduced or compromised replication ability in MDCK cells.

5 Discussion

The targets of antiviral drugs are either virus-encoded proteins or host factors that are essential for virus replication. It is well known that proteolytic processing of HA is an absolute requirement for influenza A virus infection. The responsible HA activating proteases were elucidated during the last decades. These proteases are normally provided by the host organism and occasionally by individual co-infecting microorganisms (Böttcher-Fiebertshäuser et al., 2013). The application of specific protease inhibitors seems to be possible unless inactivation of the protease causes severe adverse effects in organisms.

5.1 Furin as a drug target for prevention of HPAIV infection

Furin is a well-studied key protease which converts numerous biologically inactive protein precursor molecules into their active forms. It cleaves HA0 of highly pathogenic avian influenza virus (HPAIV) at a defined multibasic amino acid motif. The cleavage mainly occurs in the TGN before the virus particles are assembled at the plasma membrane (Fig. 1.8). Since furin is ubiquitously expressed in nearly all cells and tissues (Seidah et al., 1994), it supports the spread of HPAIV infections from endothelial cells of the respiratory tract to practically all tissues and organs under natural conditions. The spread of infection primarily occurs along endothelial cells of the blood vessel system, and thus causes systemic infections in the organisms with severe outcomes (Feldmann et al., 2000; Liem et al., 2009; Puthavathana et al., 2005). Due to furin's indispensable role during the infection of HPAIV, the efficient inhibition of furin at an early stage is thought to be a promising treatment for HPAIV infections. However, application of furin inhibitors will only be successful when other proteases unaffected by furin inhibitor can compensate for the lack of furin. Additionally, these compensatory proteases must not activate the HA of HPAIV (Garten & Klenk, 2008).

Early study showed that furin knockout mice die at an early embryonic stage because of severe defects, which indicates the physiological importance of furin during embryonic development. In contrast to the embryonic lethality of furin deficient mice, no obvious adverse effects were observed in adult transgenic mice with an interferon inducible knockout system for furin (Roebroek et al., 1998, 2004). A nearly complete elimination of furin in the liver resulted in no overt deviations from normal morphology. The natural substrates of furin, such as the proproteins of insulin receptor, albumin, α_5 -

integrin, lipoprotein receptor-related protein, vitronectin, and of α_1 -microglobulin/bikunin, were correctly proteolytically processed in the absence of furin. This indicates that an obviously redundancy for proteolytic processing of physiological proproteins provided by other members of the PCs family exist in the liver (Roebroek et al., 2004). Altogether, the absence of any severe phenotype of furin deficient adult mice raises the possibility that the treatment of HPAIV infections with furin inhibitors will be successful. Additional support for a possible application of furin inhibitors as potential drugs in adult organisms comes from furin knockout cell lines, like furin-deficient LoVo and CHO (FD11) cells, which are fully viable despite furin's inability to cleave any substrate.

The concept of furin blockage by specific inhibitors as an antiviral drug therapy has been suggested by Garten and co-workers since 1992. Initially the instable furin inhibitor dec-RVKR-cmk was used (Hallenberger et al., 1992; Stieneke-Gröber et al., 1992; Garten et al., 1994), although now it has been replaced by much more stable and efficient compounds, such as MI-701 (Becker et al., 2010; 1012).

5.2 Development and evaluation of furin inhibitors

The known furin inhibitors can be categorized into following groups: (I) peptide derivatives compounds including, such as peptidomimetics containing the furin recognition motif, (II) small synthetic non-peptidic compounds, and (III) macromolecular inhibitors, including naturally occurring proteins and genetically modified proteins (see 1.4.3.1.1 and Table 5.1).

Table 5.1: Reported furin inhibitors

Types	Inhibitors	K_i (nM)	Refs
Macromolecules*			
(Proteins)	Serine protease inhibitor, Serpin B8	53800	[1]
	α 1-Antitrypsin Portland (α 1-PDX)	1.4	[2]
	Turkey ovomucoid mutant (A15R, T17K, L18R)**	110	[3], [4]
	Eglin C variant	1.6	[5], [4]
Peptides			
	furin prodomain derived, 83-mer	154	[6]
	hFurin39–62, DYYHFWHRGVTKASLSPHRPAHSR	900	[7]
	ProSAAS derived, VLGALLRVKR-NH ₂	800	[8]
	DSHAKRHHGYKRKFHEKHHSRGGYRSNYLYDN ¹	1980	[9], [10]
	DSHAKRHHGYKRKFHEKHHSRGGY ²	2980	[9], [10]
	Polyarginine, Nona-L-Arginine	42	[8]
	Nona-D-Arginine	1.3	[11]
Peptidomimetica			
	Dec-RVKR-cmk	irreversible	[12]
	RKKR-CH=NOH	55400	[7], [10]
	Cyclo[CGTRVKR-(Ψ CH ₂ NH)-EKRIDRTRSFC]	800	[10], [13]
	Decanoyl-RVKR-(Ψ COCH ₂)-AVG-NH ₂	3.4	[14]
Small molecules			
(Non-peptidic compounds)	Andrographolide, 3 α , 14 α / β 19 Trisuccinyl mono-pyridine salt	2600	[10], [15]
	Cu(TTP)Cl ₂ , 4-[p-Tolyl]-2,2':6',2" terpyridine	5000***	[10], [16]
	Cu(MPT)Cl ₂ , 4-[4-Methoxy phenyl]2,2':6',2" terpyridine	5100***	[10], [16]
	Guanidinylated aryl 2,5-dideoxystreptamine derivatives 1e	6	[17]

[1] Dahlen et al., 1998; [2] Jean et al., 1999; [3] Lu et al., 1993; [4] Bontemps et al., 2007; [5] Liu et al., 2004; [6] Basak et al., 2010; [7] Basak & Lazure, 2003; [8] Carmeron et al., 2000; [9] Basak et al., 1997; [10] Basak, 2005; [11] Kacprzak et al., 2004; [12] Hallenberger et al., 1992; [13] Villemure et al., 2003; [14] Angliker, 1995; [15] Basak et al., 1999; [16] Podsiadlo et al., 2004; [17] Jiao et al., 2006.

* Macromolecules contain naturally occurring and genetically modified proteins. ** A15R, T17K and L18R are amino acid substitution mutations. *** IC₅₀ value. ¹ Histatin 3. ² Histatin 5.

The first small peptidomimetic inhibitors were developed on the basis of the furin recognition motif in 1990s, e. g. decanoylated tetrapeptidyl-chloromethyl ketones like the commercially available dec-RVKR-cmk, which covalently binds to the catalytic site of furin (Garten et al., 1994; Stieneke-Gröber et al., 1992; Hallenberger et al., 1992; Henrich et al., 2003). Over the last five years, such peptidomimetic furin inhibitors have been further developed and optimized. In this thesis, a series of 4-amidinobenzamide-based inhibitors were screened for an enhancement of inhibitory efficacy. Most compounds were well tolerated by MDCK cells up to a concentration of

50 μ M. In particular, the compound MI-701 was non-toxic to the cells even at higher concentrations (up to 400 μ M) (Fig. 4.2). However, the compounds MI-259, MI-232, MI-233 and MI-283 (structures are shown in Table S3 in supplementary) containing longer saturated or unsaturated P5 acyl residues with more than 11 carbon atoms showed considerable reduction of cell viability and thus they were not further investigated (Fig. 4.1). Cleavage of HA was inhibited to different extents by the listed furin inhibitors (Fig. 4.4). An optimal suppression of the spread and propagation of H7N1 and H5N1 viruses was achieved by compound MI-701. This inhibitor proved to be stable in cultured MDCK cells for several days (Fig. 4.3). Approximately 50% of MI-701 could be recovered from cell supernatants after 96h. On one hand, this observation underlines the stability of this compound. On the other hand, this fact explains the difficulties with the internalization of MI-701 into host cells. Inhibition of the intracellular activation of HA of HPAIV required a concentration of MI-701 in the micromolar range, whereas the inhibition of activation of the PA of Anthrax toxin on the cell surface required a much lower concentration of MI-701 in the nanomolar range. Hence, furin inhibitors, which are able to efficiently reach the lumina of the compartments of the intracellular secretory pathway, may have an enhanced inhibitory efficacy against HPAIV infections.

The following modifications were made to further improve the potency of the furin inhibitor MI-701: (i) N-terminal attachment of various cell penetrating peptides (CPPs), (ii) coupling of additional of D-arginine residues to the P4 arginine, (iii) replacement of valine at position P3 by tert-leucine and (iv) replacement of the P1 position 4-amidinobenzylamide group in inhibitor MI-1148 by agmatine or noragmatine (structures and results are shown in Table S4 and Fig. S5 in supplementary).

Some of the newly designed compounds such as MI-1148, the P3 Tle-analogue of the Val containing inhibitor MI-701, possesses a similar inhibitory potency as MI-701. Modifications the P5 or P1 group of MI-1148 did not enhance the antiviral activity. The attachment of CPPs facilitated the delivery of a wide variety of cargoes such as proteins, peptides, oligonucleotides, drugs, liposomes and micelles (Järver & Langel, 2006; Madani et al., 2011), but our data and data by other researchers showed that the CPP transport and penetratin induced toxicity in the cells (Saar et al., 2005). Several polyarginine-containing peptides proved to be potent furin inhibitors, such as the arginine-rich peptides modelled from the extended HA cleavage motif of H5N1 influenza virus with a K_i value of 23nM (Shiryaev et al., 2007) and the nona-D-arginine

amide (D9R) with a K_i value of 1.3nM (Kacprzak et al., 2004). In this work, attachment of one or four D-arginine residues to the N-terminal P4 arginine (MI-1184 and MI-1187) enhanced the antiviral activity against HPAIV infection.

Pharmacokinetic studies of optimized furin inhibitors still remain uncompleted. Adsorption and internalisation of MI-701 into various cells, its distribution in tissues, organs and in the whole organism, and its metabolism, degradation and elimination are of interest. Furthermore, different routes of MI-701 administration must also be examined.

5.3 Binding of furin inhibitors

The binding mode of 4-amidinobenzylamide based furin inhibitors to the active cleft of furin was initially modelled to better understand their interaction (Fig. 5.1) (Becker et al., 2010). Moreover, very recently the experimental crystal structures of inhibitors MI-227 and MI-0052 in complex with human furin have been disclosed (Dahms et al., 2014). The P1 amidinobenzylamide (Amba) group, which mimics the arginine side chain, deeply inserts into the S1 pocket of furin forming tight hydrogen bonds with the carbonyl oxygen atoms of P256 and A292 and an electrostatic interaction with D306. The P2 arginine side chain electrostatically interacts with D154 at the furin S2 pocket and forms additional interactions with N192 and D228. The backbone P3 valine binds to G255. The arginine side chain at P4 is stabilized by charged-assisted hydrogen bonds to E236, D264, Y308 and the carbonyl oxygen of G265. The N-terminal positively charged guanidinomethyl group attached in meta position to the P5 phenylacetyl group of inhibitor MI-0052 forms an electrostatic interaction with E236, a water mediated hydrogen bond to D233, and an additional hydrogen bond to the carbonyl of V231 (Fig. 5.1B) (Dahms et al., 2014).

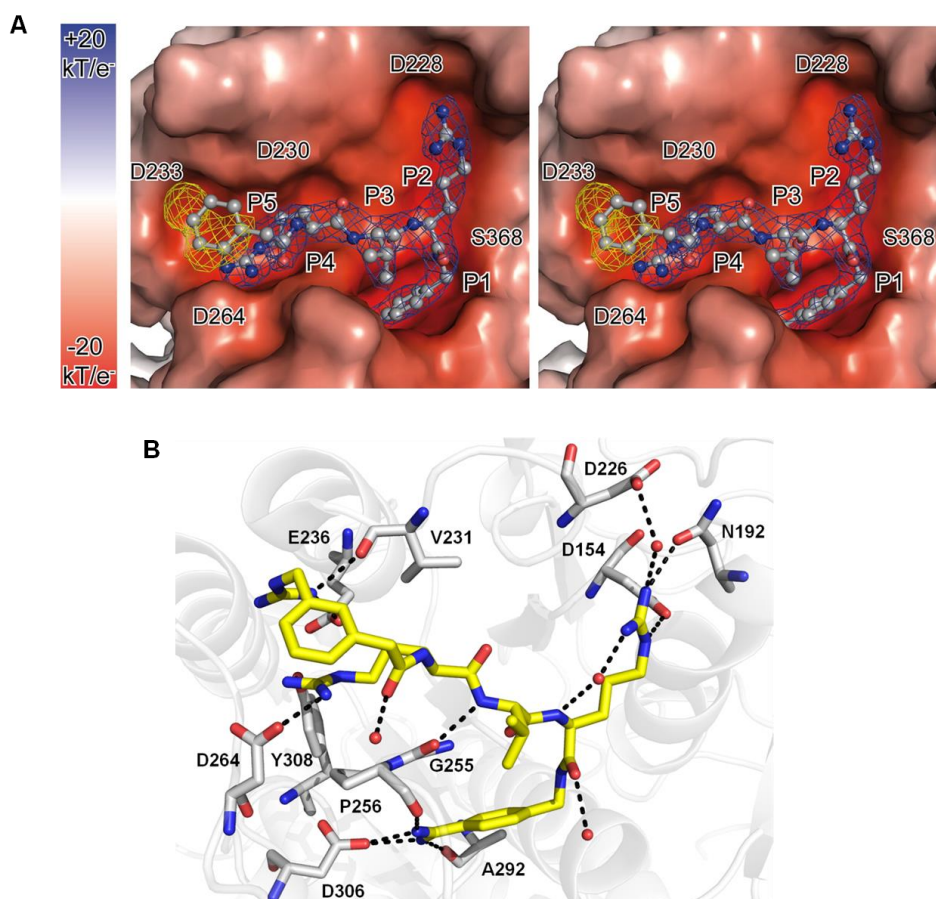


Fig. 5.1: Binding mode of synthetic inhibitors in the active site of human furin. (A) Stereoview of the complex between human furin presented with its solvent-exposed surface and inhibitor MI-227 (phenylacetyl-Arg-Val-Arg-4-amidinobenzylamide, abbreviated: Phac-RVR-Amba), whereby the inhibitor is shown with grey carbon atoms (nitrogen and oxygen atoms are shown in blue and red, respectively). The surface of furin is coloured according to the electrostatic surface potential of the catalytic domain. (B) Binding of inhibitor MI-0052, showing important hydrogen bonds. Compound MI-0052 (3-guanidinomethyl-phenylacetyl-Arg-Val-Arg-4-amidinobenzylamide, abbreviated: 3-Guame-Phac-RVR-Amba) is a close analogue of the P5 para-substituted furin inhibitor MI-701 (4-Guame-Phac-RVR-Amba), containing the N-terminal P5-guanidinomethyl group in meta position of the phenylacetyl residue. The backbone of furin is given as a cartoon representation. The carbon atoms of important furin residues involved in inhibitor binding are shown in grey. Figure (A) is taken from Dahms et al., 2014. Figure (B) was kindly provided by Kornelia Harges, Institute of Pharmaceutical Chemistry, Philipps University Marburg. The structure of MI-227 and MI-0052 are shown in Table S3 in supplementary.

5.4 Combinatorial drug treatment

In the areas of disease prevention and treatment, the use of existing drugs in combination is an important complement to monotherapy. Combination therapy has been long used for the treatment of cancer as well as diseases caused by infectious

pathogens. Streptomycin was combined with different drugs and antibiotics, including isoniazid and rifamycins to improve the therapeutic effectiveness for the treatment of *Mycobacterium tuberculosis* (Daniel, 2006). A combination of interferon plus ribavirin is currently recommended for treatment of patients with chronic hepatitis C (Hauser et al., 2014). The highly active anti-retroviral therapy (HAART) used for treatment of human immunodeficiency virus type 1 (HIV-1) is the most successful example of a combination therapy, and has changed HIV infection from an incurable disease to a chronic one (Ascierto & Marincola, 2011).

Combination therapy against influenza viruses has also been intensively studied. Early studies showed that combination of ribavirin with M2 ion channel inhibitors rimantadine or amantadine resulted in additive to synergistic antiviral effects on the influenza A viruses, including the subtypes H1N1, H3N2, H7N7 and H5N1 (Galegov et al., 1977; Hayden et al., 1980; 1984). Combination of the neuraminidase inhibitors zanamivir or oseltamivir with M2 ion channel inhibitors adamantanes resulted in enhanced therapeutic effects against different influenza A viruses subtypes, inclusively the pandemic 2009 H1N1 influenza virus (Madren et al., 1995; Smees et al., 2009; Govorkova et al., 2004). Triple combination treatment with oseltamivir, amantadine and ribavirin was proven to be highly synergistic against multiple influenza viruses, including human seasonal influenza H1N1, H3N2 viruses and the avian influenza virus H5N1 (Nguyen et al., 2009). The inhibitory efficacy of this triple combination therapy was evaluated *in vitro* and *in vivo* against the infection of amantadine-, rimantadine- and oseltamivir-resistant influenza viruses H1N1 (Nguyen et al., 2012, 2010). Subsequent pilot study in patients showed that this triple combinatorial medication had comparable pharmacokinetics as monotherapy and could be administered safely in immunocompromised patients (Seo et al., 2013).

The recent discovery of drugs with novel targets enhances the possibilities of influenza medications, including zoonotic influenza caused by HPAIV. Several novel anti-influenza compounds are in various phases of clinical development. One of these, peramivir is an intravenously administered neuraminidase inhibitor. A combination of the new neuraminidase inhibitor peramivir with ribavirin reduced H1N1 virus infection in cell cultures and in mice (Smees et al., 2002). Favipiravir (T-705) has a mechanism of action that is not fully understood, but it is suggested that it targets influenza virus RNA-dependent RNA polymerase. The combination of favipiravir, with peramivir or oseltamivir, improved the survival of influenza A H1N1 infected mice and induced

additive effects against the pandemic 2009 H1N1 influenza A virus in mice (Smee et al., 2010; Tarbet et al., 2012, 2014). Another novel combination therapy is based on the MEK inhibitor, which is a host Ras-dependent Raf/MEK/ERK mitogen-activated protein (MAP) kinase signaling pathway inhibitor. This host kinase cascade is involved in influenza virus replication. The combination of the MEK inhibitor with oseltamivir led to a synergistic effect against pandemic 2009 H1N1 influenza A virus (Haasbach et al., 2013). In addition, a combination of the host protease inhibitor BAPA and oseltamivir efficiently exhibited inhibitory potency against TMPRSS2-activated influenza A virus H1N1 and influenza B virus replication in airway epithelial cells (Böttcher-Friebertshäuser et al., 2012).

However, to date, few studies have evaluated the therapeutic effects of combination therapy on HPAIV infection. The work of Ilyushina *et al.* showed that oseltamivir-ribavirin combination therapy provided a survival advantage for mice infected with HPAIV H5N1 (Ilyushina et al., 2007). The work of An *et al.* showed that the triple combination of neuraminidase inhibitor with two immunomodulatory inhibitors statins and fibrates exhibited synergistic effects against the HPAIV H5N1 infection in mice (An et al., 2011).

This work showed that treatment with MI-701 and oseltamivir in combination resulted in significant virus titer reduction at 72h p.i. and some triple combinations of MI-701, oseltamivir and ribavirin completely blocked HPAIV KAN-1 virus yield at 72h p.i.. In contrast, the inhibitory efficacy of single drug treatment was no more observed at 72h p.i. (Fig. 5.2). Synergy analysis indicated that the combination of MI-701 and oseltamivir was largely additive against the HPAIV FPV, whereas synergy was observed in almost all tested concentrations of oseltamivir and MI-701 when they were combined with 10 μ M ribavirin (Fig. 4.15). This indicates that the antiviral activity of each drug in triple combination was increased compared to that in double combination or as a single drug. Importantly, no antagonism was observed for any combinations that were examined in this work, suggesting that combination treatment with MI-701 and oseltamivir or together with ribavirin is unlikely to lead to reduced efficacy compared to single drug treatment. Although the synergy seen in cell culture would be different from that derived in mice experiments, these results should be helpful by suggesting the concentrations of each drug that maybe needed for successful combination treatment in mice.

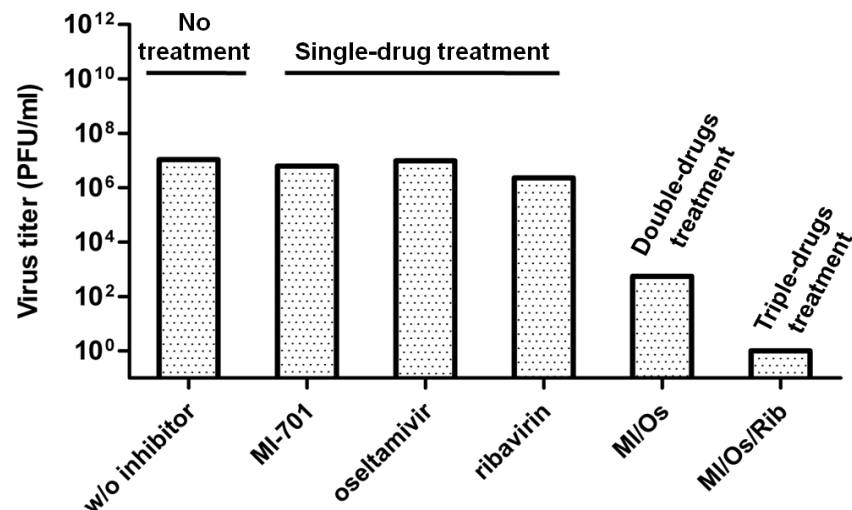


Fig. 5.2: Reduction of KAN-1 virus yield at 72h p.i. after inhibitor treatment. This figure is based on the data of figure 4.11B and figure 4.12B. Virus titer at 72h p.i. in cells treated with 50 μ M MI-701, 0.5 μ M oseltamivir, 25 μ M ribavirin alone or with 50 μ M MI-701 and 0.5 μ M oseltamivir (MI/Os), or with 50 μ M MI-701, 0.5 μ M oseltamivir and 25 μ M ribavirin in triple combination (MI/Os/Rib) were selected and compared to the virus titer in untreated infected cells.

An important factor for a successful treatment of an acute infectious disease is the starting point of medication. The work of Smee *et al.* showed that almost the same concentration of peramivir, oseltamivir or ribavirin was needed to inhibit influenza A H3N2 induced CPE when treatment was started at 0h to 12h p.i., whereas a higher concentration of each drug was required to achieve 50% inhibitory effect when treatment started at 24h p.i. or 24h before infection (Smee *et al.*, 2001). The work of Furuta *et al.* showed that favipiravir did not suppress virus yield when it was added 1h before infection or 6h to 10h after infection (Furuta *et al.*, 2005).

In this work it was demonstrated that treatment of MI-701, oseltamivir and ribavirin in combination at 0h to 6h p.i. was necessary to efficiently suppress the later rounds of virus replication (Fig. 4.16).

5.5 Development of drug-resistance during drug treatment

Selection of adamantane-resistant mutants occurred in about 30% of treated patients (Shiraishi *et al.*, 2003; Harper *et al.*, 2005). These resistant viruses were generated rapidly and frequently remain fully fit and transmissible (Herlocher *et al.*, 2002). Since 2003, the global spread of adamantane-resistant influenza A (H3N2) virus strains and isolation of adamantane-resistant pandemic 2009 H1N1 viruses during the 2009

influenza pandemic have made this class of drugs basically useless for the treatment of influenza infections. Therefore, M2 inhibitors are not recommended for treatment or prophylaxis of currently circulating influenza A virus strains (CDC³). Current options for influenza treatment are limited to neuraminidase inhibitors. However, cases of resistance to oseltamivir were observed in patients infected with the pandemic 2009 H1N1 virus and during treatment or prophylaxis for HPAIV H5N1 infection. Serial passages of human influenza A virus H3N2 in the presence of oseltamivir led to the occurrence of three amino acid substitutions, A28T in HA1 and R124M in HA2, R292K in NA. The mutations in HA caused a 10-fold decrease in susceptibility to oseltamivir, whereas the mutation R292K in NA resulted in a high level of resistance to oseltamivir (Tai et al., 1998). Passage of HPAIV H5N1 under the pressure of oseltamivir led to the development of a mutation H275Y in NA, and in one strain this mutant was combined with the mutation I223M. Both mutations resulted in significantly reduced oseltamivir susceptibility (Hurt et al., 2009). Therefore, new strategies, such as combination therapy, which can reduce the emergence of drug-resistant viruses, would be beneficial (Govorkova & Webster, 2010; Hayden, 2013).

The work of Ilyushina *et al.* showed that drug-resistant mutants emerged after five sequential passages of human influenza A/Hong Kong/156/97 (H5N1), A/Nanchang/1/99 (H1N1), and A/Panama/2007/99 (H3N2) viruses in MDCK cells in the presence of either the M2 inhibitor amantadine or neuraminidase inhibitor oseltamivir (Ilyushina et al., 2006).

In the present work HPAIV subtype H7N1 was serially passaged in the presence of either oseltamivir or furin inhibitor MI-701 alone in MDCK cells. In parallel, the same virus was serially passaged in the presence of both oseltamivir and MI-701. Propagation of HPAIV H7N1 virus in the presence of increasing concentration of furin inhibitor MI-701 did not induce the development of any mutations in HA or in NA (Fig. 4.17 and Table 4.2). Viruses that were passaged under the pressure of oseltamivir rapidly developed the mutation H275Y in NA (Fig. 4.18 and Table 4.2). And the mutation H275Y in NA occurred five passages later in the presence of oseltamivir and MI-701 than it occurred in the presence of oseltamivir alone. Besides the mutation H275Y, a single mutation N295S and a double mutation I223M/P272H in NA were also detected when viruses passaged in the presence of both MI-701 and oseltamivir.

The H275Y NA mutation is one of the most frequently occurring oseltamivir-resistant mutations in influenza A viruses. It is located in the framework region of the NA gene

and confers high resistance to oseltamivir (Govorkova, 2013) (Fig. 4.20 and Fig. 5.3). Early studies suggested that seasonal influenza A viruses H1N1 and H3N2 with the H275Y mutation were less infectious and less transmissible in humans (Carr et al., 2002; Ives et al., 2002). However, the spread of seasonal influenza A virus A/Brisbane/59/2007 with this mutation during the 2007-2009 influenza season in the absence of drug pressure indicated that the H275Y mutation may not compromise the virus fitness and transmissibility in humans (Baz et al., 2010). It was also described that HPAIV subtype H5N1 carrying the H275Y mutation in NA replicated less efficiently in the upper respiratory tract of ferrets than the wild type virus H5N1 (Le et al., 2005). In this work the dose of oseltamivir required for 50% inhibition of neuraminidase activity (IC_{50}) of HPAIV FPV_NA^{H275Y} virus was approximately 780nM, which was 140-fold higher compared to that of the wild type virus (Table 4.3). According to the WHO guideline, an influenza A virus with > 100-fold reduced IC_{50} to oseltamivir is highly resistant, whereas 10- to 100-fold reduced IC_{50} indicates reduced susceptibility. Therefore, it was demonstrated that HPAIV FPV containing the mutation H275Y confers a high resistance to oseltamivir. Replication of this mutant virus in cell cultures was comparable to the wild type virus (Fig. 4.22), which so far suggested that acquisition of H275Y mutation of HPAIV FPV did not affect the virus fitness. The mechanism for undiminished fitness of the H275Y-containing oseltamivir-resistant viruses is not completely understood, but it was suggested that the reduced substrate affinity of the NA with H275Y mutation may have restored the balance between HA receptor-binding and NA receptor-cleaving functionalities that was altered by an earlier NA mutation that increased substrate affinity (Hayden & de Jong, 2011).

The mutation N295S is also located in the framework region of NA (Fig. 5.3). Compared to the mutation H275Y it was less resistant to oseltamivir (Kiso et al., 2004; Le et al., 2005). Although the development of the mutation N295S in NA was detected in very early passage in this work, the N295S-containing FPV variant exhibited mild resistance to oseltamivir and reduced virus yield at 18h p.i. and 24h p.i. compared to that of the wild type virus.

The mutation P272H is located neither in the framework region nor in the catalytic region in the NA gene and so far it has not been observed in any other influenza virus strains (Fig. 4.20). Therefore, it is unclear if the mutation P272H is capable of conferring resistance to oseltamivir. The I223 residue is highly conserved across all influenza A and B viruses, and forms the hydrophobic pocket of the NA active site

together with arginine, serine and glutamic acid at position 224, 246, and 276 (Colman et al., 1993). The mutation at the 223 position results in the loss of the hydrophobic interaction between the side chain of I223 and oseltamivir (Hurt et al., 2009). So far different amino acid substitutions at the residue I223 have been reported. Influenza A virus H3N2 with mutation I223V was isolated from an immunocompromised child. The single I223V mutation resulted in a mild resistance to oseltamivir, whereas association with the primary oseltamivir-resistant mutation E120V led to approximately 300-fold reduction of susceptibility to oseltamivir (Baz et al., 2006). The I223R mutation was detected alone or along with H275Y in patients infected with the pandemic 2009 H1N1 virus. The I223R mutation alone resulted in reduced susceptibility to oseltamivir, zanamivir and peramivir. Enhanced resistance was also observed for I223R/H275Y recombinant viruses (Pizzorno et al., 2012). Another study showed that passaging HPAIV H5N1 in the presence of neuraminidase inhibitor induced the development of H275Y mutation in the NA gene. One strain carried a H275Y/I223M double mutation, which significantly reduced the susceptibility to oseltamivir (Hurt et al., 2009). This work showed that FPV with the double mutation I223M/P272H exhibited a mild decrease in susceptibility to oseltamivir (Table 4.3), and virus replication was slightly compromised in cell cultures compared with the wild type virus (Fig 4.22).

Although the development of oseltamivir-resistant mutations was not completely blocked in the presence of oseltamivir and furin inhibitor, the emergence of highly oseltamivir-resistant mutation H275Y was significantly delayed. It should be noted here that the initial concentration of oseltamivir influences the velocity of the development of oseltamivir-resistant mutations. Viruses passaged in the presence of oseltamivir with a higher initial concentration developed resistant mutation H275Y by the third passage, whereas viruses passaged with lower initial concentrations of oseltamivir did not develop resistant mutations before passage five (data not shown). Therefore, it is of great interest to examine the development of resistance in the presence of MI-701 and oseltamivir, and the concentration of oseltamivir starts at $0.005\mu\text{M}$, which is the 50% inhibitory concentration for the virus determined by NA enzyme inhibition assay.

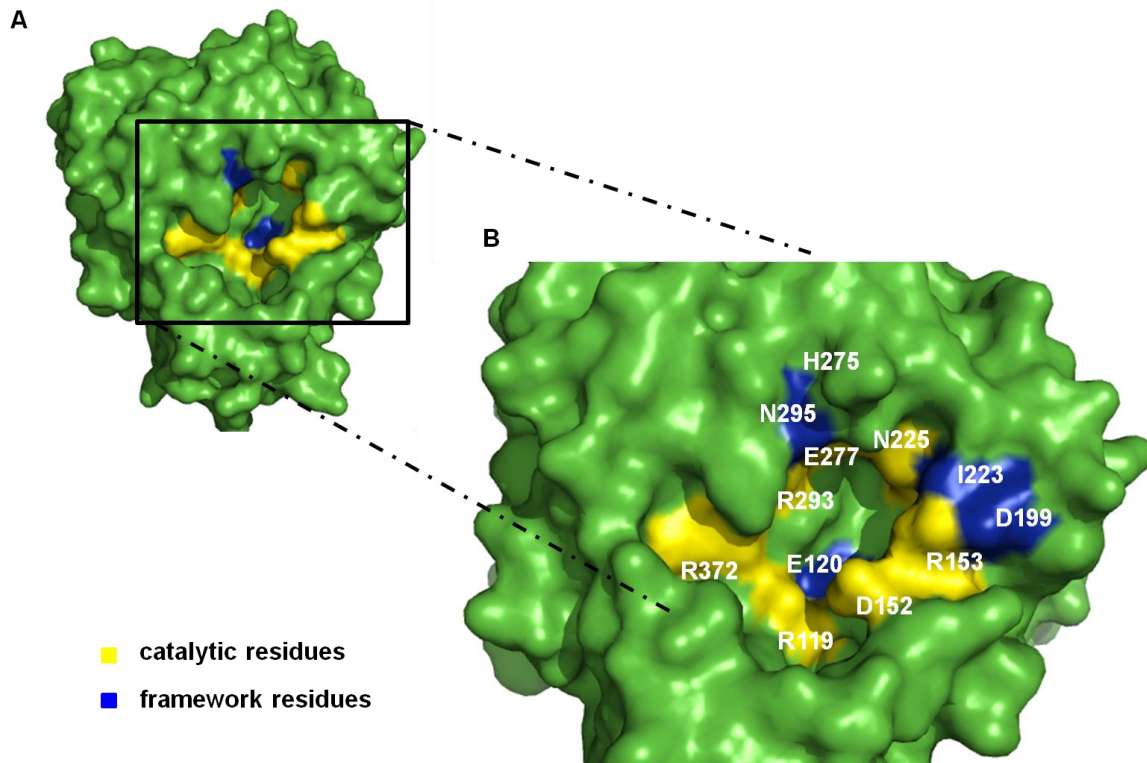


Fig. 5.3: Crystal structure of NA monomer. (A) NA monomer excised from an NA-tetramer is shown in surface representation. (B) Detailed view of NA catalytic domain is presented. Several amino acids are labelled with the number of their amino acid positions. Amino acid substitutions at these positions have been reported to confer susceptibility to neuraminidase inhibitors (N1 numbering) (Lackenby et al., 2008). The amino acids in the catalytic site of NA are indicated in yellow and amino acids belonging to the framework residues are shown in blue. The crystal structure is available from the RCSB PDB under accession codes 2HTY for the avian influenza H5N1.

Moreover, replication of FPV wild type or FPV mutants in MDCK cells in the presence of furin inhibitor MI-701 was suppressed in the same way, suggesting that furin inhibitors should be an alternative antiviral drug for treatment of oseltamivir-resistant HPAIV infection (Fig. 4.23).

5.6 Furin inhibitors block other viruses and bacterial pathogens

Currently, most prophylactic and therapeutic approaches are virus specific. Development of inhibitors with a broad substrates spectrum would be beneficial for the treatment of a wide range of severe diseases.

Furin is involved in processing the precursors of many other infectious pathogens (See 1.3.1). Besides the HA protein of HPAIV, furin is responsible for the activation of many precursors from different virus families, such as the glycoprotein of Ebola virus (EBOV)

and Marburg virus (MARV), which belongs to the family *Filoviridae* (Volchkov et al., 1998, 2000), the membrane protein of Dengue virus (DENV) (Keelapang et al., 2004) from the family *Flaviviridae*, the fusion protein of Newcastle disease virus (NDV) (Fujii et al., 1999) and respiratory syncytial virus (RSV) (Zimmer et al., 2001) from the family *Paramyxoviridae*, and glycoprotein of human immunodeficiency virus (HIV) from the family *Retroviridae* (Hallenberger et al., 1992). Furin is also responsible for the activation of various bacterial toxins, including the *Shiga* toxin (Garred et al., 1995) and *Diphtheria* toxin (Tsuneoka et al., 1993), the protective antigen of the Anthrax toxin (Klimpel et al., 1992), *Clostridium* α -toxin (Gordon et al., 1997) and *Pseudomonas* exotoxin A (Chiron et al., 1994) (Table 5.2).

Table 5.2: Cleavage motifs in the precursors of different infectious pathogens

	Infectious Pathogens	Genom	Family	Precursors	Reference
Viruses	Canine distemper virus, Measles virus, Newcastle disease virus, Mumps virus, Parainfluenza virus, Respiratory syncytial virus	(-) ssRNA	Paramyxoviridae	Fusion protein	[1], [2], [3], [4], [5], [6]
	Ebola virus, Marburg virus	(-) ssRNA	Filoviridae	Glycoprotein	[7], [8]
	Chikungunya virus	(+) ssRNA	Togaviridae	Glycoprotein	[9],
	SARS Coronavirus	(+) ssRNA	Coronaviridae	Glycoprotein	[10]
	Dengue virus, Japanese encephalitis virus, Tick borne encephalitis virus, West-Nile-virus	(+) ssRNA	Flaviviridae	Membrane protein	[11], [12], [13]
	Human immunodeficiency virus	(+) ssRNA	Retroviridae	Glycoprotein	[14]
	Epstein-Barr-virus, Human cytomegalovirus	dsDNA	Hepesviridae	Glycoprotein	[15], [16]
	Human papillomavirus	dsDNA	Papillomaviridae	Capsid protein	[17]
Bacteria	<i>Bacillus anthracis</i>			Anthrax toxin protective antigen	[18]
	<i>Clostridium perfringens</i>			Clostridium α -toxin	[19]
	<i>Corynebacterium diphtheriae</i>			Diphtheria toxin	[20]
	<i>Pseudomonas aeruginosa</i>			Pseudomonas exotoxin A	[20]
	<i>Shigella dysenteriae type 1</i>			Shiga Toxin	[21]

[1] Von Messling et al., 2004; [2] Watanabe et al., 1995; [3] Fujii et al., 1999; [4] Ortmann et al., 1994; [5] Bolt et al., 2000; [6] Zimmer et al., 2001; [7] Volchkov et al., 1998; [8] Volchkov et al., 2000; [9] Ozden et al., 2008; [10] Follis et al., 2006 [11] Keelapang et al., 2004; [12] Konishi et al., 2001; [13] Stadler et al., 1997; [14] Hallenberger et al., 1992; [15] Pellett et al., 1985; [16] Vey et al., 1995; [17] Richards et al., 2006; [18] Klimpel et al., 1992; [19] Gordon et al., 1997; [20] Chiron et al., 1994; [21] Garred et al., 1995.

In 1992 Hallenberger *et al.* showed that furin inhibitor dec-RVKR-cmk was able to inhibit the cleavage of HIV glycoprotein gp160 and reduced the yields of infectious virions (Hallenberger et al., 1992). The engineered furin inhibitor α_1 -PDX inhibited the activation of fusion protein of measles virus (MV) and the glycoprotein gB of human cytomegalovirus (HCMV) and thus led to a strong reduction of the virus titer (Watanabe et al., 1995, Jean et al., 1999). The work of Ozden *et al.* showed that furin inhibitor dec-RVKR-cmk inhibited the cleavage of the Chikungunya virus (CHIKV) glycoprotein E3E2 and significantly suppressed the virus infection in human muscle satellite cells (Ozden et al., 2008). The therapeutic effect of furin inhibitor dec-RVKR-cmk and hexa-D-arginine (D6R) for treatment of the chronic hepatitis B virus (HBV) infection was

studied by Pang and co-workers. Treatment with dec-RVCR-cmk directly inhibited HBeAg (Hepatitis B e antigen) secretion and thereby increased the expression of HBeAg precursor on the cell surface. This may terminate the host immune tolerance, and therefore it would be favourable for the early intervention in chronic HBV infection (Pang et al., 2013). In addition to the therapeutic effects against virus infections, furin inhibitors are also used for the treatment of bacterial infections. The work of Sarac *et al.* showed that furin inhibitor D6R blocked the activation of *Pseudomonas* exotoxin A (PEA) protein (Sarac et al., 2002).

The therapeutic effects of furin inhibitor MI-701 against different infectious pathogens were evaluated. The work of Becker *et al.* showed that furin inhibitor MI-701 potently inhibited the proteolytic activation of HPAIV HA and virus replication in cells cultures and the activation of Shiga toxin in HEp-2 cells (Becker et al., 2012). The syncytial formation in BHK-21 cells induced by the NDV strain Italien and RSV strain A2 was significantly suppressed in the presence of MI-701 from 10 μ M to 50 μ M, and release of NDV strain Italien was completely blocked during the course of experimentation (96h) in the presence of 50 μ M MI-701 (data not shown).

5.7 Conclusion

This thesis demonstrated the potent inhibitory efficacy of peptidomimetic furin inhibitors against HPAIV infections and the benefits of combinatorial drug treatments, which surpassed single drug treatments in cell cultures. Moreover, a significant suppression of emergency of oseltamivir resistant NA-variants was observed during double treatment with oseltamivir and furin inhibitor. These data provide a basis for further studying therapeutic efficacy of furin inhibitors in animal experiments before starting clinical trials.

6. Supplementary data

Table S1: Outbreak of HPAIV H7 subtypes in poultry since 1959.

Year	Location	Strain	Species affected
1963	England	A/turkey/England/63 (H7N3)	29,000 turkeys
1976	Victoria (Australia)	A/chicken/Victoria/76 (H7N7)	5800 chickens and ducks
1979	Germany	A/chicken/Germany/79 (H7N7)	600,000 chickens and 80 geese
1979	England	A/turkey/England/199/79 (H7N7)	9000 turkeys
1985	Victoria (Australia)	A/chicken/Victoria/85 (H7N7)	240,000 chickens
1992	Victoria (Australia)	A/chicken/Victoria/85 (H7N7)	18,000 chickens and ducks
1994	Queensland (Australia)	A/chicken/Queensland/667-6/94 (H7N3)	22,000 chickens
1997	Pakistan	A/chicken/Pakistan/447/95 (H7N3)	1,5 million chickens and other domestic birds
1997	New South Wales (Australia)	A/chicken/New South Wales/1651/97 (H7N4)	160,000 chickens and emus
1999-2000	Italy	A/turkey/Italy/99 (H7N1)	14 million chickens, turkeys, guinea-fowl quail, ducks, ostriches and pheasants
2002	Chile	A/chicken/Chile/2002 (H7N3)	700,000 chickens and turkeys
2003	Netherlands	A/chicken/Netherlands/2003 (H7N7)	> 34 million chickens and birds
2004	Canada	A/chicken/Canada-BC/2004 (H7N3)	17 million chickens
2005	North Korea	A/chicken/North Korea/2005 (H7N7)	219,000 chickens

*Table is taken from Alexander et al., 2007 and Harder & Werner, 2006 with modifications.

Table S2: Outbreaks of HPAIV H5 subtypes in poultry since 1959.

Year	Location	Strain	Species affected
1959	Scotland	A/chicken/Scotland/59 (H5N1)	2 flocks of chickens
1966	Ontario (Canada)	A/turkey/Ontario/7732/66 (H5N9)	8100 turkeys
1983-1985	Pennsylvania (USA)	A/chicken/Pennsylvania/1370/83 (H5N2)	17 million chickens and turkeys
1983	Ireland	A/turkey/Ireland/1378/83 (H5N8)	307,000 chickens, turkeys and ducks
1991	England	A/turkey/England/50-92/91 (H5N1)	8000 turkeys
1994-1995	Mexico	A/chicken/Puebla/8623-607/94 (H5N2)	360 commercial flocks of chickens
1997	Hong kong	A/chicken/Hong Kong/220/97 (H5N1)	1.4 million chickens and ducks
1997	Italy	A/chicken/Italy/330/97 (H5N2)	8000 chickens
since 2003	Asia, Europe, Africa and the Middle East	A/chicken/East Asia/2003-2005 (H5N1)	> 100 million birds
2004	Texas (USA)	A/chicken/USA-Texas/2004 (H5N2)	6600 chickens
2004	South Africa	A/ostrich/South Africa/2004 (H5N2)	30,000 ostriches
2007	England	A/turkey/England/2007 (H5N1)	160,000 turkeys

*Table is taken from Alexander et al., 2007 and Harder & Werner, 2006 with modification.

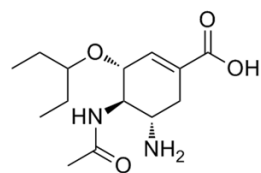
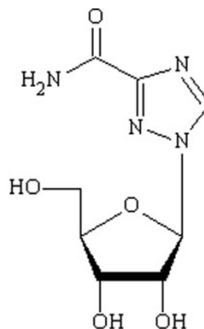
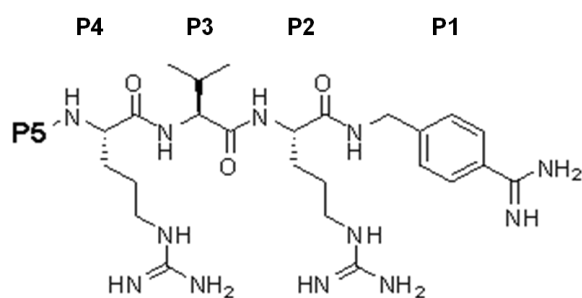
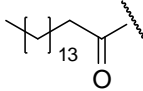
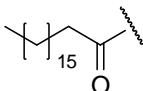
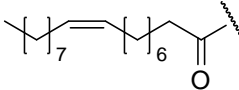
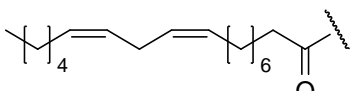
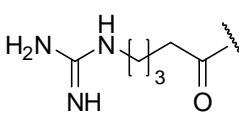
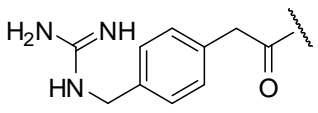
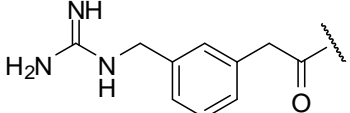
Fig. S1: Structures of oseltamivir and ribavirin.**Oseltamivir carboxylate****ribavirin**

Table S3: Structures of P5-modified furin inhibitors.

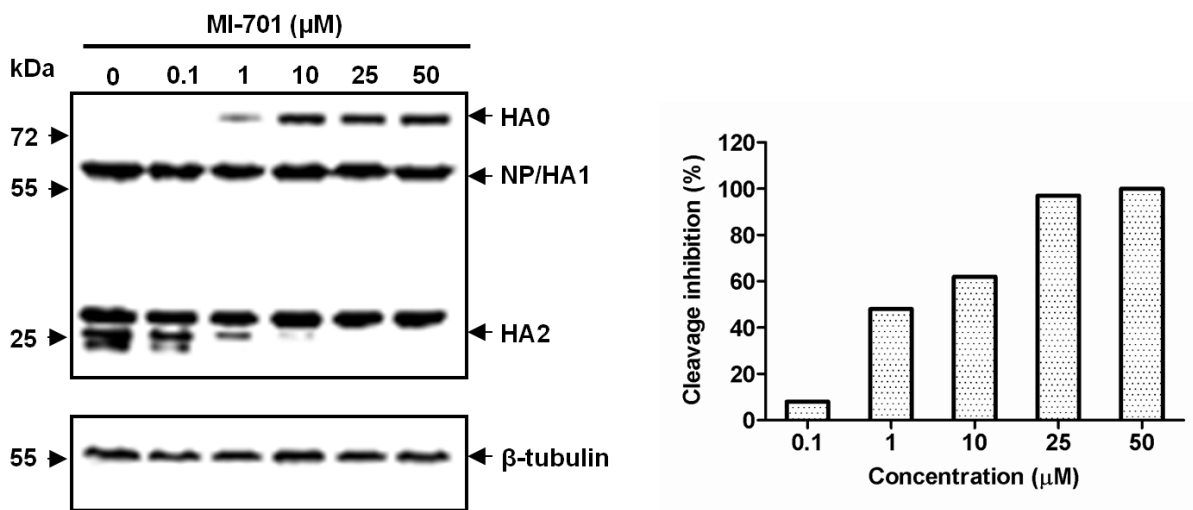
Inhibitor	P5	Sequence	K_i (nM)	IC_{50} (nM)
MI-227		Phenylacetyl-Arg-Val-Arg-4-Amba	0.81	nd
MI-230		Acetyl-Arg-Val-Arg-4-Amba	1.0	nd
MI-255		Butanoyl-Arg-Val-Arg-4-Amba	0.67	nd
MI-256		Hexanoyl-Arg-Val-Arg-4-Amba	0.78	nd
MI-257		Octanoyl-Arg-Val-Arg-4-Amba	0.67	2.3
MI-231		Decanoyl-Arg-Val-Arg-4-Amba	1.6	8.3
MI-258		Dodecanoyl-Arg-Val-Arg-4-Amba	5.6	nd
MI-259		Tetradecanoyl-Arg-Val-Arg-4-Amba	50	396

MI-232		Palmitoyl-Arg-Val-Arg-4-Amba	nd	80
MI-233		Stearyl-Arg-Val-Arg-4-Amba	nd	14010
MI-283		Oleoyl-Arg-Val-Arg-4-Amba	nd	272
MI-284		Linoyl-Arg-Val-Arg-4-Amba	5.3	22
MI-299		Guanidino-valerinoyl-Arg-Val-Arg-4-Amba	0.062	nd
MI-701		4-guanidinomethyl-phenylacetyl-Arg-Val-Arg-4-Amba	0.016	nd
MI-0052		3-guanidinomethyl-phenylacetyl-Arg-Val-Arg-4-Amba	0.008	nd

K_i values are determined under tight-binding conditions. Table is taken from Becker et al., 2012 with modification.

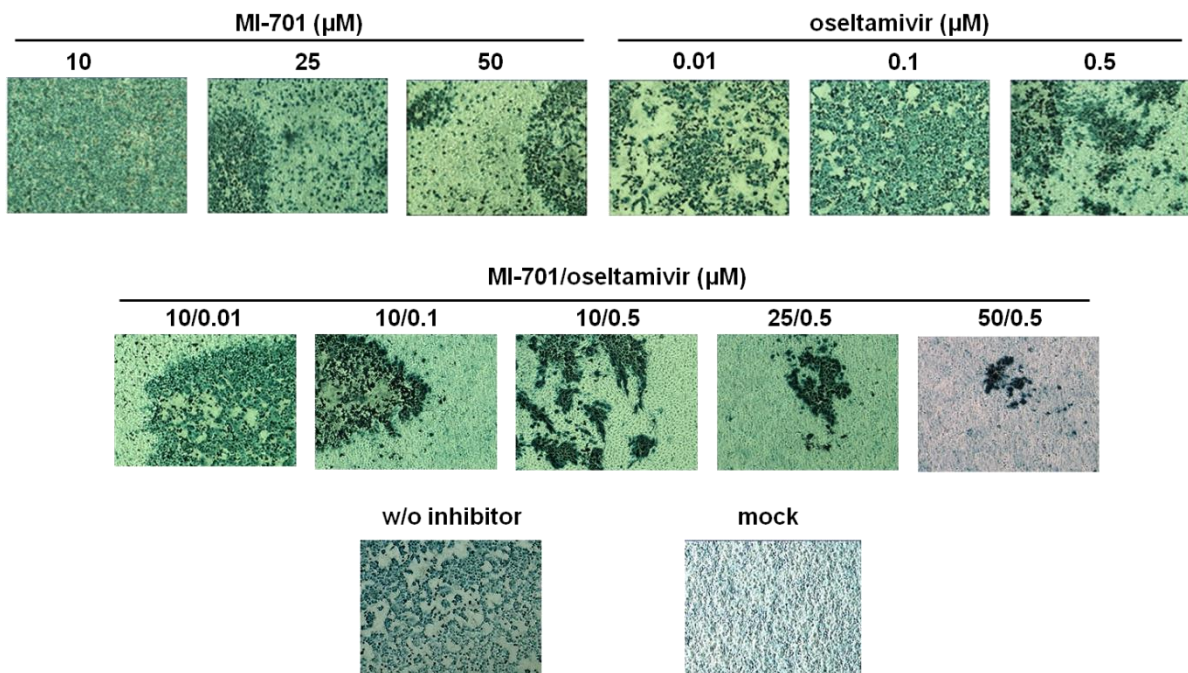
Amba= 4-amidinobenzylamide; nd = not determined.

Fig. S2: Inhibition proteolytic activation of HPAIV H5N1 subtype virus by furin inhibitor MI-701.



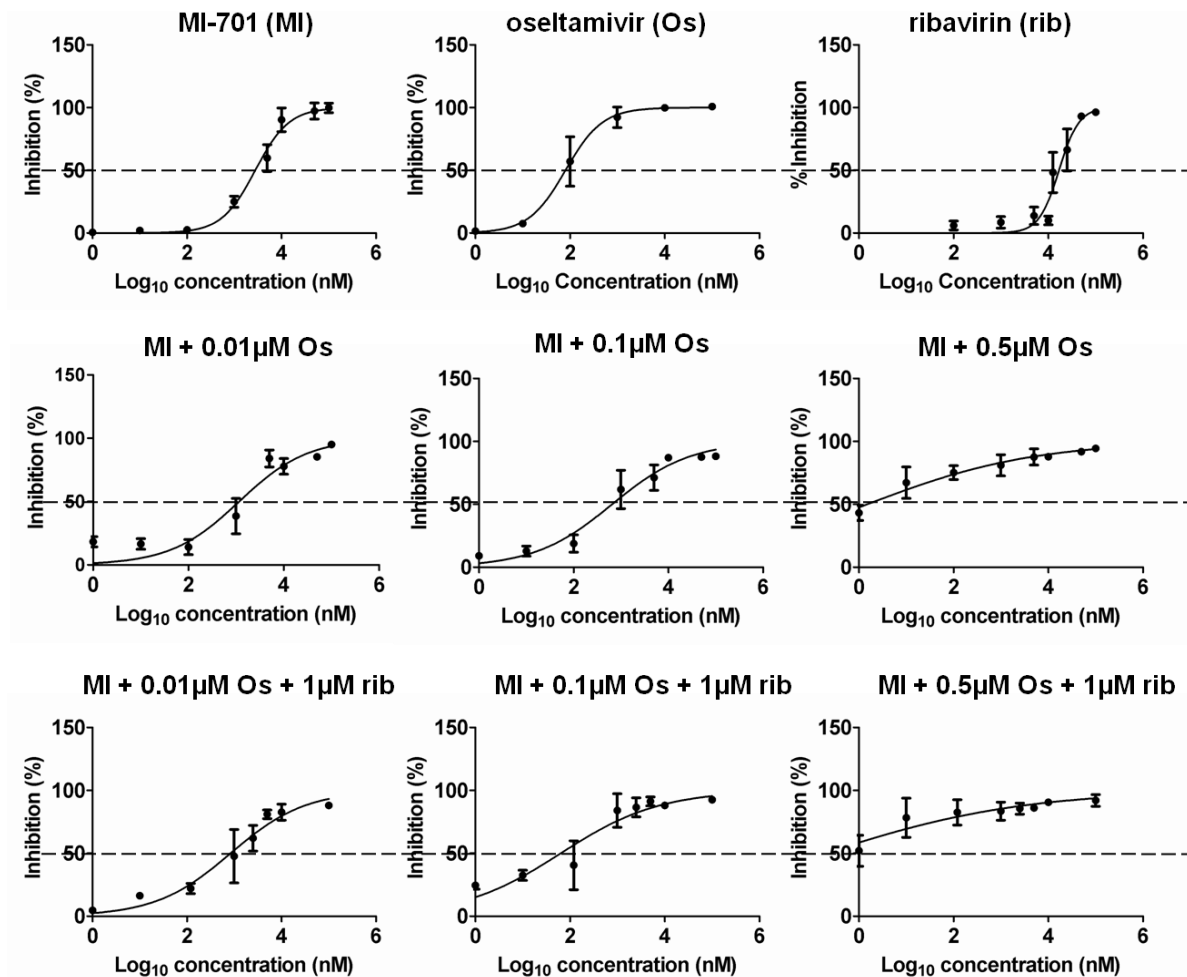
MDCK cells were infected with KAN-1 at an MOI of 10. After virus adsorption, infected cells were treated with MI-701 at concentrations of 0.1 μM , 1 μM , 10 μM , 25 μM and 50 μM , respectively or without inhibitor treatment. At 24h p.i. cell lysates were collected and subjected to SDS-PAGE and Western blot. Viral protein bands were visualized using antiserum against FPV and anti-tubulin antibody as loading control. For quantification, each HA0 band was standardized correlating to the β -tubulin bands (A) and the amount of HA0 obtained in cells treated with 50 μM MI-701 or without treatment were normalized to 100% and 0%, respectively. The intensities of protein bands were measured by the program Odyssey 2.01.

Fig. S3: Microscopy images of virus spread in the presence of MI-701 and oseltamivir alone or in combination.



MDCK cells were infected with FPV at an MOI of 0.001. Infected cells were treated with inhibitor MI-701 at a concentration of 10 μM , 25 μM or 50 μM and oseltamivir at a concentration of 0.01 μM , 0.1 μM or 0.5 μM alone or in combination. As controls, both uninfected cells (mock) and infected cells were incubated in pure medium in the absence of inhibitor. At 24h p.i. cells were fixed with 4% PFA and infected cells were immunostained using anti-FPV antibody and HRP-conjugated anti-rabbit secondary antibody.

Fig. S4: Reduction of EC₅₀ for MI-701 as single agent or in double and triple combinations.

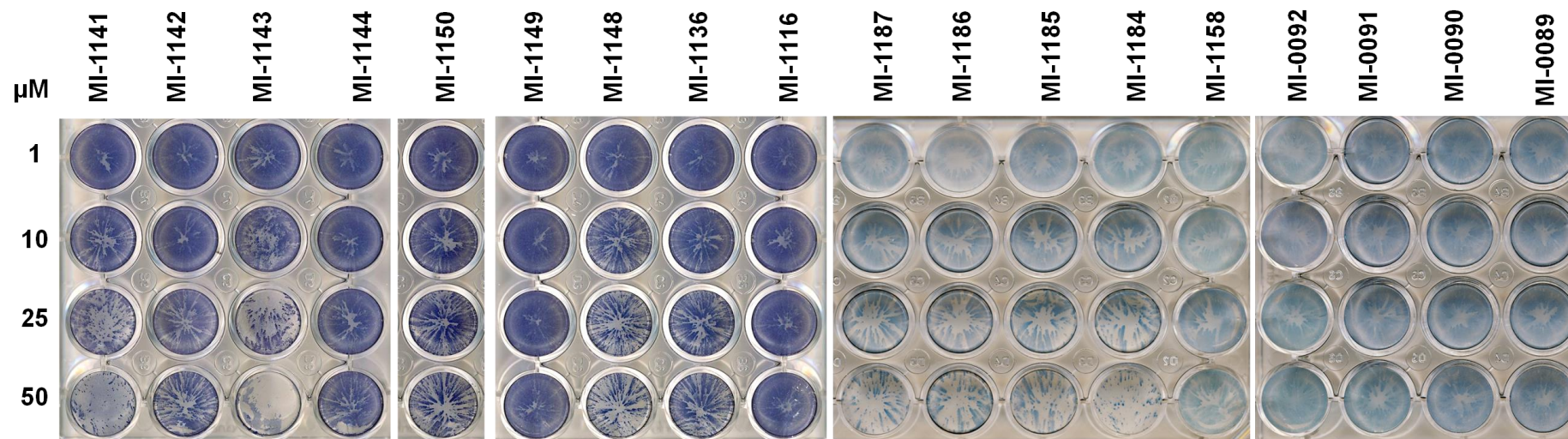


EC₅₀ calculations were made by normalizing the NR data for each well against the uninfected mock control data, which was assumed to be 100%. Normalized data were plotted as percent inhibition versus compound concentration. The data points were then fitted using four-parameter curve fitting in Graphpad Prism (Graphpad Software, La Jolla, CA) to derive the EC₅₀.

Table S4: Structures of optimized furin inhibitors.

	Inhibitor	CPPs	Sequence	Cytotoxicity
CPP derivatives	MI-1141	Penetratin	Ac-RQIKIWFQNRRMKWKKRVR-4-Amba	Yes*
	MI-1142	Tat	Ac-YGRKKRRQRRRVR-4-Amba	No
	MI-1143	Transportan	Ac-AGYLLGKINLKALAALAKKILRVR-4-Amba	Yes*
	MI-1144	Poly-Arg	Ac-RRRRRRRVR-4-Amba	No
P3 modified	MI-1116		Phac-Arg-Tle-Arg-4-Amba	No
	MI-1136		4-Ame-Phac-Arg-Tle-Arg-4-Amba	No
	MI-1148		4-Guame-Phac-Arg-Tle-Arg-4-Amba	No
	MI-1149		3-Ame-Phac-Arg-Tle-Arg-4-Amba	No
	MI-1150		3-Guame-Phac-Arg-Tle-Arg-4-Amba	No
P5 modified	MI-1158		Arg-Arg-Arg-Val-Arg-4-Amba	No
	MI-1184		H-dArg-Arg-Arg-Val-Arg-4-Amba	No
	MI-1185		H-dArg-dArg-Arg-Val-Arg-4-Amba	No
	MI-1186		H-dArg-dArg-dArg-Arg-Val-Arg-4-Amba	No
	MI-1187		H-dArg-dArg-dArg-dArg-Arg-Val-Arg-4-Amba	No
P1 modified	MI-0089		3-Guame-Phac-Arg-Tle-Arg-Noragmatin	No
	MI-0090		4-Guame-Phac-Arg-Tle-Arg-Noragmatin	No
	MI-0091		3-Guame-Phac-Arg-Tle-Arg-Agmatin	No
	MI-0092		4-Guame-Phac-Arg-Tle-Arg-Agmatin	No

The cytotoxicity of compounds was determined in MDCK cells by MTT assay (see 3.1.2).

Fig. S5: Inhibitory efficacy of newly modified furin inhibitors.

MDCK cells were infected with FPV at an MOI of 0.001. Infected cells were treated with furin inhibitors at the concentration of 1 μM , 10 μM , 25 μM or 50 μM or incubated without inhibitor treatment. At 24h p.i. cells were fixed with 4% PFA, infected cells were immunostained against anti-FPV antibody and HRP-conjugated anti-rabbit secondary antibody (structures are shown in Table S4 in supplementary).

Fig. S6: Neutral red data for synergy analysis.

A

Double combination of MI-701 and oseltamivir

Replicate 1	[DRUG]	0	0.39	0.78	1.56	3.13	6.25	12.5	25	50	3rd alone	VC	CC
		0.5	125	130	134	136	139	140	144	154	150		76
	0.25	99	114	121	125	135	137	142	142	143		74	148
	0.13	98	99	108	120	128	137	138	142	142		74	140
	0.06	77	97	90	93	114	119	137	140	140		63	145
	0.03	71	89	87	91	102	117	134	138	139		75	151
	0.02	69	76	85	88	99	115	125	134	138		78	155
	0	68	74	75	77	86	108	115	134	136		85	141

Replicate 2	[DRUG]	0	0.39	0.78	1.56	3.13	6.25	12.5	25	50	3rd alone	VC	CC
		0.5	153	161	162	170	171	172	174	175	179		115
	0.25	145	155	157	166	169	169	170	171	175		109	175
	0.13	134	142	156	163	166	168	169	169	174		108	179
	0.06	133	141	143	161	161	167	166	168	171		102	183
	0.03	121	139	141	153	163	164	165	167	170		108	183
	0.02	111	120	141	153	156	157	162	166	167		97	165
	0	101	111	121	136	136	146	158	161	162		103	169

Replicate 3	[DRUG]	0	0.39	0.78	1.56	3.13	6.25	12.5	25	50	3rd alone	VC	CC
		0.5	146	161	166	167	169	170	171	177	187		110
	0.25	113	160	161	164	165	169	170	177	177		108	189
	0.13	113	158	158	158	160	165	169	175	176		103	186
	0.06	111	154	157	157	157	162	168	173	174		117	189
	0.03	106	137	151	152	156	162	168	170	170		100	184
	0.02	103	126	133	142	154	155	166	162	170		94	187
	0	100	111	113	135	147	154	159	160	168		98	194

Vertical drug is oseltamivir (μM); Horizontal drug is MI-701 (μM); no third drug; VC = virus control; CC = cell control.

B

Triple combination of MI-701, oseltamivir and 1 μ M ribavirin

	Drug	<i>0</i>	<i>0.39</i>	<i>0.78</i>	<i>1.56</i>	<i>3.13</i>	<i>6.25</i>	<i>12.5</i>	<i>25</i>	<i>50</i>	3rd alone	VC	CC
Replicate 1	<i>0.5</i>	120	129	140	143	143	146	150	152	153	77	66	145
	<i>0.25</i>	96	102	128	136	138	140	143	146	151	67	81	143
	<i>0.13</i>	77	97	105	124	130	134	140	145	149	63	58	150
	<i>0.06</i>	72	90	88	116	117	132	139	143	147	69	68	140
	<i>0.03</i>	67	89	87	108	117	114	137	143	146	77	70	155
	<i>0.02</i>	65	72	80	84	110	113	135	139	141	67	78	140
	<i>0</i>	59	65	69	82	95	103	131	137	139	64	75	145
Replicate 2	<i>0.5</i>	153	161	162	170	171	172	174	175	179	111	115	184
	<i>0.25</i>	145	155	157	166	169	169	170	171	175	107	109	175
	<i>0.13</i>	134	142	156	163	166	168	169	169	174	106	108	179
	<i>0.06</i>	133	141	143	161	161	167	166	168	171	106	102	183
	<i>0.03</i>	121	139	141	153	163	164	165	167	170	100	108	183
	<i>0.02</i>	111	120	141	153	156	157	162	166	167	98	97	165
	<i>0</i>	101	111	121	136	136	146	158	161	162	102	103	169
Replicate 3	<i>0.5</i>	149	163	151	156	157	158	158	160	168	100	87	162
	<i>0.25</i>	139	142	149	148	150	152	155	160	157	79	77	150
	<i>0.13</i>	129	142	145	121	150	151	151	158	156	87	88	152
	<i>0.06</i>	100	133	144	119	149	148	148	150	164	113	74	157
	<i>0.03</i>	97	102	105	117	120	144	145	148	161	98	92	164
	<i>0.02</i>	95	95	100	111	115	136	140	145	154	100	99	161
	<i>0</i>	90	88	94	104	110	130	139	144	159	104	99	152

Vertical drug is oseltamivir (μ M); Horizontal drug is MI-701 (μ M); the third drug is ribavirin (μ M); VC = virus control; CC = cell control.

C

Triple combination of MI-701, oseltamivir and 10 μ M ribavirin

	Drug									3rd alone	VC	CC	
		0	0.39	0.78	1.56	3.13	6.25	12.5	25				50
Replicate 1	0.5	168	171	171	173	173	174	179	181	184	183	90	160
	0.25	166	168	166	170	172	174	179	175	186	180	111	179
	0.13	162	167	163	170	171	169	178	176	181	182	103	169
	0.06	160	166	162	169	170	168	177	174	175	178	100	168
	0.03	151	159	161	166	163	166	173	174	178	179	100	162
	0.02	150	159	159	161	162	163	172	173	178	178	104	176
	0	150	157	157	160	161	162	170	172	175	178	99	171
Replicate 2	0.5	165	168	173	171	171	178	182	183	188	178	100	160
	0.25	166	166	170	172	172	176	179	179	186	171	104	179
	0.13	162	168	166	170	171	173	178	179	181	172	101	169
	0.06	158	164	162	169	170	172	177	174	175	180	99	168
	0.03	155	159	161	166	163	166	173	175	178	180	98	162
	0.02	155	161	159	161	162	161	172	173	174	178	114	176
	0	148	153	158	161	161	165	168	168	174	188	100	171
Replicate 3	0.5	172	172	171	173	175	174	182	185	186	170	108	160
	0.25	169	168	166	172	172	174	180	175	186	180	93	179
	0.13	166	167	164	170	171	169	179	176	181	182	103	169
	0.06	160	166	162	169	170	168	175	174	175	180	98	168
	0.03	151	161	161	166	163	166	173	174	178	179	95	162
	0.02	148	159	159	161	162	163	172	173	178	175	108	176
	0	145	152	158	160	161	165	168	170	175	178	100	171

Vertical drug is oseltamivir (μ M); Horizontal drug is MI-701 (μ M); the third drug is ribavirin (μ M); VC = virus control; CC = cell control.

7. References

- Abdel-Ghafar AN, Chotpitayasunondh T, Gao Z, Hayden FG, Nguyen DH, de Jong MD, Naghdaliyev A, Peiris JSM, Shindo N, Soeroso S & Uyeki TM (2008) Update on avian influenza A (H5N1) virus infection in humans. *N. Engl. J. Med.* 358: 261–273.
- Ahmed R, Oldstone MB A & Palese P (2007) Protective immunity and susceptibility to infectious diseases: lessons from the 1918 influenza pandemic. *Nat. Immunol.* 8: 1188–1193.
- Alexander DJ (2000) A review of avian influenza in different bird species. *Vet. Microbiol.* 74: 3–13.
- Alexander DJ (2007) An overview of the epidemiology of avian influenza. *Vaccine* 25: 5637–5644.
- An SC, Xu LL, Li FD, Bao LL, Qin C & Gao ZC (2011) Triple combinations of neuraminidase inhibitors, statins and fibrates benefit the survival of patients with lethal avian influenza pandemic. *Med. Hypotheses* 77: 1054–1057.
- Angliker H (1996) Synthesis of tight binding inhibitors and their action on the proprotein-processing enzyme furin. *J. Med. Chem.* 38: 4014–4018.
- Ascierto PA & Marincola FM (2011) Combination therapy: the next opportunity and challenge of medicine. *J. Transl. Med.* 9: 115.
- Baron J, Tarnow C, Mayoli-Nüssle D, Schilling E, Meyer D, Hammami M, Schwalm F, Steinmetzer T, Guan Y, Garten W, Klenk H-D & Böttcher-Friebertshäuser E (2013) Matriptase, HAT, and TMPRSS2 activate the hemagglutinin of H9N2 influenza A viruses. *J. Virol.* 87: 1811–1820.
- Basak A (2005) Inhibitors of proprotein convertases. *J. Mol. Med. (Berl)*. 83: 844–855.
- Basak A, Chen A, Scamuffa N, Mohottalage D, Basak S & Khatib A-M (2010) Blockade of furin activity and furin-induced tumor cells malignant phenotypes by the chemically synthesized human furin prodomain. *Curr. Med. Chem.* 17: 2214–2221.
- Basak A, Cooper S, Roberge AG, Banik UK & Chre M (1999) Andrographis paniculata and their succinoyl esters. 113: 107–113.
- Basak A, Ernst B, Brewer D, Seidah NG, Munzer JS, Lazure C & Lajoie GA (1997) Histidine-rich human salivary peptides are inhibitors of proprotein convertases furin and PC7 but act as substrates for PC1. *J. Pept. Res.* 49: 596–603.
- Basak A & Lazure C (2003) Synthetic peptides derived from the prosegments of proprotein convertase 1/3 and furin are potent inhibitors of both enzymes. *Biochem. J.* 373: 231–239.
- Baz M, Abed Y, McDonald J & Boivin G (2006) Characterization of multidrug-resistant influenza A/H3N2 viruses shed during 1 year by an immunocompromised child. *Clin. Infect. Dis.* 43: 1555–1561.
- Becker GL, Lu Y, Harges K, Strehlow B, Levesque C, Lindberg I, Sandvig K, Bakowsky U, Day R, Garten W & Steinmetzer T (2012) Highly potent inhibitors of proprotein convertase furin as potential drugs for treatment of infectious diseases. *J. Biol. Chem.* 287: 21992–22003.
- Becker GL, Sielaff F, Than ME, Lindberg I, Routhier S, Day R, Lu Y, Garten W & Steinmetzer T (2010) Potent inhibitors of furin and furin-like proprotein convertases containing decarboxylated P1 arginine mimetics. *J. Med. Chem.* 53: 1067–1075.

- Belser JA, Bridges CB, Katz JM & Tumpey TM (2009) Past, present, and possible future human infection with influenza virus A subtype H7. *Emerg. Infect. Dis.* 15: 859–865.
- Bontemps Y, Scamuffa N, Calvo F & Khatib AM (2007) Potential opportunity in the development of new therapeutic agents based on endogenous and exogenous inhibitors of the proprotein convertases. *Med. Res. Rev.* 27: 631–648.
- Böttcher E, Matrosovich T, Beyerle M, Klenk HD, Garten W & Matrosovich M (2006) Proteolytic activation of influenza viruses by serine proteases TMPRSS2 and HAT from human airway epithelium. *J. Virol.* 80: 9896–9898.
- Böttcher-Friebertshäuser E, Freuer C, Sielaff F, Schmidt S, Eickmann M, Uhlendorff J, Steinmetzer T, Klenk HD & Garten W (2010) Cleavage of influenza virus hemagglutinin by airway proteases TMPRSS2 and HAT differs in subcellular localization and susceptibility to protease inhibitors. *J. Virol.* 84: 5605–5614.
- Böttcher-Friebertshäuser E, Klenk HD & Garten W (2013) Activation of influenza viruses by proteases from host cells and bacteria in the human airway epithelium. *Pathog. Dis.* 69: 87–100.
- Böttcher-Friebertshäuser E, Lu Y, Meyer D, Sielaff F, Steinmetzer T, Klenk HD & Garten W (2012) Hemagglutinin activating host cell proteases provide promising drug targets for the treatment of influenza A and B virus infections. *Vaccine* 30: 7374–7380.
- Boycott R, Klenk HD & Ohuchi M (1994) Cell tropism of influenza virus mediated by hemagglutinin activation at the stage of virus entry. *Virology* 203: 313–319.
- Bresnahan PA, Leduc R, Thomas L, Thorner J, Gibson HL, Brake AJ, Barr PJ & Thomas G (1990) Human fur gene encodes a yeast Kex2-like endoprotease that cleaves pro-beta-NGF in vivo. *J. Cell Biol.* 111: 2851–2859.
- Cameron A, Appel J, Houghten RA & Lindberg I (2000) Polyarginines are potent furin inhibitors. *J. Biol. Chem.* 275: 36741–36749.
- Capua I & Alexander DJ (2004) Avian influenza: recent developments. *Avian Pathol.* 33: 393–404.
- Carr J, Ives J, Kelly L, Lambkin R, Oxford J, Mendel D, Tai L & Roberts N (2002) Influenza virus carrying neuraminidase with reduced sensitivity to oseltamivir carboxylate has altered properties in vitro and is compromised for infectivity and replicative ability in vivo. *Antiviral Res.* 54: 79–88.
- Carrat F & Flahault A (2007) Influenza vaccine: the challenge of antigenic drift. *Vaccine* 25: 6852–6862.
- Centanni E, Savonuzzi E (1901) La peste aviaria I&II, Comunicazione fatta all'accademia delle scienze mediche e naturali de Ferrara, 1901.
- Chen R & Holmes EC (2006) Avian influenza virus exhibits rapid evolutionary dynamics. *Mol. Biol. Evol.* 23: 2336–2341.
- Chen Z & Krug RM (2000) Selective nuclear export of viral mRNAs in influenza-virus-infected cells. *Trends Microbiol.* 8: 376–383.
- Chien C, Tejero R, Huang Y, Zimmerman DE, Ríos CB, Krug RM & Montelione GT (1997) A novel RNA-binding motif in influenza A virus non-structural protein 1. *Nat. Struct. Biol.* 4: 891–895.
- Chiron MF, Fryling CM & FitzGerald DJ (1994) Cleavage of pseudomonas exotoxin and diphtheria toxin by a furin-like enzyme prepared from beef liver. *J. Biol. Chem.* 269: 18167–18176.

- Chrétien M, Seidah NG, Basak A & Mbikay M (2008) Proprotein convertases as therapeutic targets. *Expert Opin. Ther. Targets* 12: 1289–1300.
- De Clercq E (2006) Antiviral agents active against influenza A viruses. *Nat. Rev. Drug Discov.* 5: 1015–1025.
- Colman PM, Hoyne PA & Lawrence MC (1993) Sequence and structure alignment of paramyxovirus hemagglutinin-neuraminidase with influenza virus neuraminidase. *J. Virol.* 67: 2972–2980.
- Cox NJ & Subbarao K (2000) Global epidemiology of influenza: Past and present. *Annu. Rev. Med.* 51: 407–421.
- Creemers JWM, Vey M, Schafer W, Ayoubi TAY, Roebroek a. JM, Klenk HD, Garten W & Van de Ven WJM (1995) Endoproteolytic cleavage of its propeptide is a prerequisite for efficient transport of furin out of the endoplasmic reticulum. *J. Biol. Chem.* 270: 2695–2702.
- Dahlen JR, Jean F, Thomas G, Foster DC & Kisiel W (1998) Inhibition of Soluble Recombinant Furin by Human Proteinase Inhibitor 8. *J. Biol. Chem.* 273: 1851–1854.
- Dahms SO, Harges K, Becker GL, Steinmetzer T, Brandstetter H & Than ME (2014) X-ray structures of human furin in complex with competitive inhibitors. *ACS Chem. Biol.* 9: 1113–1118.
- Daniel TM (2006) The history of tuberculosis. *Respir. Med.* 100: 1862–1870.
- Delay PD, Casey HL, Ph D & Tubiash HS (1967) Comparative study of fowl plague virus and a virus isolated from man. *Public Health Rep.* 82: 615-620.
- Duguay SJ, Milewski WM, Young BD, Nakayama K & Steiner DF (1997) Processing of Wild-type and Mutant Proinsulin-like Growth Factor-1A by Subtilisin-related Proprotein Convertases. *J. Biol. Chem.* 272: 6663–6670.
- Elton D, Simpson-holley M, Archer K, Hallam R, Mccauley J, Digard P, Medcalf LIZ & Cauley JMC (2001) Interaction of the influenza virus nucleoprotein with the cellular CRM1-mediated nuclear export pathway. *J. Virol.* 75: 408-419.
- Espenshade PJ, Cheng D, Goldstein JL & Brown MS (1999) Autocatalytic Processing of Site-1 Protease Removes Propeptide and Permits Cleavage of Sterol Regulatory Element-binding Proteins. *J. Biol. Chem.* 274: 22795–22804.
- Feldmann A, Schäfer MK, Garten W & Klenk HD (2000) Targeted infection of endothelial cells by avian influenza virus A/FPV/Rostock/34 (H7N1) in chicken embryos. *J. Virol.* 74: 8018–8027.
- Follis KE, York J & Nunberg JH (2006) Furin cleavage of the SARS coronavirus spike glycoprotein enhances cell-cell fusion but does not affect virion entry. *Virology* 350: 358–369.
- Fouchier RA, Schneeberger PM, Rozendaal FW, Broekman JM, Kemink SAG, Munster V, Kuiken T, Rimmelzwaan GF, Schutten M, Van Doornum GJ, Koch G, Bosman A, Koopmans M & Osterhaus AD (2004) Avian influenza A virus (H7N7) associated with human conjunctivitis and a fatal case of acute respiratory distress syndrome. *Proc. Natl. Acad. Sci. U. S. A.* 101: 1356–1361.
- Fujii Y, Sakaguchi T, Kiyotani K & Yoshida T (1999) Comparison of substrate specificities against the fusion glycoprotein of virulent Newcastle disease virus between a chick embryo fibroblast processing protease and mammalian subtilisin-like proteases. *Microbiol. Immunol.* 43: 133–140.
- Fuller RS, Brake AJ & Thorner J (1989) Intracellular targeting and structural conservation of a prohormone-processing endoprotease. *Science* 246: 482–486.

- Furuta Y, Takahashi K, Fukuda Y, Kuno M, Kamiyama T, Kozaki K, Nomura N, Egawa H, Minami S, Watanabe Y, Shiraki K & Narita H (2002) In Vitro and In Vivo Activities of Anti-Influenza Virus Compound T-705. *Antimicrob Agents Chemother.* 46: 977-981.
- Furuta Y, Takahashi K, Kuno-maekawa M, Sangawa H, Uehara S, Kozaki K, Nomura N, Egawa H & Shiraki K (2005) Mechanism of action of T-705 against influenza virus. *Antimicrob. Agents Chemother.* 49: 981-986.
- Gabriel G, Klingel K, Otte A, Thiele S, Hudjetz B, Arman-Kalcek G, Sauter M, Shmidt T, Rother F, Baumgarte S, Keiner B, Hartmann E, Bader M, Brownlee GG, Fodor E & Klenk HD (2011) Differential use of importin- α isoforms governs cell tropism and host adaptation of influenza virus. *Nat. Commun.* 2: 156.
- Gagnon H, Beauchemin S, Kwiatkowska A, Couture F, D'Anjou F, Levesque C, Dufour F, Desbiens AR, Vaillancourt R, Bernard S, Desjardins R, Malouin F, Dory YL & Day R (2014) Optimization of furin inhibitors to protect against the activation of influenza hemagglutinin H5 and Shiga toxin. *J. Med. Chem.* 57: 29-41.
- Galegov GA, Pushkarskaya NL, Obrosova-Serova NP & Zhdanov VM (1977) Combined action of ribovirin and rimantadine in experimental myxovirus infection. *Experientia* 33: 905-906.
- Galloway SE, Reed ML, Russell CJ & Steinhauer DA (2013) Influenza HA subtypes demonstrate divergent phenotypes for cleavage activation and pH of fusion: implications for host range and adaptation. *PLoS Pathog.* 9: e1003151.
- García-Sastre A, Egorov A, Matassov D, Brandt S, Levy DE, Durbin JE, Palese P & Muster T (1998) Influenza A virus lacking the NS1 gene replicates in interferon-deficient systems. *Virology* 252: 324-330.
- Garred O, van Deurs B & Sandvig K (1995) Furin-induced cleavage and activation of Shiga toxin. *J. Biol. Chem.* 270: 10817-10821.
- Garten W, Hallenberger S, Ortmann D, Schäfer W, Vey M, Angliker H, Shaw E & Klenk HD (1994) Processing of viral glycoproteins by the subtilisin-like endoprotease furin and its inhibition by specific peptidylchloroalkylketones. *Biochimie* 76: 217-225.
- Garten W & Klenk HD (2008) Cleavage Activation of the Influenza Virus Hemagglutinin and Its Role in Pathogenesis. 156-167.
- Garten W, Stieneke A, Shaw E, Wikstrom P & Klenk HD (1989) Inhibition of proteolytic activation of influenza virus hemagglutinin by specific peptidyl chloroalkyl ketones. *Virology.* 172: 25-31.
- Gordon VM, Benz R, Fujii K, Leppla SH, Tweten RK, Gordon VM, Benz R, Fujii K & Leppla SH (1997) Clostridium septicum alpha-toxin is proteolytically activated by furin. *Infect. Immun.* 65: 4130-4134.
- Gotoh B, Ogasawara T, Toyoda T, Inocencio NM, Hamaguchi M & Nagai Y (1990) An endoprotease homologous to the blood clotting factor X as a determinant of viral tropism in chick embryo. *EMBO J.* 9: 4189-4195.
- Govorkova EA (2013) Consequences of resistance: in vitro fitness, in vivo infectivity, and transmissibility of oseltamivir-resistant influenza A viruses. *Influenza Other Respi. Viruses* 7 Suppl 1: 50-57.
- Govorkova EA & Webster RG (2010) Combination chemotherapy for influenza. *Viruses* 2: 1510-1529.
- Govorkova EA, Fang HB, Tan M & Webster RG (2004) Neuraminidase inhibitor-rimantadine combinations exert additive and synergistic anti-influenza virus effects in MDCK cells. *Antimicrob. Agents Chemother.* 48: 4855-4863.

- Haasbach E, Hartmayer C & Planz O (2013) Combination of MEK inhibitors and oseltamivir leads to synergistic antiviral effects after influenza A virus infection in vitro. *Antiviral Res.* 98: 319–324.
- Hale BG, Randall RE, Ortín J & Jackson D (2008) The multifunctional NS1 protein of influenza A viruses. *J. Gen. Virol.* 89: 2359–2376.
- Hallenberger S, Bosch V, Angliker H, Shaw E, Klenk HD & Garten W (1992) Inhibition of furin-mediated cleavage activation of HIV-1 glycoprotein gp160. *Nature* 360: 358–361.
- Harper SA, Fukuda K, Uyeki TM, Cox NJ & Bridges CB (2005) Prevention and control of influenza. Recommendations of the Advisory Committee on Immunization Practices (ACIP). *MMWR. Recomm. Rep.* 54: 1–40.
- Harrison SC (2008) Viral membrane fusion. *Nat. Struct. Mol. Biol.* 15: 690–698.
- Hauser G, Awad T, Thorlund K, Stimac D, Mabrouk M & Gluud C (2014) Peginterferon alpha-2a versus peginterferon alpha-2b for chronic hepatitis C. *Cochrane database Syst. Rev.* 2: CD005642.
- Hayden FG (2013) Newer influenza antivirals, biotherapeutics and combinations. *Influenza Other Respi. Viruses* 7 Suppl 1: 63–75.
- Hayden FG, Douglas RG & Simons R (1980) Enhancement of activity against influenza viruses by combinations of antiviral agents. *Antimicrob. Agents Chemother.* 18: 536–541.
- Hayden FG & de Jong MD (2011) Emerging influenza antiviral resistance threats. *J. Infect. Dis.* 203: 6–10.
- Hayden FG, Schlepshkin AN & Pushkarskaya NL (1984) Combined interferon-alpha 2, rimantadine hydrochloride, and ribavirin inhibition of influenza virus replication in vitro. *Antimicrob. Agents Chemother.* 25: 53–57.
- Henrich S, Cameron A, Bourenkov GP, Kiefersauer R, Huber R, Lindberg I, Bode W & Than ME (2003) The crystal structure of the proprotein processing proteinase furin explains its stringent specificity. *Nat. Struct. Biol.* 10: 520–526.
- Herlocher ML, Carr J, Ives J, Elias S, Truscon R, Roberts N & Monto AS (2002) Influenza virus carrying an R292K mutation in the neuraminidase gene is not transmitted in ferrets. *Antiviral Res.* 54: 99–111.
- Hirst GK (1942) The quantitative determination of influenza virus and antibodies by means of red cell agglutination. *J. Exp. Med.* 75: 49–64.
- Horimoto T, Nakayama K, Smeekens SP & Kawaoaka Y (1994) Proprotein-processing endoproteases PC6 and furin both activate hemagglutinin of virulent avian influenza viruses. *J. Virol.* 68: 6074–6078.
- Hurt AC, Holien JK, Parker M, Kelso A & Barr IG (2009) Zanamivir-resistant influenza viruses with a novel neuraminidase mutation. *J. Virol.* 83: 10366–10373.
- Ibricevic A, Pekosz A, Walter MJ, Newby C, Battaile JT, Brown EG, Holtzman MJ & Brody SL (2006) Influenza virus receptor specificity and cell tropism in mouse and human airway epithelial cells. *J. Virol.* 80: 7469–7480.
- Ikematsu H & Kawai N (2011) Laninamivir octanoate: a new long-acting neuraminidase inhibitor for the treatment of influenza. *Expert Rev. Anti. Infect. Ther.* 9: 851–857.

- Ilyushina NA, Bovin NV, Webster RG & Govorkova EA (2006) Combination chemotherapy, a potential strategy for reducing the emergence of drug-resistant influenza A variants. *Antiviral Res.* 70: 121–131.
- Ilyushina NA, Hoffmann E, Salomon R, Webster RG & Govorkova EA (2007) Amantadine-oseltamivir combination therapy for H5N1 influenza virus infection in mice. *Antivir. Ther.* 12: 363–370.
- Ives JAL, Carr JA, Mendel DB, Tai CY, Lambkin R, Kelly L, Oxford JS, Hayden FG & Roberts NA (2002) The H274Y mutation in the influenza A/H1N1 neuraminidase active site following oseltamivir phosphate treatment leave virus severely compromised both in vitro and in vivo. *Antiviral Res.* 55: 307–317.
- Jagger BW, Wise HM, Kash JC, Walters K, Wills NM, Xiao YL, Dunfee RL, Schwartzman LM, Ozinsky A, Bell GL, Dalton RM, Lo A, Efstathiou S, Atkins JF, Firth AE, Taubenberger JK & Digard P (2012) An overlapping protein-coding region in influenza A virus segment 3 modulates the host response. *Science* 337: 199–204.
- Järver P & Langel U (2006) Cell-penetrating peptides--a brief introduction. *Biochim. Biophys. Acta* 1758: 260–263.
- Jean F, Thomas L, Molloy SS, Liu G, Jarvis MA, Nelson JA & Thomas G (2000) A protein-based therapeutic for human cytomegalovirus infection. *Proc. Natl. Acad. Sci. U. S. A.* 97: 2864–2869.
- Jiao GS, Cregar L, Wang J, Millis SZ, Tang C, O'Malley S, Johnson AT, Sareth S, Larson J & Thomas G (2006) Synthetic small molecule furin inhibitors derived from 2,5-dideoxystreptomine. *Proc. Natl. Acad. Sci. U. S. A.* 103: 19707–19712.
- De Jong MD, Tran TT, Truong HK, Vo MH, Smith GJ, Nguyen VC, Bach VC, Phan TQ, Do QH, Guan Y, Peiris JSM, Tran TH & Farrar J (2005) Oseltamivir resistance during treatment of influenza A (H5N1) infection. *N. Engl. J. Med.* 353: 2667–2672.
- Jonges M, Liu WM, van der Vries E, Jacobi R, Pronk I, Boog C, Koopmans M, Meijer A & Soethout E (2010) Influenza virus inactivation for studies of antigenicity and phenotypic neuraminidase inhibitor resistance profiling. *J. Clin. Microbiol.* 48: 928–940.
- Kacprzak MM, Peinado JR, Than ME, Appel J, Henrich S, Lipkind G, Houghten RA, Bode W & Lindberg I (2004) Enzyme catalysis and regulation: inhibition of furin by nona-d-arginine inhibition of furin by polyarginine-containing peptides. *J. Biol. Chem.* 279: 36788-36794.
- Keelapang P, Sriburi R, Supasa S, Panyadee N, Songjaeng A, Jairungsri A, Puttikhunt C, Kasinrerak W, Malasit P & Sittisombut N (2004) Alterations of pr-M cleavage and virus export in pr-M junction chimeric dengue viruses. *J. Virol.* 78: 2367–2381.
- Kido H, Yokogoshi Y, Sakai K, Tashiro M, Kishino Y, Fukutomi A & Katunuma N (1992) Isolation and characterization of a novel trypsin-like protease found in rat bronchiolar epithelial Clara cells. A possible activator of the viral fusion glycoprotein. *J. Biol. Chem.* 267: 13573–13579.
- Kiefer MC, Tucker JE, Joh R, Landsberg KE, Saltman D & Barr PJ (1991) Identification of a second human subtilisin-like protease gene in the fes/fps region of chromosome 15. *DNA Cell Biol.* 10: 757–769.
- Kilbourne ED (2006) Influenza pandemics of the 20th century. *Emerg. Infect. Dis.* 12: 9–14.
- Kiso M, Mitamura K, Sakai-Tagawa Y, Shiraishi K, Kawakami C, Kimura K, Hayden FG, Sugaya N & Kawaoka Y (2004) Resistant influenza A viruses in children treated with oseltamivir: descriptive study. *Lancet* 364: 759–765.

- Klenk HD, Rott R, Orlich M & Blödorn J (1975) Activation of influenza A viruses by trypsin treatment. *Virology* 68: 426–439.
- Klimpel KR, Molloy SS, Thomas G & Leppla SH (1992) Anthrax toxin protective antigen is activated by a cell surface protease with the sequence specificity and catalytic properties of furin. *Proc. Natl. Acad. Sci. U. S. A.* 89: 10277–10281.
- Kumlin U, Olofsson S, Dimock K & Arnberg N (2008) Sialic acid tissue distribution and influenza virus tropism. *Influenza Other Respi. Viruses* 2: 147–154.
- Kurtz J, Manvell RJ & Banks J (1996) Avian influenza virus isolated from a woman with conjunctivitis. *Lancet* 348: 901–902.
- Kyhse-Andersen J (1984) Electrophoretic transfer of multiple gels: a simple apparatus without buffer tank for rapid transfer of proteins from polyacrylamide to nitrocellulose. *J. Biochem. Biophys. Methods* 10: 203–209.
- Lackenby A, Thompson CI & Democratis J (2008) The potential impact of neuraminidase inhibitor resistant influenza. *Curr. Opin. Infect. Dis.* 21: 626–638.
- Laemmli UK (1970) Cleavage of Structural Proteins during the Assembly of the Head of Bacteriophage T4. *Nature* 227: 680–685.
- Lamb RA, Zebedee SL & Richardson CD (1985) Influenza virus M2 protein is an integral membrane protein expressed on the infected-cell surface. *Cell* 40: 627–633.
- Langebeek N, Sprenger HG, Gisolf EH, Reiss P, Sprangers M a G, Legrand J, Richter C & Nieuwkerk PT (2014) A simplified combination antiretroviral therapy regimen enhances adherence, treatment satisfaction and quality of life: results of a randomized clinical trial. *HIV Med.* 15: 286–290.
- Lazarowitz SG & Choppin PW (1975) Enhancement of the infectivity of influenza A and B viruses by proteolytic cleavage of the hemagglutinin polypeptide. *Virology* 68: 440–454.
- Le QM, Kiso M, Someya K, Sakai YT, Nguyen TH, Nguyen KHL, Pham ND, Ngyen HH, Yamada S, Muramoto Y, Horimoto T, Takada A, Goto H, Suzuki T, Suzuki Y & Kawaoka Y (2005) Avian flu: isolation of drug-resistant H5N1 virus. *Nature* 437: 1108.
- Leduc R, Molloy SS, Thorne BA & Thomas G (1992) Activation of human furin precursor processing endoprotease occurs by an intramolecular autoproteolytic cleavage. *J. Biol. Chem.* 267: 14304–14308.
- Liem NT, Tung CV, Hien ND, Hien TT, Chau NQ, Long HT, Hien NT, Mai LQ, Taylor WRJ, Wertheim H, Farrar J, Khang DD & Horby P (2009) Clinical features of human influenza A (H5N1) infection in Vietnam: 2004-2006. *Clin. Infect. Dis.* 48: 1639–1646.
- Liu Z, Fei H & Chi C (2004) Two engineered eglin c mutants potently and selectively inhibiting kexin or furin. *FEBS Lett.* 556: 116–120.
- Lu W, Zhang W, Molloy SS, Thomas G, Ryan K, Chiang Y, Anderson S & Laskowski M (1993) Arg15-Lys17-Arg18 turkey ovomucoid third domain inhibits human furin. *J. Biol. Chem.* 268: 14583–14585.
- Lupiani B & Reddy SM (2009) The history of avian influenza. *Comp. Immunol. Microbiol. Infect. Dis.* 32: 311–323.
- Madani F, Lindberg S, Langel U, Futaki S & Gräslund A (2011) Mechanisms of cellular uptake of cell-penetrating peptides. *J. Biophys.* 2011: 414729.

- Malakhov MP, Aschenbrenner LM, Donald F, Wandersee MK, Sidwell RW, Larisa V, Mishin VP, Hayden FG, Kim H, Ing A, Campbell ER, Yu M, Smee DF, Gubareva L V, Kim DH & Fang F (2006) Sialidase fusion protein as a novel broad-spectrum inhibitor of influenza virus infection. *Antimicrob Agents Chemother.* 50: 1470-1479.
- Marathe BM, Lévêque V, Klumpp K, Webster RG & Govorkova EA (2013) Determination of neuraminidase kinetic constants using whole influenza virus preparations and correction for spectroscopic interference by a fluorogenic substrate. *PLoS One* 8: e71401.
- Maruyama S, Koda M, Oi S & Murawaki Y (2013) Successful treatment of myelodysplastic syndrome and chronic hepatitis C using combined peginterferon- α -2b and ribavirin therapy. *Hepatol. Res.* 1–18.
- Matrosovich MN, Matrosovich TY, Gray T, Roberts NA, Klenk HD (2004) Human and avian influenza viruses target different cell types in cultures of human airway epithelium. *Proc Natl Acad Sci USA* 101:4620-4624.
- Matrosovich M, Matrosovich T, Garten W & Klenk HD (2006) New low-viscosity overlay medium for viral plaque assays. *Viol. J.* 3: 63.
- McKimm-Breschkin JL (2000) Resistance of influenza viruses to neuraminidase inhibitors--a review. *Antiviral Res.* 47: 1–17.
- Mitchison DA (2012) Prevention of drug resistance by combined drug treatment of tuberculosis. *Handb. Exp. Pharmacol.* 87–98.
- Mosmann T (1983) Rapid colorimetric assay for cellular growth and survival: application to proliferation and cytotoxicity assays. *J. Immunol. Methods* 65: 55–63.
- Moss RB, Hansen C, Sanders RL, Hawley S, Li T & Steigbigel RT (2012) A phase II study of DAS181, a novel host directed antiviral for the treatment of influenza infection. *J. Infect. Dis.* 206: 1844–1851.
- Mullis KB & Faloona FA (1987) Specific synthesis of DNA in vitro via a polymerase-catalyzed chain reaction. *Methods Enzymol.* 155: 335-350
- Murakami M, Towatari T, Ohuchi M, Shiota M, Akao M, Okumura Y, Parry MA & Kido H (2001) Miniplasmin found in the epithelial cells of bronchioles triggers infection by broad-spectrum influenza A viruses and Sendai virus. *Eur. J. Biochem.* 268: 2847–2855.
- Muramoto Y, Noda T, Kawakami E, Akkina R & Kawaoka Y (2013) Identification of novel influenza A virus proteins translated from PA mRNA. *J. Virol.* 87: 2455–2462.
- Nakayama K (1997) Furin: a mammalian subtilisin/Kex2p-like endoprotease involved in processing of a wide variety of precursor proteins. *Biochem. J.* 327: 625–635.
- Nayak DP, Balogun RA, Yamada H, Zhou ZH & Barman S (2009) Influenza virus morphogenesis and budding. *Virus Res.* 143: 147–161.
- Nguyen JT, Hoopes JD, Le MH, Smee DF, Patick AK, Faix DJ, Blair PJ, de Jong MD, Prichard MN & Went GT (2010) Triple combination of amantadine, ribavirin, and oseltamivir is highly active and synergistic against drug resistant influenza virus strains in vitro. *PLoS One* 5: e9332.
- Nguyen JT, Hoopes JD, Smee DF, Prichard MN, Driebe EM, Engelthaler DM, Le MH, Keim PS, Spence RP & Went GT (2009) Triple combination of oseltamivir, amantadine, and ribavirin displays synergistic activity against multiple influenza virus strains in vitro. *Antimicrob. Agents Chemother.* 53: 4115–4126.

- Nguyen JT, Smee DF, Barnard DL, Julander JG, Gross M, de Jong MD & Went GT (2012) Efficacy of combined therapy with amantadine, oseltamivir, and ribavirin in vivo against susceptible and amantadine-resistant influenza A viruses. *PLoS One* 7: e31006.
- Noda T (2011) Native morphology of influenza virions. *Front. Microbiol.* 2: 269.
- O'Neill RE, Talon J & Palese P (1998) The influenza virus NEP (NS2 protein) mediates the nuclear export of viral ribonucleoproteins. *EMBO J.* 17: 288–296.
- Okumura Y, Takahashi E, Yano M, Ohuchi M, Daidoji T, Nakaya T, Böttcher E, Garten W, Klenk HD & Kido H (2010) Novel type II transmembrane serine proteases, MSPL and Tmprss13, proteolytically activate membrane fusion activity of the hemagglutinin of highly pathogenic avian influenza viruses and induce their multicycle replication. *J. Virol.* 84: 5089–5096.
- Ozden S, Lucas-Hourani M, Ceccaldi PE, Basak A, Valentine M, Benjannet S, Hamelin J, Jacob Y, Mamchaoui K, Mouly V, Desprès P, Gessain A, Butler-Browne G, Chrétien M, Tangy F, Vidalain PO & Seidah NG (2008) Inhibition of Chikungunya virus infection in cultured human muscle cells by furin inhibitors: impairment of the maturation of the E2 surface glycoprotein. *J. Biol. Chem.* 283: 21899–21908.
- Pang YJ, Tan XJ, Li DM, Zheng ZH, Lei RX & Peng XM (2013) Therapeutic potential of furin inhibitors for the chronic infection of hepatitis B virus. *Liver Int.* 33: 1230–1238.
- Pellett PE, Biggin MD, Barrell B & Roizman B (1985) Epstein-Barr virus genome may encode a protein showing significant amino acid and predicted secondary structure homology with glycoprotein B of herpes simplex virus 1. *J. Virol.* 56: 807–813.
- Perdue ML, García M, Senne D & Fraire M (1997) Virulence-associated sequence duplication at the hemagglutinin cleavage site of avian influenza viruses. *Virus Res.* 49: 173–186.
- Perroncito E. (1878) Epizoozia tifoide nei gallinacei. *Annali Accad Agri Torino* 1878;21:87–126.
- Prichard, MN, Prichard LE & Shipman C Jr (1993). Strategic design and three-dimensional analysis of antiviral drug combinations. *Antimicrob. Agents Chemother.* 37:540–545.
- Prichard, MN & Shipman C Jr (1990). A three-dimensional model to analyze drug-drug interactions. *Antivir. Res.* 14:181–205.
- Pirrone V, Thakkar N, Jacobson JM, Wigdahl B & Krebs FC (2011) Combinatorial approaches to the prevention and treatment of HIV-1 infection. *Antimicrob. Agents Chemother.* 55: 1831–1842.
- Pizzorno A, Abed Y, Bouhy X, Beaulieu E, Mallett C, Russell R & Boivin G (2012) Impact of mutations at residue I223 of the neuraminidase protein on the resistance profile, replication level, and virulence of the 2009 pandemic influenza virus. *Antimicrob. Agents Chemother.* 56: 1208–1214.
- Podsiadlo P, Komiyama T, Fuller S, Blum O & Fuller RS (2004) Furin Inhibition by compounds of copper and zinc furin inhibition by compounds of copper and Zinc. *J. Biol. Chem.* 279: 36219-36227.
- Potier M, Mameli L, Bélisle M, Dallaire L & Melançon SB (1979) Fluorometric assay of neuraminidase with a sodium (4-methylumbelliferyl- α -D-N-acetylneuraminate) substrate. *Anal. Biochem.* 94: 287–296.
- Presti RM, Zhao G, Beatty WL, Mihindukulasuriya K a, da Rosa AP , Popov VL, Tesh RB, Virgin HW & Wang D (2009) Quarantfil, Johnston Atoll, and Lake Chad viruses are novel members of the family Orthomyxoviridae. *J. Virol.* 83: 11599–11606.

- Puthavathana P, Auewarakul P, Charoenying PC, Sangsiriwut K, Pooruk P, Boonnak K, Khanyok R, Thawachsupha P, Kijphati R & Sawanpanyalert P (2005) Molecular characterization of the complete genome of human influenza H5N1 virus isolates from Thailand. *J. Gen. Virol.* 86: 423–433.
- Qian X, Alonso-Caplen F & Krug RM (1994) NS1 protein are required for regulation of Two Functional Domains of the Influenza Virus NS1 Protein Are Required for Regulation of Nuclear Export of mRNA. 68.
- Repetto G, del Peso A & Zurita JL (2008) Neutral red uptake assay for the estimation of cell viability/cytotoxicity. *Nat. Protoc.* 3: 1125–1131.
- Richards RM, Lowy DR, Schiller JT & Day PM (2006) Cleavage of the papillomavirus minor capsid protein, L2, at a furin consensus site is necessary for infection. *Proc. Natl. Acad. Sci. U. S. A.* 103: 1522–1527.
- Roebroek AJ, Schalken JA, Leunissen JA, Onnekink C, Bloemers HP & Van de Ven WJ (1986) Evolutionary conserved close linkage of the c-fes/fps proto-oncogene and genetic sequences encoding a receptor-like protein. *EMBO J.* 5: 2197–2202.
- Roebroek AJ, Taylor NA, Pauli I, Smeijers L, Lauwers A, Von de Van WJ, Hartmann D, Creemers JW (2004) Modification , and Degradation: Limited Redundancy of the Proprotein Convertase Furin in Mouse Liver. *J. Bio.I Chem.* 279: 53442-53450.
- Roebroek AJ, Umans L, Pauli IG, Robertson EJ, van Leuven F, Van de Ven WJ & Constam DB (1998) Failure of ventral closure and axial rotation in embryos lacking the proprotein convertase Furin. *Development.* 125: 4863–4876.
- Rothberg MB, Haessler SD & Brown RB (2008) Complications of viral influenza. *Am. J. Med.* 121: 258–264.
- Russell RJ, Haire LF, Stevens DJ, Collins PJ, Lin YP, Blackburn GM, Hay AJ, Gamblin SJ & Skehel JJ (2006) The structure of H5N1 avian influenza neuraminidase suggests new opportunities for drug design. *Nature* 443: 45–49.
- Saar K, Lindgren M, Hansen M, Eiríksdóttir E, Jiang Y, Rosenthal-Aizman K, Sassian M & Langel U (2005) Cell-penetrating peptides: a comparative membrane toxicity study. *Anal. Biochem.* 345: 55–65.
- Sarac MS, Cameron A & Lindberg I (2002) The furin inhibitor hexa-D-arginine blocks the activation of *Pseudomonas aeruginosa* exotoxin A in vivo. *Infect. Immun.* 70: 7136–7139.
- Sato M, Yoshida S, Iida K, Tomozawa T, Kido H & Yamashita M (2003) A novel influenza A virus activating enzyme from porcine lung: purification and characterization. *Biol. Chem.* 384: 219–227.
- Schäfer W, Stroh A, Berghöfer S, Seiler J, Vey M, Kruse ML, Kern HF, Klenk HD & Garten W (1995) Two independent targeting signals in the cytoplasmic domain determine trans-Golgi network localization and endosomal trafficking of the proprotein convertase furin. *EMBO J.* 14: 2424–2435.
- Schnell JR & Chou JJ (2008) Structure and mechanism of the M2 proton channel of influenza A virus. *Nature* 451: 591–595.
- Scholtissek C (1990) Pigs as “Mixing Vessels” for the creation of new pandemic influenza A viruses. *Med. Princ. Pract.* 2: 65–71.
- Seidah NG, Benjannet S, Wickham L, Marcinkiewicz J, Stifani S, Basak A, Prat A & Chre M (2002) The secretory proprotein convertase neural Liver regeneration and neuronal differentiation. 1.

- Seidah NG & Chretien M (1999) Interactive report proprotein and prohormone convertases: a family of subtilases generating diverse bioactive polypeptides 1.
- Seidah NG, Chrétien M & Day R (1994) The family of subtilisin/kexin like pro-protein and pro-hormone convertases: divergent or shared functions. *Biochimie* 76: 197–209.
- Seidah NG & Prat A (2012) The biology and therapeutic targeting of the proprotein convertases. *Nat. Rev. Drug Discov.* 11: 367–383.
- Seo S, Englund JA, Nguyen JT, Pukrittayakamee S, Lindegardh N, Tarning J, Tambyah PA, Renaud C, Went GT, de Jong MD & Boeckh MJ (2013) Combination therapy with amantadine, oseltamivir and ribavirin for influenza A infection: safety and pharmacokinetics. *Antivir. Ther.* 18: 377–386.
- Shetty AK & Peek LA (2012) Peramivir for the treatment of influenza. *Expert Rev. Anti. Infect. Ther.* 10: 123–143.
- Shiraishi K, Mitamura K, Sakai-Tagawa Y, Goto H, Sugaya N & Kawaoka Y (2003) High frequency of resistant viruses harboring different mutations in amantadine-treated children with influenza. *J. Infect. Dis.* 188: 57–61.
- Shiryaev SA, Remacle AG, Ratnikov BI, Nelson NA, Savinov AY, Wei G, Bottini M, Rega MF, Parent A, Desjardins R, Fugere M, Day R, Sabet M, Pellecchia M, Liddington RC, Smith JW, Mustelin T, Guiney DG, Lebl M & Strongin AY (2007) Targeting host cell furin proprotein convertases as a therapeutic strategy against bacterial toxins and viral pathogens. *J. Biol. Chem.* 282: 20847–20853.
- Shortridge KF, Zhou NN, Guan Y, Gao P, Ito T, Kawaoka Y, Kodihalli S, Krauss S, Markwell D, Murti KG, Norwood M, Senne D, Sims L, Takada A, Webster RG (1998) Characterization of avian H5N1 influenza viruses from poultry in Hong Kong. *Virology* 252: 331–342.
- Skehel JJ & Wiley DC (2002) Influenza haemagglutinin. *Vaccine*. 20 Suppl 2: S51–4.
- Smee DF, Bailey KW, Morrison AC & Sidwell RW (2002) Combination treatment of influenza A virus infections in cell culture and in mice with the cyclopentane neuraminidase inhibitor RWJ-270201 and ribavirin. *Chemotherapy* 48: 88–93.
- Smee DF, Huffman JH, Morrison AC, Barnard DL & Sidwell RW (2001) Cyclopentane neuraminidase inhibitors with potent in vitro anti-influenza virus activities. *Antimicrob. Agents Chemother.* 45: 743–748.
- Smee DF, Hurst BL, Wong M-H, Bailey KW & Morrey JD (2009) Effects of double combinations of amantadine, oseltamivir, and ribavirin on influenza A (H5N1) virus infections in cell culture and in mice. *Antimicrob. Agents Chemother.* 53: 2120–2128.
- Smee DF, Hurst BL, Wong M-H, Bailey KW, Tarbet EB, Morrey JD & Furuta Y (2010) Effects of the combination of favipiravir (T-705) and oseltamivir on influenza A virus infections in mice. *Antimicrob. Agents Chemother.* 54: 126–133.
- Smith GJ, Vijaykrishna D, Bahl J, Lycett SJ, Worobey M, Pybus OG, Ma SK, Cheung CL, Raghvani J, Bhatt S, Peiris JS, Guan Y & Rambaut A (2009) Origins and evolutionary genomics of the 2009 swine-origin H1N1 influenza A epidemic. *Nature* 459: 1122–1125.
- Stevens J, Blixt O, Paulson JC & Wilson IA (2006) Glycan microarray technologies: tools to survey host specificity of influenza viruses. *Nat Rev Microbiol.* 4: 857–864.
- Stieneke-Gröber A, Vey M, Angliker H, Shaw E, Thomas G, Roberts C, Klenk HD & Garten W (1992) Influenza virus hemagglutinin with multibasic cleavage site is activated by furin, a subtilisin-like endoprotease. *EMBO J.* 11: 2407–2414.

- Suzuki H, Saito R, Masuda H, Oshitani H, Sato M & Sato I (2003) Emergence of amantadine-resistant influenza A viruses: epidemiological study. *J. Infect. Chemother.* 9: 195–200.
- Tai CY, Escarpe PA, Sidwell RW, Williams MA, Lew W, Wu H, Kim CU & Mendel DB (1998) Characterization of human influenza virus variants selected in vitro in the presence of the neuraminidase inhibitor GS 4071. *Antimicrob. Agents Chemother.* 42: 3234–3241.
- Tarbet EB, Maekawa M, Furuta Y, Babu YS, Morrey JD & Smee DF (2012) Combinations of favipiravir and peramivir for the treatment of pandemic influenza A/California/04/2009 (H1N1) virus infections in mice. *Antiviral Res.* 94: 103–110.
- Tarbet EB, Vollmer AH, Hurst BL, Barnard DL, Furuta Y & Smee DF (2014) In vitro activity of favipiravir and neuraminidase inhibitor combinations against oseltamivir-sensitive and oseltamivir-resistant pandemic influenza A (H1N1) virus. *Arch. Virol.* 159: 1279–1291.
- Taubenberger JK, Reid AH, Krafft AE, Bijwaard KE & Fanning TG (1997) Initial genetic characterization of the 1918 “Spanish” influenza virus. *Science.* 275: 1793–1796.
- Thomas G (2002) Furin at the cutting edge: from protein traffic to embryogenesis and disease. *Nat. Rev. Mol. Cell Biol.* 3: 753–766.
- Toltzis P & Huang AS (1986) Effect of ribavirin on macromolecular synthesis in vesicular stomatitis virus-infected cells. *Antimicrob. Agents Chemother.* 29: 1010–1016.
- Tong S, Li Y, Rivaller P, Conrardy C, Castillo DA, Chen LM, Recuenco S, Ellison JA, Davis CT, York IA, Turmelle AS, Moran D, Rogers S, Shi M, Tao Y, Weil MR, Tang K, Rowe LA, Sammons S, Xu X, Frace M, Lindblade KA, Cox NJ, Anderson LJ, Rupprecht CE & Donis RO (2012) A distinct lineage of influenza A virus from bats. *Proc. Natl. Acad. Sci. U. S. A.* 109: 4269–4274.
- Tong S, Zhu X, Li Y, Shi M, Zhang J, Bourgeois M, Yang H, Chen X, Recuenco S, Gomez J, Chen LM, Johnson A, Tao Y, Dreyfus C, Yu W, McBride R, Carney PJ, Gilbert AT, Chang J, Guo Z, Davis CT, Paulson JC, Stevens J, Rupprecht CE, Holmes EC, Wilson IA & Donis RO (2013) New world bats harbor diverse influenza A viruses. *PLoS Pathog.* 9: e1003657.
- Tosh PK, Jacobson RM & Poland GA (2010) Influenza vaccines: from surveillance through production to protection. *Mayo. Clin. Proc.* 83: 257–273.
- Tran TH, Nguyen TL, Nguyen TD, Luong TS, Pham PM, Nguyen van VC, Pham TS, Vo CD, Le TQM, Ngo TT, Dao BK, Le PP, Nguyen TT, Hoang TL, Cao VT, Le TG, Nguyen DT, Le HN, Nguyen KT, Le HS, Le VT, Christiane D, Tran TT, Menno de J, Schultsz C, Cheng P, Lim W, Horby P & Farrar J (2004) Avian influenza A (H5N1) in 10 patients in Vietnam. *N. Engl. J. Med.* 350: 1179–1188.
- Tsuneoka M, Nakayama K, Hatsuzawa K, Komada M, Kitamura N & Mekada E (1993) Evidence for involvement of furin in cleavage and activation of diphtheria toxin. *J. Biol. Chem.* 268: 26461–26465.
- Vey M, Schäfer W, Reis B, Ohuchi R, Britt W, Garten W, Klenk HD & Radsak K (1995) Proteolytic processing of human cytomegalovirus glycoprotein B (gpUL55) is mediated by the human endoprotease furin. *Virology* 206: 746–749.
- Villemure M, Fournier A, Gauthier D, Rabah N, Wilkes BC & Lazure C (2003) Barley serine proteinase inhibitor 2-derived cyclic peptides as potent and selective inhibitors of convertases PC1/3 and furin. *Biochemistry* 42: 9659–9668.
- Volchkov VE, Feldmann H, Volchkova VA & Klenk HD (1998) Processing of the Ebola virus glycoprotein by the proprotein convertase furin. *Proc. Natl. Acad. Sci. U. S. A.* 95: 5762–5767.

- Volchkov VE, Volchkova VA, Ströher U, Becker S, Dolnik O, Cieplik M, Garten W, Klenk HD & Feldmann H (2000) Proteolytic processing of Marburg virus glycoprotein. *Virology* 268: 1-6.
- Van der Vries E, Stelma FF & Boucher CAB (2010) Emergence of a multidrug-resistant pandemic influenza A (H1N1) virus. *N. Engl. J. Med.* 363: 1381–1382.
- Watanabe M, Hirano A, Stenglein S, Nelson J, Thomas G, Watanabe M, Hirano A, Stenglein S, Nelson JA, Thomas G & Wong TC (1995) Engineered serine protease inhibitor prevents furin-catalyzed activation of the fusion glycoprotein and production of infectious measles virus. *J. Virol.* 69: 3206-3210.
- Webster RG, Bean WJ, Gorman OT, Chambers TM & Kawaoka Y (1992) Evolution and ecology of influenza A viruses. *Microbiol. Rev.* 56: 152-179.
- Wilks S, de Graaf M, Smith DJ & Burke DF (2012) A review of influenza haemagglutinin receptor binding as it relates to pandemic properties. *Vaccine* 30: 4369-4376.
- Wise HM, Hutchinson EC, Jagger BW, Stuart AD, Kang ZH, Robb N, Schwartzman LM, Kash JC, Fodor E, Firth AE, Gog JR, Taubenberger JK & Digard P (2012) Identification of a novel splice variant form of the influenza A virus M2 ion channel with an antigenically distinct ectodomain. *PLoS Pathog.* 8: e1002998.
- Wise HM, Foeglein A, Sun J, Dalton RM, Patel S, Howard W, Anderson EC, Barclay WS & Digard P (2009) A complicated message: Identification of a novel PB1-related protein translated from influenza A virus segment 2 mRNA. *J. Virol.* 83: 8021–8031.
- Zhirnov OP, Vorobjeva I V, Ovcharenko A V & Klenk HD (2003) Intracellular cleavage of human influenza a virus hemagglutinin and its inhibition. *Biochem.* 68: 1020–1026.
- Zimmer G, Budz L & Herrler G (2001) Proteolytic activation of respiratory syncytial virus fusion protein. Cleavage at two furin consensus sequences. *J. Biol. Chem.* 276: 31642–31650.

Other references

- Knipe, David M.; Howley, Peter M. (2006) Title: Fields Virology, 5th Edition, 2006.
- Harder TC & Werner O (2006). "Avian influenza". <http://www.influenzareport.com/ir/ai.htm>

CDC

- 1 <http://www.cdc.gov/flu/professionals/acip/>
- 2 http://wwwnc.cdc.gov/eid/article/17/10/11-0117_article
- 3 <http://www.cdc.gov/flu/professionals/antivirals/summary-clinicians.htm>

WHO

- 1 http://www.who.int/influenza/human_animal_interface/virology_laboratories_and_vaccines/influenza_virus_infections_humans_feb14.pdf?ua=1

2

http://www.who.int/influenza/human_animal_interface/influenza_h7n9/140225_H7N9RA_for_w eb_20140306FM.pdf?ua=1

3

http://www.who.int/influenza/human_animal_interface/Influenza_Summary_IRA_HA_interface _24January14.pdf?ua=1

4

http://www.who.int/influenza/human_animal_interface/EN_GIP_20140124CumulativeNumber H5N1cases.pdf

5

http://www.who.int/mediacentre/news/statements/2009/h1n1_pandemic_phase6_20090611/en /

Abbreviations

Ac	acetyl
Amba	amidinobenzylamide
Ame	aminomethyl
APS	ammonium peroxydisulfate
BSL	biosafety level
C-terminal	carboxyl-terminal
cDNA	complementary DNA
CPE	cytopathic effects
def (PBS _{def})	deficient
d (dH ₂ O)	deionized
D6R	hexa-D-arginine
DENV	Dengue virus
DMEM	Dulbecco's Modified Eagle medium
DMSO	dimethyl sulfoxide
DNA	deoxyribonucleic acid
EB	ethidium bromide
EC ₅₀	50% effective concentration
EDTA	ethylenediaminetetraacetic acid
ELISA	enzyme-linked immunosorbent assay
dNTP	deoxynucleoside triphosphate
ds (ds RNA)	double stranded
EBOV	Ebola virus
ER	endoplasmic reticulum
FCS	fetal calf serum
FPV	A/chicken/fowl plague virus/Rostock/1934, H7N1
Guame	guanidinomethyl
HA	hemagglutinin
HAART	highly active antiretroviral therapy
HAU	hemagglutination unit
HEPES	2-[4-(2-hydroxyethyl)piperazin-1-yl]ethanesulfonic acid
HFRS	haemorrhagic fever with renal syndrome
HIV	human immunodeficiency virus
HPAIV	highly pathogenic avian influenza virus
HPLC	high performance liquid chromatography
HRP	horseradish peroxidase
IC ₅₀	50% inhibitory concentration
IFN	interferon
KAN-1	A/Thailand/1(KAN-1)/2004, H5N1

LPAIV	low pathogenic avian influenza virus
MDCK	Madin-Darby Canine Kidney
MAP	mitogen-activated protein
MARV	Marburg virus
2 x MEM	2 x Modified Eagle Medium
mM	millimolar
mm	millimeter
Mock	uninfected and untreated cells
M1	matrix protein 1
MOI	multiplicity of infection
mRNA	messenger RNA
M2	matrix protein 2
MTT	3-(4,5-dimethylthiazol-2-yl)-2,5-diphenyltetrazolium bromide
MUNANA	2'-(4-Methylumbelliferyl)- α -D-N-acetylneuraminic acid
4-MU	4-methylumbelliferone
4-MUSS	4-methyumbelliferone sodium salt
NDV	Newcastle disease virus
NA	neuraminidase (influenza)
NP	nucleoprotein (influenza)
NR	neutral red
μ M	micromolar
nM	nanomolar
Os	oseltamivir
PA	polymerase acid (influenza)
PB1	polymerase basic 1 (influenza)
PB2	polymerase basic 2 (influenza)
PCR	polymerase chain reaction
PDB	protein data bank
PFU	plaque forming units
Phac	phenylacetyl
PFA	paraformaldehyde
p.i.	post infection
P/S	penicillin/streptavidin
RFU	relative fluorescence units
rib	ribavirin
RNA	ribonucleic acid
RNP	ribonucleoprotein
rpm	revolutions per minute
RSV	respiratory syncytial virus
RT-PCR	reverse transcription polymerase chain reaction

RT	reverse transcription
SA	sialic acid
SDS	sodium dodecyl sulphate
SDS-PAGE	sodium dodecyl sulfate polyacrylamide gel electrophoresis
SPF	specific pathogen free
ss	single stranded
TEMED	N,N,N',N'-tetramethylethanediamine
TGN	<i>trans</i> -Golgi network
UV	ultraviolet
VSV	Vesicular stomatitis virus
WB	Western blot

Amino acids

A (Ala)	alanine
C (Cys)	cysteine
E (Glu)	glutamic acid
D (Asp)	aspartic acid
G (Gly)	glycine
H (His)	histidine
I (Ile)	isoleucine
K (Lys)	lysine
L (Leu)	leucine
M (Met)	methionine
N (Asn)	asparagine
P (Pro)	proline
Q (Gln)	glutamine
R (Arg)	arginine
S (Ser)	serine
T (Thr)	threonine
W (Trp)	tryptophan
V (Val)	valine
Y (Tyr)	tyrosine

Figures

Fig. 1.1: Recorded human influenza pandemics since 1918.	8
Fig. 1.2: Structure of influenza A virus.	10
Fig. 1.3: Influenza virus life cycle.	13
Fig. 1.4: Crystal structure of hemagglutinin (HA).	15
Fig. 1.5: The role of swine for influenza virus genetic reassortment.	16
Fig. 1.6: Cleavage of hemagglutinin of influenza A viruses.	17
Fig. 1.7: Scheme of the furin structure.	20
Fig. 1.8: Sites of substrates activation by furin.	21
Fig. 1.9: M2 protein inhibitors.	24
Fig. 1.10: Neuraminidase inhibitors.	25
Fig. 1.11: Structure of furin inhibitor MI-701.	28
Fig. 1.12: Antiviral agents target different steps during influenza virus replication.	30
Fig. 3.1: Scheme of propagation of FPV in the presence and absence of antivirals in MDCK cells.	53
Fig. 4.1: Cytotoxicity determination of different furin inhibitors <i>in vitro</i> .	58
Fig. 4.2: Dose-dependent cytotoxicity determination of different inhibitors.	59
Fig. 4.3: Stability measurement of furin inhibitors.	60
Fig. 4.4: Cleavage of HA in the presence of different furin inhibitors (A) and quantification of HA cleavage inhibition (B).	61
Fig. 4.5: Cleavage of HA0 in the presence of inhibitor MI-701 at various concentrations.	63
Fig. 4.6: Virus spread in the presence of furin inhibitor MI-701.	64
Fig. 4.7: Inhibition of HPAIV multicycle replication in cell cultures.	65
Fig. 4.8: Inhibition of the FPV_mutant_HA _{mono} multicycle replication in cell cultures.	66
Fig. 4.9: Cytotoxicity of MI-701 in double and triple combination with anti-influenza drugs.	68
Fig. 4.10: Virus spread in the presence of MI-701 and oseltamivir.	69
Fig. 4.11: HPAIV multicycle replication in the presence of double drugs.	70
Fig. 4.12A: Multicycle replication of HPAIV subtype H7N1 in the presence of triple drugs.	72
Fig. 4.12B: Multicycle replication of HPAIV subtype H5N1 in the presence of triple drugs.	73
Fig. 4.13: Viability of inhibitor treated infected cells at 96h p.i..	74
Fig. 4.14: Vesicular Stomatitis Virus control infection.	75
Fig. 4.15: Synergistic inhibition of MI-701 in double combination and triple combination against FPV.	77
Fig. 4.16: Time of inhibitor addition.	79
Fig. 4.17: Susceptibility of passaged FPV to furin inhibitor MI-701.	81
Fig. 4.18: Susceptibility of passaged FPV to oseltamivir.	82
Fig. 4.19: Sequence analysis is represented in chromatogram.	84

Fig. 4.20: Crystal structure of group-1 (N1) NA monomer in ribbons representation (A) and NA tetramer in surface representation (B).	85
Fig. 4.21: NA enzyme inhibition assay of FPV mutants.	86
Fig. 4.22: Growth FPV wild type and FPV mutants in cell cultures.	88
Fig. 4.23: Effect of MI-701 on FPV mutants replication.	89
Fig. 5.1: Binding mode of synthetic inhibitors in the active site of human furin.	95
Fig. 5.2: Reduction of KAN-1 virus yield at 72h p.i. after inhibitor treatment.	98
Fig. 5.3: Neuraminidase inhibitor resistant mutations.	102
Fig. S1: Structures of oseltamivir and ribavirin.	107
Fig. S2: Inhibition proteolytic activation of HPAIV H5N1 subtype virus by furin inhibitor MI-701.	110
Fig. S3: Microscopy images of virus spread in the presence of MI-701 and oseltamivir alone or in combination.	111
Fig. S4: Reduction of EC ₅₀ for MI-701 as single agent or in double and triple combinations.	112
Fig. S5: Inhibitory efficacy of newly modified furin inhibitors.	114
Fig. S6: Neutral red data for synergy analysis.	115-117
Table 1.1: Human cases of influenza A virus H7 subtype infection since 1996.	5
Table 1.2: Confirmed human H5N1 cases from 2003 to 2014.	7
Table 1.3: Functions of influenza viral proteins.	11
Table 4.1: Reduction of EC ₅₀ for MI-701 as single agent or in double and triple combinations.	76
Table 4.2: Sequence analysis of FPV variants in the presence of drugs <i>in vitro</i> .	83
Table 4.3: Susceptibility of FPV mutants to oseltamivir.	87
Table 5.1: Reported furin inhibitors.	92
Table 5.2: Cleavage motifs in the precursors of different infectious pathogens.	104
Table S1: Outbreak of HPAIV H7 subtypes in poultry since 1959.	106
Table S2: Outbreaks of HPAIV H5 subtypes in poultry since 1959.	107
Table S3: Structures of P5-modified furin inhibitors.	108
Table S4: Structures of optimized furin inhibitors.	115

Curriculum vitae

Name: Yinghui Lu
Birthday: 21st Nov.1983
Birth place: Shanghai, China
Nationality: chinese

Education

2007-2009 Philipps university Marburg
Master programme 'Molecular and Cellular Biology'
Degree: Master of Science
2002-2006 Bioscience, Shanghai Normal University
Degree: Bachelor of Science
1999-2002 Shangnan high school in Pudong New Distrcit, Shanghai
1996-1999 The Subsidiary Experimental School of College of
education in Pudong New Distrcit, Shanghai
1990-1995 Pusanlu primary school in Pudong New Distrcit, Shanghai

Scholarships

09/2009-06/2011 PhD student, LOEWE-Stiftung, Hessen
(Prof. Dr. Wolfgang Garten)
05/2010-08/2010 Research & Teaching Assistantships (DAAD)
07/2011-11/2011 Roland und Elfriede-Schauer-Stiftung, PhD scholarship
12/2011-08/2013 FAZIT-Stiftung, PhD scholarship
09-2013-12-2014 PhD student, Collaboration research center 593,
project B1 (Prof. Dr. Hans-Dieter Klenk)

Publications

Becker GL, Sielaff F, Than ME, Lindberg I, Routhier S, Day R, **Lu Y**, Garten W & Steinmetzer T (2010) Potent inhibitors of furin and furin-like proprotein convertases containing decarboxylated P1 arginine mimetics. *J. Med. Chem.* 53: 1067–1075.

Becker GL, **Lu Y**, Harges K, Strehlow B, Levesque C, Lindberg I, Sandvig K, Bakowsky U, Day R, Garten W & Steinmetzer T (2012) Highly potent inhibitors of proprotein convertase furin as potential drugs for treatment of infectious diseases. *J. Biol. Chem.* 287: 21992–22003.

Böttcher-Friebertshäuser E, **Lu Y**, Meyer D, Sielaff F, Steinmetzer T, Klenk H-D & Garten W (2012) Hemagglutinin activating host cell proteases provide promising drug targets for the treatment of influenza A and B virus infections. *Vaccine* 30: 7374–7380.

Paper in preparation

Lu Y, Harges K, Böttcher-Friebertshäuser E, Steinmetzer T, Klenk HD, and Garten W (2014) Synergistic inhibition of highly pathogenic avian influenza viruses by combinatorial treatment with oseltamivir, ribavirin, and a peptidomimetic furin inhibitor

Poster presentations

21th Annual Meeting of the Society for Virology, Freiburg, Germany. (2011)

“Newly designed peptidomimetics inhibit specific host cell subtilases necessary for propagation of distinct viruses.” **Lu Y**, Fehling SK, Strecker T, Becker G, Steinmetzer T and Garten W.

“Importance of activated viral glycoprotein for spread of Borna disease virus in various cell cultures.” Bayer K, Lennartz F, **Lu Y**, Becker G, Steinmetzer T, Kehr K, Herden C and Garten W.

22th Annual Meeting of the Society for Virology, Essen, Germany. (2012)

“Synergistic blockage of virus propagation by host cell protease inhibitors combined approved drugs.” Fehling SK, **Lu Y**, Strecker T, Becker G, Steinmetzer T and Garten W.

“Inhibition of IBV infection in Vero cells and chicken tracheal organ cultures by an Inhibitor of the cellular protease furin.” Winter C, **Lu Y**, Herrler G, Steinmetzer T and Garten W.

International Symposium of the SFB 593 “Mechanisms of Cellular Compartmentalization.” (2012)

“Synergistic inhibition of virus replication by combination of host cell protease inhibitors and approved drugs.” Fehling SK, **Lu Y**, Strecker T, Becker G, Steinmetzer T and Garten W.

3rd International Influenza Meeting, Muenster, Germany. (2012)

“Newly designed furin-specific inhibitors exhibit potent inhibitory efficacy against highly pathogenic influenza viruses.” **Lu Y**, Becker G, Steinmetzer T and Garten W.

23th Annual Meeting of the Society for Virology, Kiel, Germany. (2013)

The proteolytic cleavage of the IBV spike protein by furin or other host proteases depends on the cell type.” Winter C, **Lu Y**, Garten W, Steinmetzer T and Herrler G.

“Propagation of highly pathogenic influenza virus is blocked by combinatorial treatment with GS4017, ribavirin and furin inhibitor MI-701.” **Lu Y**, Becker G, Steinmetzer T and Garten W.

Oral presentation**24th Annual Meeting of the Society for Virology, Alpbach, Austria. (2014)**

“Combinatorial treatment with oseltamivir, ribavirin and furin inhibitor MI-701 inhibits propagation of highly pathogenic avian influenza virus and suppresses the development of drug-resistant virus mutants.” **Lu Y**, Becker G, Steinmetzer T, Klenk HD and Garten W.

Acknowledgements

This research project would not have been possible without support from of many people.

First and foremost, I would like to express my profound gratitude to my advisor, *Prof. Dr. Wolfgang Garten*, who offered guidance and suggestions throughout my PhD study. I am also very grateful for his scientific advice, knowledge and many insightful discussions and suggestions.

A special thanks goes to *Prof. Dr. Steinmetzer* and his team, *Dr. Gero Becker* and *Kornelia Harges*, Institute of Pharmaceutical Chemistry, Philipps University Marburg, who steadily supplied me with the peptidomimetic inhibitors and gave me lots of valuable advice.

I would like to make a grateful acknowledgement to *Prof. Dr. Hans-Dieter Klenk*, Institute of Virology, Marburg, for his interest in and generous support of my work. I also like to thank *Dr. Mikhail Matrosovich*, Institute of Virology, Marburg, who made the influenza virus A/Thailand/1(KAN-1)/2004 (H5N1) from *Dr. Puthavathana Mahidol*, University, Bangkok, Thailand, available for my research.

I would like to thank *Dr. Eva Friebertshäuser* for her helpful discussions and advice.

I am grateful for *Emi Takashita*, PhD at the Influenza Virus Research Center, National Institute of Infectious Disease, Tokyo, Japan, for her useful advices about virus inactivation, which made it possible to measure the neuraminidase activity of highly pathogenic influenza virus in the BSL 2 lab.

Many thanks go to *Prof. Dr. Mark N. Prichard*, Department of Pediatrics, Division of Infectious Diseases, University of Alabama at Birmingham, for kindly providing the program MacSynergy III for the synergy analysis.

I am grateful for *Dr. Vasundara Srinivasan* (LOEWE Center for Synthetic Microbiology-SYNNMIKRO) at the Philipps University Marburg, for kindly showing me how to present the 3D model of influenza NA protein using the program Pymol.

I would also like to acknowledge *Vanessa Körner* and *Cornelia Stoiber* for testing several furin inhibitors against the infections caused by Newcastle disease virus and respiratory syncytial virus in cell cultures.

I'm thankful for *Dr. Volker Czudai-Matwich's* kind help and advice about neuraminidase assays.

I am also appreciative of *Prof. Dr. Wolfgang Buckel*, *Prof. Dr. Erhard Bremer* and *Prof. Dr. Susanne Önel*, for their friendly support and effort in the thesis committee of the Faculty Biology at the Philipps University Marburg.

I am obliged to all of the people in Institute of Virology, Marburg, especially the present and past members of our lab, *Dr. Eva Friebertshäuser*, *Dr. Thomas Strecker*, *Dr. Sarah Katharina Fehling*, *Dr. Catharina Peitsch*, *Dr. Frank Lennartz*, *Dr. Katrin Schlie*, *Carolin Tarnow*, *Annika Arendt*, *Petra Neubauer-Rädel*, *Vanessa Körner* and *Cornelia Stoiber*, who gave me assistance and an enjoyable work environment during my study here.

I'd like to give my special thanks to *Leah Demakovsky* for her elaborative linguistic correction of my thesis.

I'd like to thank *Prof. Dr. Stephan Becker* for the opportunity to perform my thesis at the Institute of Virology and for his ongoing support.

I'd like to thank to the *Deutsche Forschungsgemeinschaft Sonderforschungsbereich 593*, *LOEWE-Stiftung*, *FAZIT-Stiftung*, *Roland und Elfriede-Schauer Stiftung* for providing financial aid by turns.

Last but not least, my utmost gratitude goes to my family. Words fail me to express my deepest love for my parents and my sister. Thanks for your understanding and endless love. Lastly I'd like to take this opportunity to thank all of my friends for their support.

Erklärung

Ich erkläre, daß ich meine Dissertation

**Potent inhibition of highly pathogenic influenza virus infection using a
peptidomimetic furin inhibitor alone or in combination with conventional
antiviral agents**

selbständig, ohne unerlaubte Hilfe angefertigt und mich dabei keiner anderen als der von mir ausdrücklich bezeichneten Quellen und Hilfen bedient habe. Die Dissertation wurde in der jetzigen oder einer ähnlichen Form noch keiner anderen Hochschule eingereicht und hat noch keinen sonstigen Prüfungszwecken gedient.

Marburg, 14.08.2014

Yinghui Lu